

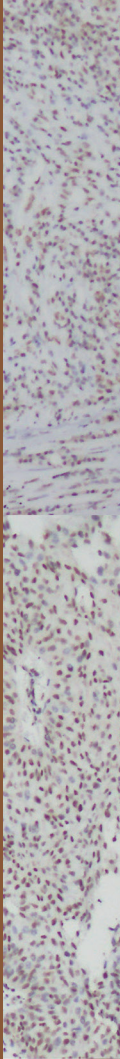
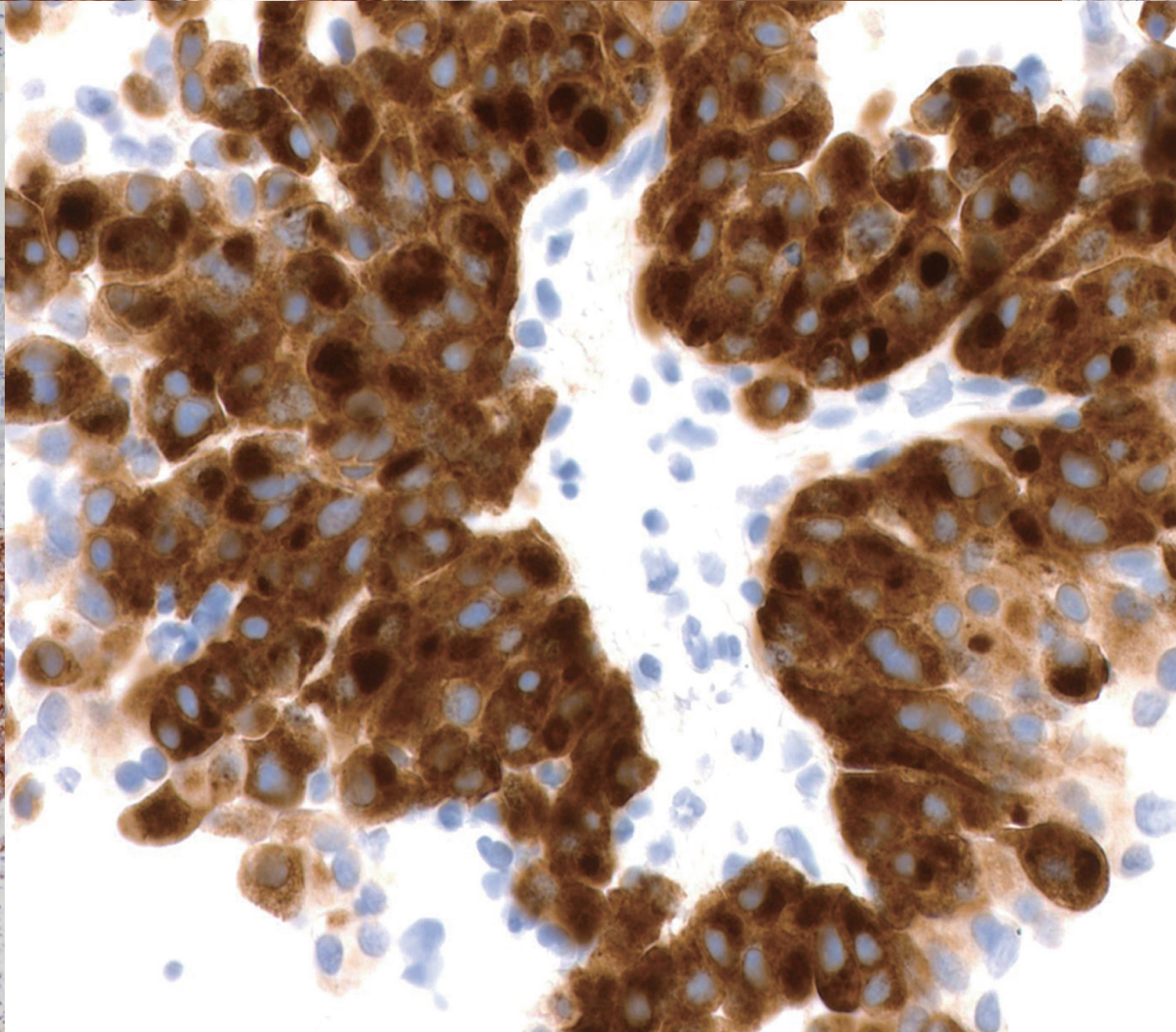
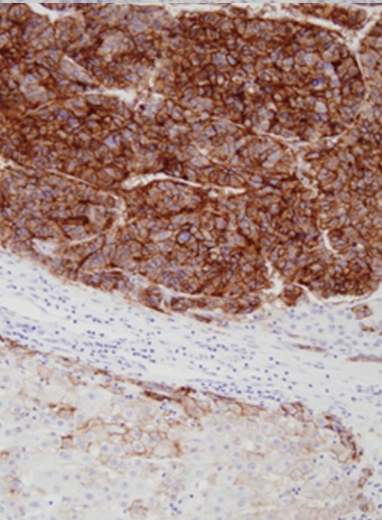
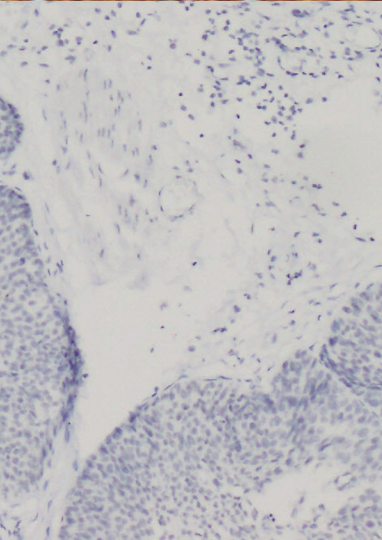
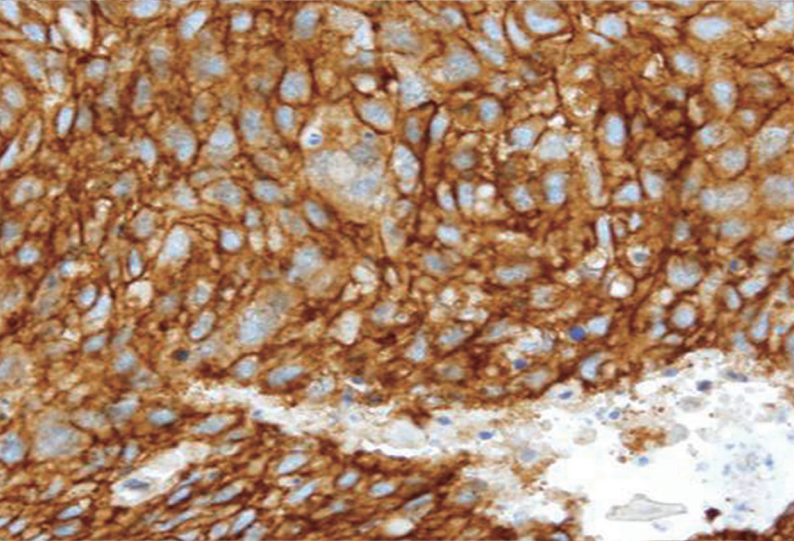
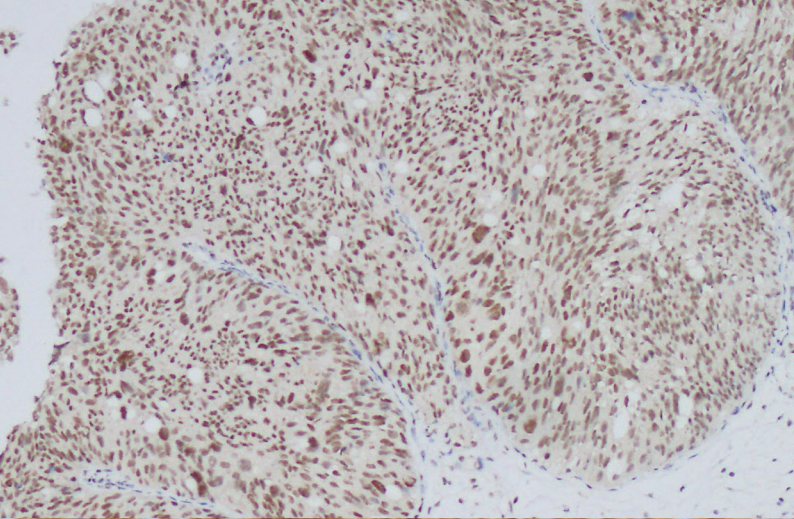
JPTM

Journal of Pathology
and Translational Medicine

September 2015
Vol. 49 / No. 5
jpatholm.org
pISSN: 2383-7837
eISSN: 2383-7845



*Cytology Specimen
Management, Triage and
Standardized Reporting
of Fine Needle Aspiration
Biopsies of the Pancreas*



Aims & Scope

The *Journal of Pathology and Translational Medicine* is an open venue for the rapid publication of major achievements in various fields of pathology, cytopathology, and biomedical and translational research. The Journal aims to share new insights into the molecular and cellular mechanisms of human diseases and to report major advances in both experimental and clinical medicine, with a particular emphasis on translational research. The investigations of human cells and tissues using high-dimensional biology techniques such as genomics and proteomics will be given a high priority. Articles on stem cell biology are also welcome. The categories of manuscript include original articles, review and perspective articles, case studies, brief case reports, and letters to the editor.

Subscription Information

To subscribe to this journal, please contact the Korean Society of Pathologists/the Korean Society for Cytopathology. Full text PDF files are also available at the official website (<http://jpatholm.org>). *Journal of Pathology and Translational Medicine* is indexed by PubMed, PubMed Central, Scopus, KoreaMed, KoMCI, WRPIM and CrossRef. Circulation number per issue is 700.

Editors-in-Chief

Hong, Soon Won, M.D. (*Yonsei University, Korea*)

Kim, Chong Jai, M.D. (*University of Ulsan, Korea*)

Associate Editors

Choi, Yoon Jung, M.D. (*National Health Insurance Service, Ilsan Hospital, Korea*)

Han, Jee Young, M.D. (*Inha University, Korea*)

Editorial Board

Ali, Syed Z. (*Johns Hopkins Hospital, U.S.A.*)

Avila-Casado, Maria del Carmen (*University of Toronto, Toronto General Hospital UHN, Canada*)

Cho, Kyung-Ja (*University of Ulsan, Korea*)

Choi, Yeong-Jin (*Catholic University, Korea*)

Chung, Jin-Haeng (*Seoul National University, Korea*)

Gong, Gyung Yub (*University of Ulsan, Korea*)

Grignon, David J. (*Indiana University, U.S.A.*)

Ha, Seung Yeon (*Gachon University, Korea*)

Jang, Se Jin (*University of Ulsan, Korea*)

Jeong, Jin Sook (*Dong-A University, Korea*)

Kang, Gyeong Hoon (*Seoul National University, Korea*)

Katoh, Ryohei (*University of Yamaguchi, Japan*)

Kerr, Keith M. (*Aberdeen University Medical School, U.K.*)

Kim, Aeree (*Korea University, Korea*)

Kim, Kyoung Mee (*Sungkyunkwan University, Korea*)

Kim, Kyu Rae (*University of Ulsan, Korea*)

Kim, Se Hoon (*Yonsei University, Korea*)

Kim, Seok-Hyung (*Sungkyunkwan University, Korea*)

Kim, Woo Ho (*Seoul National University, Korea*)

Kim, Youn Wha (*Kyung Hee University, Korea*)

Ko, Young Hyeoh (*Sungkyunkwan University, Korea*)

Koo, Ja Seung (*Yonsei University, Korea*)

Lee, C. Soon (*University of Western Sydney, Australia*)

Lee, Hye Seung (*Seoul National University, Korea*)

Lee, Kyung Han (*Sungkyunkwan University, Korea*)

Lee, Sug Hyung (*Catholic University, Korea*)

Lim, Beom Jin (*Yonsei University, Korea*)

Moon, Woo Sung (*Chonbuk University, Korea*)

Park, Chan-Sik (*University of Ulsan, Korea*)

Park, Sanghui (*Ewha Womans University, Korea*)

Park, So Yeon (*Seoul National University, Korea*)

Park, Young Nyun (*Yonsei University, Korea*)

Ro, Jae Y. (*Cornell University, The Methodist Hospital, U.S.A.*)

Romero, Roberto (*National Institute of Child Health and Human Development, U.S.A.*)

Schmitt, Fernando (*IPATIMUP [Institute of Molecular Pathology and Immunology of the University of Porto], Portugal*)

Shin, Eunah (*Cha University, Korea*)

Sung, Chang Ohk (*University of Ulsan, Korea*)

Tan, Puay Hoon (*National University of Singapore, Singapore*)

Than, Nandor Gabor (*Semmelweis University, Hungary*)

Tse, Gary M. (*Prince of Wales Hospital, Hongkong*)

Vielh, Philippe (*International Academy of Cytology Gustave Roussy Cancer Campus Grand Paris, France*)

Wildman, Derek (*University of Illinois, U.S.A.*)

Yatabe, Yasushi (*Aichi Cancer Center, Japan*)

Yoon, Bo Hyun (*Seoul National University, Korea*)

Yoon, Sun Och (*Yonsei University, Korea*)

Statistics Editors

Kim, Dong Wook (*National Health Insurance Service Ilsan Hospital, Korea*)

Yoo, Hanna (*Yonsei University, Korea*)

Manuscript Editor

Chang, Soo-Hee (*InfoLumi Co., Korea*)

Contact the Korean Society of Pathologists/the Korean Society for Cytopathology

Publishers: Changsuk Kang, MD, So Young Jin, MD

Editors-in-Chief: Soon Won Hong, MD, Chong Jai Kim, MD

Published by the Korean Society of Pathologists/the Korean Society for Cytopathology

Editorial Office

Room 1209 Gwanghwamun Officia, 92 Saemunan-ro, Jongno-gu,

Seoul 110-999, Korea/#406 Lilla Swami Bldg, 68 Dongsan-ro,

Seocho-gu, Seoul 03186, Korea

Tel: +82-2-795-3094/+82-2-593-6943

Fax: +82-2-790-6635/+82-2-593-6944

E-mail: office@jpatholm.org

Printed by ML communications Co., Ltd.

Jungang Bldg. 18-8 Wonhyo-ro 89-gil, Yongsan-gu, Seoul 04314, Korea

Tel: +82-2-717-5511 Fax: +82-2-717-5515 E-mail: ml@smileml.com

Manuscript Editing by InfoLumi Co.

210-202, 421 Pangyo-ro, Bundang-gu, Seongnam 13522, Korea

Tel: +82-70-8839-8800 E-mail: infolumi.chang@gmail.com

Front cover image: Immunohistochemistry of this issue. p366, p375, p383, p392, p393.

© Copyright 2015 by the Korean Society of Pathologists/the Korean Society for Cytopathology

© Journal of Pathology and Translational Medicine is an Open Access journal under the terms of the Creative Commons Attribution Non-Commercial License (<http://creativecommons.org/licenses/by-nc/3.0>).

© This paper meets the requirements of KS X ISO 9706, ISO 9706-1994 and ANSI/NISO Z.39.48-1992 (Permanence of Paper).

This journal was supported by the Korean Federation of Science and Technology Societies Grant funded by the Korean Government.

CONTENTS

REVIEWS

- 355 **Current Issues and Clinical Evidence in Tumor-Infiltrating Lymphocytes in Breast Cancer**
Sung Gwe Ahn, Joon Jeong, SoonWon Hong, Woo Hee Jung
- 364 **Cytology Specimen Management, Triage and Standardized Reporting of Fine Needle Aspiration Biopsies of the Pancreas**
Won Jae Yoon, Martha Bishop Pitman

ORIGINAL ARTICLES

- 373 **SALL4 Expression in Hepatocellular Carcinomas Is Associated with EpCAM-Positivity and a Poor Prognosis**
Hyejin Park, Hyejung Lee, An Na Seo, Jai Young Cho, Young Rok Choi, Yoo-Seok Yoon, Ho-Seong Han, Young Nyun Park, Haeryoung Kim
- 382 **Membranous Insulin-like Growth Factor-1 Receptor (IGF1R) Expression Is Predictive of Poor Prognosis in Patients with Epidermal Growth Factor Receptor (EGFR)-Mutant Lung Adenocarcinoma**
Eunhyang Park, Soo Young Park, Hyojin Kim, Ping-Li Sun, Yan Jin, Suk Ki Cho, Kwahanmien Kim, Choon-Taek Lee, Jin-Haeng Chung
- 389 **Parafibromin Staining Characteristics in Urothelial Carcinomas and Relationship with Prognostic Parameters**
Serap Karaarslan, Banu Yaman, Hakan Ozturk, Banu Sarsik Kumbaraci
- 396 **Comparison of Cytologic Characteristics between Adenoid Cystic Carcinoma and Adenoid Basal Carcinoma in the Uterine Cervix**
Juhyeon Jeong, Seung Yeon Ha, Hyun Yee Cho, Dong Hae Chung, Jungsuk An

CASE REPORTS

- 403 **Paediatric Primary Pachymeningeal Xanthogranuloma with Scattered Foci Displaying Reticulohistiocytoma-like Features**
Miguel Fdo. Salazar, María del Rocío Estrada Hernández, Erick Gómez Apo, Laura G. Chávez Macías, Carlos Alfonso Rodríguez Álvarez
- 409 **Human Herpesvirus 8-Negative and Epstein-Barr Virus-Positive Effusion-Based Lymphoma in a Patient with Human Immunodeficiency Virus**
Jung-Woo Choi, Younghye Kim, Ju-Han Lee, Young-Sik Kim
- 413 **Oncocytic Renal Cell Carcinoma with Tubulopapillary Growth Having a Fat Component**
Na Rae Kim, Hyun Yee Cho

-
- 418 **Multifocal Polypoid Endometriosis Mimicking Malignancy in a Young Woman with a History of Hormonal Treatment**
Ji-Young Kim, Tae-Jong Song, Hye-Kyung Choi, Jeong Yun Shim
- 421 **Gastric Langerhans Cell Histiocytosis: Case Report and Review of the Literature**
So Jung Lee, Chung Su Hwang, Gi Young Huh, Chang Hun Lee, Do Youn Park

Instructions for Authors for *Journal of Pathology and Translational Medicine* are available at <http://jpatholm.org/authors/authors.php>

Current Issues and Clinical Evidence in Tumor-Infiltrating Lymphocytes in Breast Cancer

Sung Gwe Ahn · Joon Jeong
SoonWon Hong¹ · Woo Hee Jung¹

Departments of Surgery and ¹Pathology,
Gangnam Severance Hospital, Yonsei University
College of Medicine, Seoul, Korea

Received: July 19, 2015
Revised: July 22, 2015
Accepted: July 28, 2015

Corresponding Author

Joon Jeong, MD
Department of Surgery, Gangnam Severance
Hospital, Yonsei University College of Medicine,
211 Eonju-ro, Gangnam-gu, Seoul 06273, Korea
Tel: +82-2-2019-3379
Fax: +82-2-3462-5994
E-mail: gsjjoon@yuhs.ac

With the advance in personalized therapeutic strategies in patients with breast cancer, there is an increasing need for biomarker-guided therapy. Although the immunogenicity of breast cancer has not been strongly considered in research or practice, tumor-infiltrating lymphocytes (TILs) are emerging as biomarkers mediating tumor response to treatments. Earlier studies have provided evidence that the level of TILs has prognostic value and the potential for predictive value, particularly in triple-negative and human epidermal growth factor receptor 2-positive breast cancer. Moreover, the level of TILs has been associated with treatment outcome in patients undergoing neoadjuvant chemotherapy. To date, no standardized methodology for measuring TILs has been established. In this article, we review current issues and clinical evidence for the use of TILs in breast cancer.

Key Words: Breast neoplasms; Immune system; Lymphocytes, tumor-infiltrating; Triple negative breast neoplasms

Molecular medicine has shown that all cancers are caused by mutations accumulated in various genes. Cancerous tissues harboring genetic mutations frequently create a new class of tumor-specific antigens.^{1,2} The presentation of neoantigen by tumor cells induces an immune response and triggers antitumor immunity. These neoantigens are displayed on the surfaces of tumor cells and are increased in relation to mutational load because mutations increase the efficiency with which a peptide is presented by MHC molecules.¹ Recent findings based on whole-exome sequencing have revealed that different tumors have different mutational loads, suggesting that neoantigen repertoire varies according to tumor type.³ That study showed that breast cancer has an average of one somatic mutation per megabase (Mb) of coding DNA and is expected to have moderate immunogenicity among human cancers.

Though the immunogenicity of breast cancer has not been traditionally considered in clinical practice or cancer research, the presence of tumor-infiltrating lymphocytes (TILs) in the tumor or peritumoral site has emerged as a biomarker of antitumor immune response in breast cancer. Despite the heterogeneity of TILs and the absence of a standardized methodology of

evaluating TILs, recent studies have suggested that the presence of TILs is correlated with good outcome in patients with breast cancer.⁴⁻⁷ With advances in understanding of the role of the immune system during carcinogenesis and tumor progression, TILs have been recognized as important biomarkers reflecting anti-tumor immune response in several malignancies, such as epithelial ovarian carcinoma^{8,9} and endometrial cancer,¹⁰⁻¹⁴ as well as breast cancer.

Recent achievements in immune therapy such as adoptive T-cell therapy or dendritic cell therapy, which reactivate the anti-tumor immune response and immune check-points inhibiting monoclonal antibodies, have been applied in practice and have ameliorated outcomes in patients with advanced malignancies.¹⁵ Understanding the biology and clinical utilization of TILs might offer novel therapeutic options in management of breast cancer.

In this article, we review three issues of TILs in patients with breast cancer: (1) biology of TILs, (2) methodology defining TILs, and (3) clinical evidence of TILs as biomarkers with clinical utility.

THE BIOLOGY OF TUMOR-INFILTRATING LYMPHOCYTES IN BREAST CANCER

The components of TILs

Infiltrating immune cells are frequently observed in tumors, but the proportion of immune cells comprising the host immune system is diverse and depends on the type and organ sites of malignancies.¹⁶ Previous evidence from animal and clinical studies has shown that leukocyte subsets predominantly contribute to either tumor-suppressive or tumor-stimulating activities. In murine models, myeloid lineage leukocytes, such as dendritic cells, myeloid-derived suppressor cells, and tumor-associated macrophages, have been identified and are thought to principally act to modulate the immune microenvironment toward either an antitumor milieu or a tumor-promoting milieu. T cells that migrate to tumor and/or peritumor sites are activated or inactivated and, in turn, regulate macrophage differentiation via polarization toward pro-tumorigenic M2 or antitumor M1 functional phenotypes, suggesting the importance of cell-to-cell cross-talk in the immune milieu.¹⁷

Most TILs are T lymphocytes.¹⁸⁻²⁰ Tumor-infiltrating B lymphocytes are less common and are poorly defined.²¹ The composition of TILs has been well studied in two recent publications.¹⁹ These studies showed similar results that T lymphocytes constituted 75% of TILs, B lymphocytes made up fewer than 20%, monocytes constituted fewer than 10%, and natural killer and natural killer T cells made up fewer than 5% of all leukocytes.

To understand the role of T-lymphocyte-dominant TILs in antitumor response through adaptive immunity, it is necessary to understand the biologic characteristics and sub-classification of T cells. T cells, which are distinguished from other lymphocytes such as B cells and natural killer cells, have a T-cell receptor on the cell surface. There are several subgroups of T lymphocytes, each with a unique function. CD8+ T cells are known as cytotoxic T cells and destroy tumor cells by binding to antigen presented by MHC class I molecules, which are expressed on the membranes of all nucleated cells. These cytotoxic CD8+ T cells are regulated and can be inactivated by regulatory T cells (Treg), interleukin (IL) 10, and other cytokines, which prevent autoimmune diseases.

T helper cells (Th cells), which are also known as CD4+ T cells, mediate the immune response of other white blood cells. They assist in maturation of B cells into plasma cells and memory B cells and activate CD8+ T cells and macrophages. Th cells are activated when they come into contact with peptide antigens expressed by MHC class II molecules, which exist on the sur-

faces of antigen-presenting cells (APCs). This type of immune reaction is classified as type II immunity, which is distinguished from type I immunity, which is mainly conveyed by CD8+ T cells.²² When Th cells are activated, they undergo rapid division and release cytokines mediating the active immunologic reaction. According to signaling from APCs, Th cells differentiate into various types such as Th1, Th2, Th3, Th17, Th9, or tumor-infiltrated follicular helper (Tfh) and release different cytokines to promote various active immune reactions. Among Th cells, Treg cells develop either in the thymus or in peripheral lymphoid organs. Treg cells developed in a peripheral lymphoid organ regulate adaptive immune responses.²³ The expression of forkhead box P3 protein (FOXP3) is used to identify Treg cells.

Several studies have highlighted the importance of T cells and TILs in breast cancer. Regarding the prognostic effect of cytotoxic CD8+ T cells, it is evident that the presence of these cells is significantly associated with prolonged survival outcome^{5,24} and good response to chemotherapy.²⁵ The presence of CD8+ T cells is also associated with different subtypes of breast cancer. In a study with more than 1,200 breast cancer cases, high level of CD8+ T cells was found in the less aggressive subtypes, such as luminal cancer. In contrast, low level of CD8+ T cells was observed in HER2-positive or basal-like breast cancer.²⁶

In contrast to the studies with CD8+ T cells, the prognostic effect of CD4+ T cells in breast cancer is variously reported and remains inconclusive. Th1 cells, which are the primary sources of interferon- γ , were reported to correlate with favorable prognostic outcome,¹⁹ whereas Th2 cells were reported to counteract Th1 cells and attenuate the antitumor response based on analyses with immune-gene signatures.²⁷ A recent study defined the existence of Tfh cells and showed that an increase in CXCL13-producing Tfh cells in tertiary lymphoid structures adjacent to breast tumors is positively associated with treatment outcome and might modulate an effective and durable antitumor immune response.¹⁹ Th17 cells also contribute to the tumor microenvironment. Particularly, the balance between Th17 cells and IL-17 family, which have pro-inflammatory functions, has an important role in regulating tumor angiogenesis. The effect of Th17 cells near tumors seems to be variable depending on the cytokine milieu.²⁸ The antitumor or pro-tumor effect of Th17 cells might be different depending on the type of tumor.²⁸

Studies with CD4+ Treg cells expressing FOXP3 remain controversial because the presence of Treg cells has been associated with both immunosuppressive and immunostimulatory activity.^{18,29,30} The effects of Treg cells on prognosis differed according to immunohistochemistry (IHC) marker and type of CD4+ T

cells. Interestingly, the ratio of CD8+ to FOXP3+ is correlated with molecular subtype²⁶ and is characterized to define medullary cancer.³¹ Furthermore, a recent study showed that this ratio can be used to identify patients with good response to neoadjuvant chemotherapy in triple-negative breast cancer (TNBC).³²

Currently, little is known regarding the role of tumor-infiltrating B cells (CD20+) as components of TILs.^{33,34} Some authors have reported that increased expression of immunoglobulin κ C by B cells is associated with favorable prognosis of breast cancer according to the database of gene-expression profiling.³⁵

Factors affecting recruitment of TILs

There are several factors responsible for lymphocyte recruitment in tumors. High endothelial venules (HEV) interact with blood vessels and contribute to lymphocyte infiltration in breast cancer.³⁶ The high density of HEV is related to lymphotoxin- β produced by mature dendritic cells³⁷ and is associated with improved survival outcome in patients with breast cancer. It has been noted that HEV density is increased in ductal carcinoma *in situ* compared to invasive ductal carcinoma.

Indoleamine-2,3-dioxygenase (IDO), which catalyzes the conversion of tryptophan to kynurenine, is one of the enzymes affecting lymphocytic infiltration of tumors. Tryptophan depletion inhibits both tumor cells and lymphocytes, and kynurenine has cytotoxic activity against tumors.³⁸ Therefore, the catalytic activity of IDO might inhibit or stimulate both tumor growth and antitumor immune functions.³⁹

Factors affecting TIL count and recruitment of TILs have been studied. High TIL count has been observed in patients with TNBC.²⁵ The presence of TILs has been shown to inversely correlate with expression of human leukocyte antigen-G, which might be involved in tumor escape.⁴⁰ The TIL count has also been reported to be associated with expression of stem cell makers or epithelial-mesenchymal transition markers in cancer cells.²⁵

Stromal TILs and intratumoral TILs

Depending on lymphocyte-infiltrated site, TILs are classified as infiltrated lymphocytes in the tumor stroma (stromal TILs) or in the tumor cell islets (intratumoral TILs). Stromal TILs are defined as lymphocytes dispersed in the stroma and are distinguished from intratumoral TILs, which are located within carcinoma nests and are in direct contact with tumor cells.⁴¹ To date, most clinical trials have suggested that stromal TILs are likely to be more stable and reproducible markers than intratumoral TILs because of their increased frequency.

Efforts in methodological agreement in evaluation of TILs in breast cancer

There are many hurdles to utilizing TILs as prognostic or predictive markers because of their heterogeneity and the absence of standardized methods of evaluation. Moreover, the methodology based on IHC assessment of TILs demonstrates enormous variation in analytical practice and limits the value of TIL measurement to experimental research or specific studies. Consequently, TIL determination is not yet feasible in routine clinical practice and urgently demands a consensus in the development of a standardized measurement system.

The initial method for measuring TILs was proposed by Denkert *et al.* in 2010,⁴² which evaluated TILs in specimens from core biopsies. Since then, the majority of researchers investigating TILs have used that method, which has now been supported by robust findings. With this background, an International TIL Working Group was recently organized, and participants with experience in evaluation of TILs in specimens from phase III clinical trials were surveyed regarding topics in the methodology of TILs evaluation. Consequently, they reported current recommendations to reconcile the method of evaluating TILs (Table 1).⁴³

Clinical evidence of TILs in adjuvant or neoadjuvant studies

Major adjuvant or neoadjuvant studies testing TILs are presented in Tables 2 and 3.^{5,24,25,35,41,42,44-57} Most of these studies evaluated both stromal and intratumoral TILs. As described above, the measurement of stromal TILs is more reproducible among studies and has superior clinical value. Some studies have evaluated TILs using IHC, whereas others have identified the immune components of TILs based on databases of gene-expression profiling.

In 2010, the clinical significance of TILs as biomarkers associated with pathologic response was identified by Denkert *et al.*⁴² using samples from large clinical trials. This pivotal study was the first to evaluate TILs using the protocol of the International TIL Working Group. From that time, many researchers have focused on the association between presence of TILs and clinical outcome in various cohorts.

Among these translational studies with TILs in the adjuvant setting, the most important finding is the prognostic value of stromal TILs in TNBC. The positive correlation between increase of stromal TILs and survival outcome in TNBC was initially reported using data from the BIG 2-98 trial.⁴⁵ This correlation was validated in independent cohorts of two clinical trials.⁴⁶ Interestingly, the level of TILs was not prognostic in

Table 1. International TIL Working Group recommendations for assessing TILs in breast cancer

- 1) TILs should be reported for the stromal compartment (= % stromal TILs). The denominator used to determine the % stromal TILs is the area of stromal tissue (i.e., area occupied by mononuclear inflammatory cells over total intratumoral stromal area), not the number of stromal cells (i.e., fraction of total stromal nuclei that represent mononuclear inflammatory cell nuclei).
- 2) TILs should be evaluated within the borders of the invasive tumor.
- 3) Exclude TILs outside of the tumor border and around DCIS and normal lobules.
- 4) Exclude TILs in tumor zones with crush artifacts, necrosis, regressive hyalinization as well as in the previous core biopsy site.
- 5) All mononuclear cells (including lymphocytes and plasma cells) should be scored, but polymorphonuclear leukocytes are excluded.
- 6) One section (4–5 µm, magnification ×200–400) per patient is currently considered to be sufficient.
- 7) Full sections are preferred over biopsies whenever possible. Cores can be used in the pretherapeutic neoadjuvant setting; currently no validated methodology has been developed to score TILs after neoadjuvant treatment.
- 8) A full assessment of average TILs in the tumor area by the pathologist should be used. Do not focus on hotspots.
- 9) The working group's consensus is that TILs may provide more biological relevant information when scored as a continuous variable, since this will allow more accurate statistical analyses, which can later be categorized around different thresholds. However, in daily practice, most pathologists will rarely report for example 13.5% and will round up to the nearest 5%–10%, in this example thus 15%. Pathologist should report their scores in as much detail as the pathologist feels comfortable with.
- 10) TILs should be assessed as a continuous parameter. The percentage of stromal TILs is a semiquantitative parameter for this assessment, for example, 80% stromal TILs means that 80% of the stromal area shows a dense mononuclear infiltrate. For assessment of percentage values, the dissociated growth pattern of lymphocytes needs to be taken into account. Lymphocytes typically do not form solid cellular aggregates; therefore, the designation '100% stromal TILs' would still allow some empty tissue space between the individual lymphocytes.
- 11) No formal recommendation for a clinically relevant TIL threshold(s) can be given at this stage. The consensus was that a valid methodology is currently more important than issues of thresholds for clinical use, which will be determined once a solid methodology is in place. Lymphocyte predominant breast cancer can be used as a descriptive term for tumors that contain 'more lymphocytes than tumor cells'. However, the thresholds vary between 50% and 60% stromal lymphocytes.

Adopted from Salgado R, Denkert C, Demaria S, Sirtaine N, Klauschen F, Pruneri G, Wienert S, Van den Eynden G, Baehner FL, Penault-Llorca F, Perez EA, Thompson EA, Symmans WF, Richardson AL, Brock J, Criscitiello C, Bailey H, Ignatiadis M, Floris G, Sparano J, Kos Z, Nielsen T, Rimm DL, Allison KH, Reis-Filho JS, Loibl S, Sotiriou C, Viale G, Badve S, Adams S, Willard-Gallo K, Loi S. The evaluation of tumor infiltrating lymphocytes (TILs) in breast cancer: recommendations by an International TILs Working Group 2014. *Ann Oncol* 2015; 26: 259-71, with permission of Oxford University Press.⁴³
TIL, tumor-infiltrating lymphocytes; DCIS, ductal carcinoma *in-situ*.

patients with estrogen receptor (ER)-positive cancer receiving adjuvant chemotherapy. Consequently, these findings suggest that stromal TILs can be utilized as prognostic markers in a subset of breast cancer such as TNBC but not in ER-positive breast cancer. Despite the reproducibility of TILs as prognostic markers for patients with TNBC, TILs should not be used as predictive markers for chemotherapy response because of the absence of data from patients with TNBC not treated with chemotherapy.

The pronounced prognostic effect of TILs particularly in TNBC can be explained by the neoantigens described in the introduction because TNBC has higher mutational load than do non-TNBC tumors.⁵⁸ The higher mutational load of TNBC tumors enhances immunogenicity and might result in increased TIL recruiting.

Some studies have attempted to verify the prognostic significance of TILs in patients with HER2-positive breast cancer treated with adjuvant trastuzumab. Recent data from the FINHER study suggested that increased TILs are associated with better response to adjuvant trastuzumab. In the study, patients with TIL-predominant tumors showed a superior survival outcome compared to patients with non-TIL-predominant tumors after adjuvant trastuzumab.⁴ Recently published data from the N9831 study, which tested the benefit of trastuzumab in HER2-

positive breast cancer, also showed that patients with immunogenic tumors defined by mRNA expression of immune genes had improved survival in response to trastuzumab treatments.⁵⁹ However, there are major caveats to the results of the FINHER trial. The number of patients was small (n = 209), and the prognostic value of TILs was not confirmed in multivariate analysis. Moreover, based on the same samples from the N9831 study, Perez *et al.*⁵⁰ demonstrated conflicting results. In exploratory analyses of TIL evaluation, stromal TILs were associated with improved relapse-free survival in patients treated with chemotherapy alone but were not shown to be associated with recurrence-free survival in patients treated with chemotherapy plus trastuzumab.

Therefore, based on the current findings, the effect of TILs in mediating the response to adjuvant trastuzumab is not conclusive. Despite the controversy regarding the role of TILs in response to HER2-targeted therapy, previous studies have suggested that TILs mediate the antitumor response of trastuzumab and have the potential to be predictive markers of trastuzumab response.⁴

In addition to stromal TILs identified by hematoxylin and eosin exam, several studies have shown the prognostic value of CD8+ intratumoral TILs in adjuvant settings. Furthermore, genomic data might accelerate the discovery of immune markers or

Table 2. Adjuvant studies evaluating TILs and prognosis

Reference	Study	Manner of sample collection	Regimen	Assay	Marker	Type of TILs	Sample size	Correlation with clinical outcome (multivariate analysis)a
West <i>et al.</i> (2011) ⁴⁴	Single institute	Retrospective	CMF, AC, CEF, or CAF	TMA	CD3	CD3-IHC alone	255 for anthracyclines	CD3+ T cells: HR 0.24 for DFS (p = .016, univariate)
Mahmoud <i>et al.</i> (2011) ⁵	Single institute	Retrospective	CMF	TMA	CD8	Total TIL identified by CD8	1,334	CD8+ total TIL: HR 0.55 for BCSS in training set (p = .001) HR 0.58 for BCSS in validation set (p = .002)
Liu <i>et al.</i> (2012) ²⁴	Single institute	Retrospective	MF, AC, FAC, or no CTx	TMA	CD8	sTIL, iTIL, and total TIL	497 TNBC	CD8+ iTIL: HR 0.48 for BCSS (p < .001)
Loi <i>et al.</i> (2013) ⁴⁵	BIG 02-98	Prospective	A followed by CMF or AC followed by CMF	H&E	TILs	sTIL iTIL	2,009 Total 256 TNBC	None sTIL (continuous): HR 0.83 for OS (p = .023) LPBC (binary ≥ 50%): HR 0.29 for OS (p = .036)
Adams <i>et al.</i> (2014) ⁴⁶	ECOG2197 ECOG1199	Prospective	AC vs AC AC followed by D or P	H&E	TILs	sTIL iTIL	481 TNBC	sTIL (continuous, per 10% increase): HR 0.79 for OS (p = .003)
Liu <i>et al.</i> (2014) ⁴⁷	FINHER	Prospective	D or V followed by FEC or FEC with trastuzumab if HER2+	H&E	TILs	sTIL iTIL	934 Total 134 TNBC 209 HER2+	None sTIL (continuous): HR 0.77 for DDFS (p = .02) sTIL (continuous): HR 0.82 of DDPS (p = .025, univariate) only for trastuzumab arm
Ali <i>et al.</i> (2014) ⁴⁸	Four cohorts including NEAT trial	Retrospective	Various regimen	TMA	CD8	sTIL and iTIL identified by CD8	12,439	CD8+ iTIL: HR 0.72 for BCSS (p = .00003) CD8+ sTIL: HR 0.79 for BCSS (p = .004)
Liu <i>et al.</i> (2012) ²⁴	Single institute	Retrospective	MF, AC, FAC, or no CTx	TMA	CD8, FOXP3	sTIL, iTIL, and total TIL	88 ER-/HER2+ with CD8+TIL-positive	FOXP3+ iTIL: HR 0.48 for BCSS (p = .047)
Schalper <i>et al.</i> (2014) ⁴⁹	Single institute	Retrospective	Various regimen	mRNA assay H&E	PD-L1 mRNA TILs	Nonspecific TILs	328	Positive PD-L1 mRNA expression: HR 0.27 for RFS (p = .009)
Perez <i>et al.</i> ⁵⁰ (abstract only)	N9831 arm A and C	Prospective	AC followed by P or P with trastuzumab	H&E	TILs	sTIL	489 Treated without trastuzumab 456 Treated with trastuzumab	LPBC (binary ≥ 60%): HR 0.20 for RFS (p = .007) LPBC (binary ≥ 60%): HR 1.1 for RFS (p = .87)

TIL, tumor-infiltrating lymphocyte; CMF, cyclophosphamide, methotrexate, 5-fluorouracil; AC, doxorubicin/cyclophosphamide; CEF, Canadian cyclophosphamide, epirubicin, 5-fluorouracil; CAF, cyclophosphamide, doxorubicin, 5-fluorouracil; TMA, tissue microarray; IHC, immunohistochemistry; HR, hazard ratio; DFS, disease-free survival; BCSS, breast cancer specific survival; MF, methotrexate, 5-fluorouracil; FAC, 5-fluorouracil, doxorubicin, cyclophosphamide; CTx, chemotherapy; sTIL, stromal tumor-infiltrating lymphocyte; iTIL, intratumoral tumor-infiltrating lymphocyte; TNBC, triple-negative breast cancer; H&E, hematoxylin and eosin; OS, overall survival; LPBC, lymphocyte predominant breast cancer; D, docetaxel; P, paclitaxel; V, vinorelbine; FEC, 5-fluorouracil, epirubicin, cyclophosphamide; HER2, human epidermal growth factor receptor 2; DDPS, distant disease-free survival; DDPS, distant disease relapse-free survival; FOXP3, forkhead box P3 protein; ER, estrogen receptor; RFS, recurrence-free survival.

Table 3. The association between TILs and pathologic response in neoadjuvant studies

Reference	Study	Manner of sample collection	Regimen	Assay	Marker	Type of TILs	Sample size	Definition of pCR	Correlation with pCR
Hornychova et al. (2008) ⁴¹	Single institute	Retrospective	Anthracycline-taxane-based regimens	IHC	CD3	iTIL	73	ypT0/Tis ypN0	CD3+iTIL (p = .004, univariate)
Denkert et al. (2010) ⁴²	GeparDuo GeparTrio	Prospective	EC-Doc (GeparDuo) TAC ± vinorelbine/ capecitabine (GeparTrio)	H&E	TILs	sTIL iTIL	1,058	ypT0/Tis ypN0	sTILs (continuous, per 10% increase) (p = .001, multivariate) LPBC (binary ≥60%) (p = .001, multivariate)
Denkert et al. (2015) ⁵¹	Geparsixto	Prospective	Anthracycline-taxane plus carboplatin vs Anthracycline-taxane	H&E mRNA assay	TILs 12 immune mRNA markers	sTIL iTIL	580 481	ypT0/Tis ypN0	sTILs (continuous, per 10% increase) (p = .001, multivariate) 12 immune mRNA markers were predictive for increased pCR
West et al. (2011) ⁴⁴	Public gene expression data from EORTC 10994/BIG00-01	Prospective	FEC vs TET	Gene expression data	Gene expression data	Not associated	99	Undefined	High TIL signature correlate with pCR (p = .001, multivariate)
Ono et al. (2012) ⁵²	Single institute	Retrospective	Anthracycline-based; cyclophosphamide-based or taxane-based regimens	H&E	TILs	sTIL iTIL	92 TNBC	ypT0	Total TILs correlate with pCR (p = .015, multivariate)
Yamaguchi et al. (2012) ⁵³	Single institute	Retrospective	Anthracycline-taxane-based regimens	H&E	TILs	Total TILs	68	ypT0/Tis	Total TILs correlate with pCR (p < .001, multivariate)
Oda et al. (2012) ⁵⁴	Institutional	Retrospective	Paclitaxel followed by FEC	IHC	CD8, FOXP3, IL17F	iTIL	180	ypT0ypN0	FOXP3 positively correlated with pCR (p = .014, multivariate)
Schmidt et al. (2012) ³⁵	Public gene expression data (7 cohorts)	Retrospective	Anthracycline-based regimen	Gene expression data	Gene expression data	Not associated	845	Undefined	IGKC positively correlated with pCR (p < .001)
Issa-Nummer et al. (2013) ⁵⁵	GeparQuinto Predict study	EC-D	EC followed by D	H&E	TILs	sTIL iTIL	313 HER2-	ypT0ypN0	sTILs and LPBC associated with pCR (p = .01, multivariate) LPBC associated with pCR (p = .003, multivariate)
Seo et al. (2013) ²⁵	Single institute	Retrospective	Anthracycline-taxane-based regimens	IHC	CD8, CD4, FOXP3	iTILs	153	ypT0ypN0	CD8 positively correlated with pCR (p = .003, multivariate)
Lee et al. (2013) ⁵⁶	Single institute	Retrospective	Anthracycline-taxane-based regimens	H&E IHC	TILs, CD3, CD8, FOXP3	sTILs	175	ypT0ypN0	sTIL positively correlated with pCR (p = .024, multivariate)
Nabholz et al. (2014) ⁵⁷	Phase II TVA study	Prospective	FEC with/without D with panitumumab	IHC	CD8	Not associated	47	ypT0/Tis ypN0	CD8 positively correlated with pCR (p = .000003, univariate)

CD8 positively correlated with pCR (p = .000003, univariate).
 TIL, tumor-infiltrating lymphocyte; pCR, pathological complete response; IHC, immunohistochemistry; iTIL, intratumoral tumor-infiltrating lymphocyte; H&E, hematoxylin and eosin; sTIL, stromal tumor-infiltrating lymphocyte; LPBC, lymphocyte predominant breast cancer; FEC, 5-fluorouracil, epirubicin, cyclophosphamide; TEI, docetaxel, epirubicin and docetaxel; TNBC, triple-negative breast cancer; IL, interleukin; IGKC, gene encoding for immunoglobulin kappa constant; D, docetaxel; HER2, human epidermal growth factor receptor 2; FOXP3, forkhead box P3 protein.

immune signatures associated with TILs or treatment outcome.

TILs have been evaluated in the samples of core biopsies from more than 3,000 patients receiving neoadjuvant chemotherapy. These studies used clinical information from prospective trials, as well as from single institutional cohorts. In an early study of a cohort of limited size, the numbers of intratumoral TILs detected by CD3 expression were significantly higher in patients with pathological complete response (pCR).⁴¹ Patients who achieved pCR also had significantly higher dendritic cell (CD83+) counts in specimens of core biopsies. The potential of TILs as biomarkers predicting pCR was independently confirmed using much larger cohorts of patients enrolled in the GeparDuo and GeparTrio trials. These studies showed that the percentage of intratumoral TILs is an independent predictor of pCR.⁴² The studies investigating the role of TILs in patients undergoing neoadjuvant chemotherapy are summarized in Table 3. In summary, data of both histologically assessed TILs and molecular genetic signatures indicate that increased immune markers are related to higher pCR rates independent of other clinico-pathological factors or type of chemotherapy. A recent meta-analysis of TILs in neoadjuvant studies also supported the hypothesis that higher TIL level is associated with higher pCR rate.⁶⁰

CONCLUSION

Accumulating preclinical and clinical evidence supports the use of TILs as predictive and prognostic markers in breast cancer. However, it is essential to establish a standard definition of TILs and to develop a consensus for morphological evaluation of TILs before they can be applied in routine clinical practice. The heterogeneity of types and functions of lymphocytes and activating mechanisms demands molecular and functional characterization of TILs in order to improve their value. The incorporation of other biomarkers in breast cancer, such as the remaining hurdle with interobserver variability in determination of Ki-67, suggests that a biomarker cannot be widely applied in daily practice until a standardized approach has been validated in multiple studies including prospective trials. Further scientific research with TILs will offer unique insights and information on the role of the immune systems in malignancy and in treatment response.

Conflicts of Interest

No potential conflict of interest relevant to this article was reported.

REFERENCES

1. Heemskerk B, Kvistborg P, Schumacher TN. The cancer antigenome. *EMBO J* 2013; 32: 194-203.
2. Schumacher TN, Schreiber RD. Neoantigens in cancer immunotherapy. *Science* 2015; 348: 69-74.
3. Alexandrov LB, Nik-Zainal S, Wedge DC, *et al.* Signatures of mutational processes in human cancer. *Nature* 2013; 500: 415-21.
4. Loi S, Michiels S, Salgado R, *et al.* Tumor infiltrating lymphocytes are prognostic in triple negative breast cancer and predictive for trastuzumab benefit in early breast cancer: results from the FinHER trial. *Ann Oncol* 2014; 25: 1544-50.
5. Mahmoud SM, Paish EC, Powe DG, *et al.* Tumor-infiltrating CD8+ lymphocytes predict clinical outcome in breast cancer. *J Clin Oncol* 2011; 29: 1949-55.
6. Menard S, Tomasic G, Casalini P, *et al.* Lymphoid infiltration as a prognostic variable for early-onset breast carcinomas. *Clin Cancer Res* 1997; 3: 817-9.
7. Mohammed ZM, Going JJ, Edwards J, Elsberger B, Doughty JC, McMillan DC. The relationship between components of tumour inflammatory cell infiltrate and clinicopathological factors and survival in patients with primary operable invasive ductal breast cancer. *Br J Cancer* 2012; 107: 864-73.
8. Tomsova M, Melichar B, Sedlakova I, Steiner I. Prognostic significance of CD3+ tumor-infiltrating lymphocytes in ovarian carcinoma. *Gynecol Oncol* 2008; 108: 415-20.
9. Zhang L, Conejo-Garcia JR, Katsaros D, *et al.* Intratumoral T cells, recurrence, and survival in epithelial ovarian cancer. *N Engl J Med* 2003; 348: 203-13.
10. de Jong RA, Leffers N, Boezen HM, *et al.* Presence of tumor-infiltrating lymphocytes is an independent prognostic factor in type I and II endometrial cancer. *Gynecol Oncol* 2009; 114: 105-10.
11. Giatromanolaki A, Bates GJ, Koukourakis MI, *et al.* The presence of tumor-infiltrating FOXP3+ lymphocytes correlates with intratumoral angiogenesis in endometrial cancer. *Gynecol Oncol* 2008; 110: 216-21.
12. Ino K, Yamamoto E, Shibata K, *et al.* Inverse correlation between tumoral indoleamine 2,3-dioxygenase expression and tumor-infiltrating lymphocytes in endometrial cancer: its association with disease progression and survival. *Clin Cancer Res* 2008; 14: 2310-7.
13. Kondratiev S, Sabo E, Yakirevich E, Lavie O, Resnick MB. Intratumoral CD8+ T lymphocytes as a prognostic factor of survival in endometrial carcinoma. *Clin Cancer Res* 2004; 10: 4450-6.
14. Yamagami W, Susumu N, Tanaka H, *et al.* Immunofluorescence-detected infiltration of CD4+FOXP3+ regulatory T cells is relevant to the prognosis of patients with endometrial cancer. *Int J Gynecol*

- Cancer 2011; 21: 1628-34.
15. Taube JM, Klein A, Brahmer JR, *et al.* Association of PD-1, PD-1 ligands, and other features of the tumor immune microenvironment with response to anti-PD-1 therapy. *Clin Cancer Res* 2014; 20: 5064-74.
 16. Galon J, Angell HK, Bedognetti D, Marincola FM. The continuum of cancer immunosurveillance: prognostic, predictive, and mechanistic signatures. *Immunity* 2013; 39: 11-26.
 17. Coussens LM, Pollard JW. Leukocytes in mammary development and cancer. *Cold Spring Harb Perspect Biol* 2011; 3: a003285.
 18. Gobert M, Treilleux I, Bendriss-Vermare N, *et al.* Regulatory T cells recruited through CCL22/CCR4 are selectively activated in lymphoid infiltrates surrounding primary breast tumors and lead to an adverse clinical outcome. *Cancer Res* 2009; 69: 2000-9.
 19. Gu-Trantien C, Loi S, Garaud S, *et al.* CD4(+) follicular helper T cell infiltration predicts breast cancer survival. *J Clin Invest* 2013; 123: 2873-92.
 20. Ruffell B, Au A, Rugo HS, Esserman LJ, Hwang ES, Coussens LM. Leukocyte composition of human breast cancer. *Proc Natl Acad Sci U S A* 2012; 109: 2796-801.
 21. Cimino-Mathews A, Ye X, Meeker A, Argani P, Emens LA. Metastatic triple-negative breast cancers at first relapse have fewer tumor-infiltrating lymphocytes than their matched primary breast tumors: a pilot study. *Hum Pathol* 2013; 44: 2055-63.
 22. Gutcher I, Becher B. APC-derived cytokines and T cell polarization in autoimmune inflammation. *J Clin Invest* 2007; 117: 1119-27.
 23. Abbas AK, Benoist C, Bluestone JA, *et al.* Regulatory T cells: recommendations to simplify the nomenclature. *Nat Immunol* 2013; 14: 307-8.
 24. Liu S, Lachapelle J, Leung S, Gao D, Foulkes WD, Nielsen TO. CD8+ lymphocyte infiltration is an independent favorable prognostic indicator in basal-like breast cancer. *Breast Cancer Res* 2012; 14: R48.
 25. Seo AN, Lee HJ, Kim EJ, *et al.* Tumour-infiltrating CD8+ lymphocytes as an independent predictive factor for pathological complete response to primary systemic therapy in breast cancer. *Br J Cancer* 2013; 109: 2705-13.
 26. Liu F, Lang R, Zhao J, *et al.* CD8(+) cytotoxic T cell and FOXP3(+) regulatory T cell infiltration in relation to breast cancer survival and molecular subtypes. *Breast Cancer Res Treat* 2011; 130: 645-55.
 27. Teschendorff AE, Gomez S, Arenas A, *et al.* Improved prognostic classification of breast cancer defined by antagonistic activation patterns of immune response pathway modules. *BMC Cancer* 2010; 10: 604.
 28. Qi W, Huang X, Wang J. Correlation between Th17 cells and tumor microenvironment. *Cell Immunol* 2013; 285: 18-22.
 29. Bates GJ, Fox SB, Han C, *et al.* Quantification of regulatory T cells enables the identification of high-risk breast cancer patients and those at risk of late relapse. *J Clin Oncol* 2006; 24: 5373-80.
 30. West NR, Kost SE, Martin SD, *et al.* Tumour-infiltrating FOXP3(+) lymphocytes are associated with cytotoxic immune responses and good clinical outcome in oestrogen receptor-negative breast cancer. *Br J Cancer* 2013; 108: 155-62.
 31. Anz D, Eiber S, Scholz C, *et al.* In breast cancer, a high ratio of tumour-infiltrating intraepithelial CD8+ to FoxP3+ cells is characteristic for the medullary subtype. *Histopathology* 2011; 59: 965-74.
 32. Miyashita M, Sasano H, Tamaki K, *et al.* Tumor-infiltrating CD8+ and FOXP3+ lymphocytes in triple-negative breast cancer: its correlation with pathological complete response to neoadjuvant chemotherapy. *Breast Cancer Res Treat* 2014; 148: 525-34.
 33. An T, Sood U, Pietruk T, Cummings G, Hashimoto K, Crissman JD. *In situ* quantitation of inflammatory mononuclear cells in ductal infiltrating breast carcinoma: relation to prognostic parameters. *Am J Pathol* 1987; 128: 52-60.
 34. Mahmoud SM, Lee AH, Paish EC, Macmillan RD, Ellis IO, Green AR. The prognostic significance of B lymphocytes in invasive carcinoma of the breast. *Breast Cancer Res Treat* 2012; 132: 545-53.
 35. Schmidt M, Hellwig B, Hammad S, *et al.* A comprehensive analysis of human gene expression profiles identifies stromal immunoglobulin kappa C as a compatible prognostic marker in human solid tumors. *Clin Cancer Res* 2012; 18: 2695-703.
 36. Martinet L, Garrido I, Filleron T, *et al.* Human solid tumors contain high endothelial venules: association with T- and B-lymphocyte infiltration and favorable prognosis in breast cancer. *Cancer Res* 2011; 71: 5678-87.
 37. Martinet L, Filleron T, Le Guellec S, Rochemaux P, Garrido I, Girard JP. High endothelial venule blood vessels for tumor-infiltrating lymphocytes are associated with lymphotoxin beta-producing dendritic cells in human breast cancer. *J Immunol* 2013; 191: 2001-8.
 38. Melichar B, Ferrandina G, Verschraegen CF, Loercher A, Abbruzzese JL, Freedman RS. Growth inhibitory effects of aromatic fatty acids on ovarian tumor cell lines. *Clin Cancer Res* 1998; 4: 3069-76.
 39. Jacquemier J, Bertucci F, Finetti P, *et al.* High expression of indoleamine 2,3-dioxygenase in the tumour is associated with medullary features and favourable outcome in basal-like breast carcinoma. *Int J Cancer* 2012; 130: 96-104.
 40. Dong DD, Yie SM, Li K, *et al.* Importance of HLA-G expression and tumor infiltrating lymphocytes in molecular subtypes of breast cancer. *Hum Immunol* 2012; 73: 998-1004.
 41. Hornychova H, Melichar B, Tomsova M, Mergancova J, Urminska H, Ryska A. Tumor-infiltrating lymphocytes predict response to neoadjuvant chemotherapy in patients with breast carcinoma. *Cancer Invest* 2008; 26: 1024-31.

42. Denkert C, Loibl S, Noske A, *et al.* Tumor-associated lymphocytes as an independent predictor of response to neoadjuvant chemotherapy in breast cancer. *J Clin Oncol* 2010; 28: 105-13.
43. Salgado R, Denkert C, Demaria S, *et al.* The evaluation of tumor-infiltrating lymphocytes (TILs) in breast cancer: recommendations by an International TILs Working Group 2014. *Ann Oncol* 2015; 26: 259-71.
44. West NR, Milne K, Truong PT, Macpherson N, Nelson BH, Watson PH. Tumor-infiltrating lymphocytes predict response to anthracycline-based chemotherapy in estrogen receptor-negative breast cancer. *Breast Cancer Res* 2011; 13: R126.
45. Loi S, Sirtaine N, Piette F, *et al.* Prognostic and predictive value of tumor-infiltrating lymphocytes in a phase III randomized adjuvant breast cancer trial in node-positive breast cancer comparing the addition of docetaxel to doxorubicin with doxorubicin-based chemotherapy: BIG 02-98. *J Clin Oncol* 2013; 31: 860-7.
46. Adams S, Gray RJ, Demaria S, *et al.* Prognostic value of tumor-infiltrating lymphocytes in triple-negative breast cancers from two phase III randomized adjuvant breast cancer trials: ECOG 2197 and ECOG 1199. *J Clin Oncol* 2014; 32: 2959-66.
47. Liu S, Foulkes WD, Leung S, *et al.* Prognostic significance of FOXP3+ tumor-infiltrating lymphocytes in breast cancer depends on estrogen receptor and human epidermal growth factor receptor-2 expression status and concurrent cytotoxic T-cell infiltration. *Breast Cancer Res* 2014; 16: 432.
48. Ali HR, Provenzano E, Dawson SJ, *et al.* Association between CD8+ T-cell infiltration and breast cancer survival in 12,439 patients. *Ann Oncol* 2014; 25: 1536-43.
49. Schalper KA, Velcheti V, Carvajal D, *et al.* *In situ* tumor PD-L1 mRNA expression is associated with increased TILs and better outcome in breast carcinomas. *Clin Cancer Res* 2014; 20: 2773-82.
50. Perez EA, Ballman KV, Anderson SK, *et al.* Stromal tumor-infiltrating lymphocytes (S-TILs): in the alliance N9831 trial S-TILs are associated with chemotherapy benefit but not associated with trastuzumab benefit. In: San Antonio Breast Cancer Symposium (SABCS); 2014 Dec 2; Redwood, CA, USA; Abstract S1-06.
51. Denkert C, von Minckwitz G, Brase JC, *et al.* Tumor-infiltrating lymphocytes and response to neoadjuvant chemotherapy with or without carboplatin in human epidermal growth factor receptor 2-positive and triple-negative primary breast cancers. *J Clin Oncol* 2015; 33: 983-91.
52. Ono M, Tsuda H, Shimizu C, *et al.* Tumor-infiltrating lymphocytes are correlated with response to neoadjuvant chemotherapy in triple-negative breast cancer. *Breast Cancer Res Treat* 2012; 132: 793-805.
53. Yamaguchi R, Tanaka M, Yano A, *et al.* Tumor-infiltrating lymphocytes are important pathologic predictors for neoadjuvant chemotherapy in patients with breast cancer. *Hum Pathol* 2012; 43: 1688-94.
54. Oda N, Shimazu K, Naoi Y, *et al.* Intratumoral regulatory T cells as an independent predictive factor for pathological complete response to neoadjuvant paclitaxel followed by 5-FU/epirubicin/cyclophosphamide in breast cancer patients. *Breast Cancer Res Treat* 2012; 136: 107-16.
55. Issa-Nummer Y, Darb-Esfahani S, Loibl S, *et al.* Prospective validation of immunological infiltrate for prediction of response to neoadjuvant chemotherapy in HER2-negative breast cancer—a substudy of the neoadjuvant GeparQuinto trial. *PLoS One* 2013; 8: e79775.
56. Lee HJ, Seo JY, Ahn JH, Ahn SH, Gong G. Tumor-associated lymphocytes predict response to neoadjuvant chemotherapy in breast cancer patients. *J Breast Cancer* 2013; 16: 32-9.
57. Nabholz JM, Abrial C, Mouret-Reynier MA, *et al.* Multicentric neoadjuvant phase II study of panitumumab combined with an anthracycline/taxane-based chemotherapy in operable triple-negative breast cancer: identification of biologically defined signatures predicting treatment impact. *Ann Oncol* 2014; 25: 1570-7.
58. Shah SP, Roth A, Goya R, *et al.* The clonal and mutational evolution spectrum of primary triple-negative breast cancers. *Nature* 2012; 486: 395-9.
59. Perez EA, Thompson EA, Ballman KV, *et al.* Genomic analysis reveals that immune function genes are strongly linked to clinical outcome in the North Central Cancer Treatment Group n9831 Adjuvant Trastuzumab Trial. *J Clin Oncol* 2015; 33: 701-8.
60. Mao Y, Qu Q, Zhang Y, Liu J, Chen X, Shen K. The value of tumor infiltrating lymphocytes (TILs) for predicting response to neoadjuvant chemotherapy in breast cancer: a systematic review and meta-analysis. *PLoS One* 2014; 9: e115103.

Cytology Specimen Management, Triage and Standardized Reporting of Fine Needle Aspiration Biopsies of the Pancreas

Won Jae Yoon
Martha Bishop Pitman^{1,2}

Department of Internal Medicine, Inje University Seoul Paik Hospital, Inje University College of Medicine, Seoul, Korea; ¹Department of Pathology, Massachusetts General Hospital, Boston, MA; ²Harvard Medical School, Boston, MA, USA

Received: July 16, 2015
Accepted: July 19, 2015

Corresponding Author

Martha Bishop Pitman, MD
Department of Pathology, Massachusetts General Hospital, 55 Fruit Street, Boston, MA 02114, USA
Tel: +1-617-726-3185
Fax: +1-617-724-6564
E-mail: mpitman@mgh.harvard.edu

The recent advances in pancreas cytology specimen sampling methods have enabled a specific cytologic diagnosis in most cases. Proper triage and processing of the cytologic specimen is pivotal in making a diagnosis due to the need for ancillary testing in addition to cytological evaluation, which is especially true in the diagnosis of pancreatic cysts. Newly proposed terminology for pancreaticobiliary cytology offers a standardized language for reporting that aims to improve communication among patient caregivers and provide for increased flexibility in patient management. This review focuses on these updates in pancreas cytology for the optimal evaluation of solid and cystic lesions of the pancreas.

Key Words: Pancreas; Cytology; Biopsy, fine-needle; Triage; Terminology

The advances in techniques of pancreas cytology specimen sampling have improved the yield of specimen for diagnosis in various pancreatic diseases. Proper triage and processing of specimens that maximizes the use of the aspirated specimen or cyst fluid for ancillary testing are pivotal in making a specific diagnosis, or in some cases, a sufficiently specific diagnosis, which when combined with the clinical and imaging characteristics of the case, allow for proper patient management. Recently proposed terminology for pancreaticobiliary cytology aims to standardize the language of reporting to improve communication among the patient's caregivers as well as to provide for increasingly conservative patient management options.¹

CLINICAL INDICATIONS FOR SAMPLING

Pancreas cytology specimen sampling is indicated when the information obtained by specimen sampling has the potential to affect the patient management. This includes (1) differentiating benign from malignant lesions; (2) staging of cancer; and (3) diagnosis of malignancy before chemotherapy and/or radiation therapy.^{2,3}

TECHNIQUES OF CYTOLOGY SPECIMEN SAMPLING

Techniques of pancreas cytology specimen sampling include percutaneous computed tomography- or ultrasound-guided fine needle aspiration (FNA), endoscopic retrograde cholangiopancreatography (ERCP)-guided brush cytology of the pancreatic duct, and the distal common bile duct, and endoscopic ultrasound-guided FNA (EUS-FNA).⁴ ERCP-guided specimen sampling is rarely used, as the yield of exfoliative cytology from the aspirated pancreatic juice is low, and the risk of pancreatitis from ductal brushing is significant.⁴ Compared to EUS-FNA, percutaneous FNA suffers from lower diagnostic yield in pancreatic tumors with diameter less than 3 cm,⁵ and is suggested to have higher complication rates.⁶ Currently, EUS-FNA is considered to be the first-line technique when sampling of a suspected pancreatic cancer is indicated.⁷

EUS-FNA of solid pancreatic lesions is performed using linear echoendoscopes. Doppler imaging is used to identify and avoid blood vessels when passing the needle into the lesion.⁸ Lesions in the head/uncinate process of the pancreas are accessed via trans-

duodenal approach; lesions in the body or the tail of the pancreas are accessed via a transgastric route.⁴ Selection of appropriate EUS needles is based on the vascularity of the target lesion, difficulty in accessing the lesion, and the type of specimen needed for the diagnosis.⁴ For cytology, simple aspiration needles of 22- or 25-gauge are used.⁹ A recent meta-analysis concluded that the EUS-FNA using 25-gauge needles are more sensitive than that using 22-gauge needles for diagnosis of pancreatic malignancy.¹⁰ Histologic samples may be obtained by standard 19-gauge and 22-gauge FNA needles. Recently, 19-gauge and 22-gauge core biopsy needles have become available.¹¹ Core needle biopsies are often critical in procuring sufficient tissue for a specific diagnosis, which is especially true for diseases dependent on some tissue architecture such as autoimmune pancreatitis, or morphologically similar tumors distinguished by immunohistochemical studies such as neuroendocrine neoplasms, acinar cell carcinoma and solid-pseudopapillary neoplasms.¹²

When the lesion is identified, the needle, occluded by a stylet, is placed into the target lesion with one quick thrust. Once the lesion is placed into the solid lesion, the stylet is removed, and the needle is moved to and fro within the lesion with or without application of suction.⁴ Use of a stylet is very important as it minimizes gastrointestinal contamination of the specimen which can cause significant diagnostic difficulty.¹³ Using fanning technique during needle handling enables sampling from multiple areas within the lesion and increases the yield of cytology.¹⁴ Multiple needle passes are usually needed for diagnosis.¹⁵

After each needle pass in EUS-FNA of solid masses, the procured material is expelled onto glass slides. Core particles are placed in formalin solution. Smears are prepared on glass slides and fixed in ethanol, or air-dried. In the case of EUS-FNA of pancreatic cystic lesions, the procedure is similar to that of solid pancreatic lesions except that direct smears are not made. All fluid should be aspirated using suction with one needle pass,¹⁶ and any solid component separately aspirated. Direct smears should be made of this aspirate, which could be evaluated on-site if so desired. Antibiotics are used to minimize the risk of cyst infection.¹⁷

Tumor cell seeding following EUS-FNA has been reported anecdotally, but relative to the number of biopsies performed, the rate is very low. Seeding of neoplastic mucinous cysts is of particular concern in Asian countries; however, a recent study has shown that there is no difference in peritoneal seeding or pseudomyxoma peritonei in patients who did and did not have EUS-FNA prior to resection.¹⁸

SPECIMEN TRIAGE AND PROCESSING

Specimen aspirated from the pancreas can be prepared using direct smears, cytopins (Thermo-Shandon Instruments, Asheville, NC, USA), liquid based preparations—ThinPrep (Hologic Corporation, Marlborough, MA, USA) or SurePath Prep (Becton-Dickinson, Burlington, NC, USA), and as formalin-fixed paraffin-embedded tissue (cellblocks and core biopsies). The preparation technique used will depend on the type of lesion, and the preferences of the laboratory and pathologists assessing the samples. In order to perform a rapid on-site evaluation (ROSE) at the time of biopsy, direct smears will have to be made.

RAPID ON-SITE EVALUATION

The purpose of ROSE is to ensure that the FNA is adequately cellular for diagnosis and that the tissue aspirated is appropriately prepared and triaged for diagnosis. ROSE has been shown to be beneficial for solid mass lesions of the pancreas,¹⁹⁻²² but since ROSE does not direct repeat biopsies of a cystic lesion, and the aspirated cyst fluid is usually so scant, ROSE is not recommended for cystic lesions that produce liquid cystic fluid. If the cyst has a solid component, it is separately sampled with direct smears made for cytological analysis.

PROCESSING OF ASPIRATES FROM SOLID MASSES

The best method of processing specimen from FNAs of solid masses is with direct smears, as long as good direct smears can be made (see below). Processing specimen for cellblock preparation is recommended even if core biopsies are also planned as not all core biopsies are representative. Specimen in paraffin provides small tissue fragments for cytohistological evaluation and provides readily accessible tissue for immunohistochemical and molecular studies, which may be essential for an accurate and specific diagnosis. A dedicated biopsy pass can be triaged for microbiologic cultures, electron microscopy, and flow cytometric analysis.¹²

Direct smears

Direct smears are made from aspirates that is solid enough to be smeared, which may include some aspirates from thick cyst contents. Direct smears may be air-dried or fixed with an alcohol based fixative. Air-dried smears are stained with a Romanowsky stain, such as Diff-Quik, which provides details of the cy-

toplasmic features and background mesenchymal elements. Fixed smears are stained with either a standard Papanicolaou stain or hematoxylin and eosin stain, which provides nuclear details. Regardless of the stain used, all require good quality smears for accurate interpretation. The person responsible for making the smears should have proper training.

Prior to expressing the aspirate onto slides to make the direct smears, the outside of the needle should be wiped clean of contaminating cells and mucus from the gastrointestinal tract. Aspirated specimen should be spread across the slide in a relatively thin layer with an even distribution, and without crush, air-drying or obscuring artifact. A poorly prepared smear may not be interpretable, or worse, may lead to a false-positive or false-negative interpretation. Critical to an optimal smear is to remove needle casts of clotted specimen from the slides, which are expressed as “worms” of clotted specimen and which may contain valuable specimen (Fig. 1). All such specimen clots should be gently lifted from the glass slide with the tip of a needle and placed in formalin for cellblock preparation.

Liquid based preparations

The two most common liquid based cytology (LBC) methods include ThinPrep (Hologic Inc., Marlborough, MA, USA) and SurePath (Becton-Dickinson, Burlington, NC, USA). The proprietary alcohol-based fixatives (Cytolyt [Hologic Corp., Marlborough, MA, USA] for ThinPrep and Cytorich Red [Becton-Dickinson, Burlington, NC, USA] for SurePath) reduce the potentially obscuring background elements such as blood and inflammation. Extracellular mucin, however, will be diluted and attenuated making morphological interpretation challenging. For this reason as well as the inability to perform biochemical

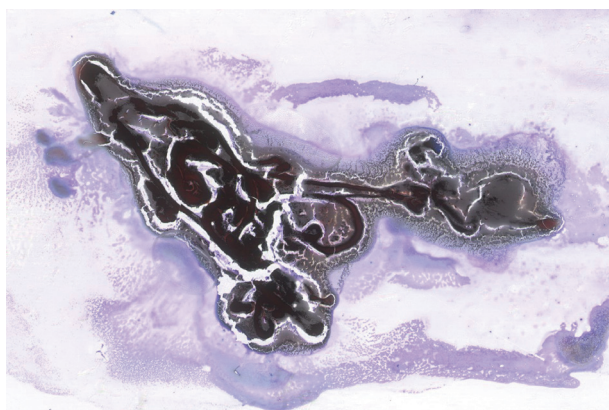


Fig. 1. Needle casts of blood clot expressed onto a glass slide should be placed in formalin for cellblock processing. Tissue entrapped in blood clot is not evaluable on cytology.

testing, LBC is not recommended for cyst fluids. For solid masses, however, a liquid-based preparation is far more desirable than poorly prepared direct smears with artifact.

Formalin-fixed paraffin embedded specimen

Needle rinsings after expression of the aspirate on the slide coupled with a dedicated biopsy for rinsing only, often provide specimen for cellblock preparation. The cellular content of needle rinsing fluid is spun down into a cell button, which is then fixed in formalin and processed as a routine histology specimen (Fig. 2).

There are different methods of agglutinating the cells. A common method is the plasma-thrombin clot method using outdat-

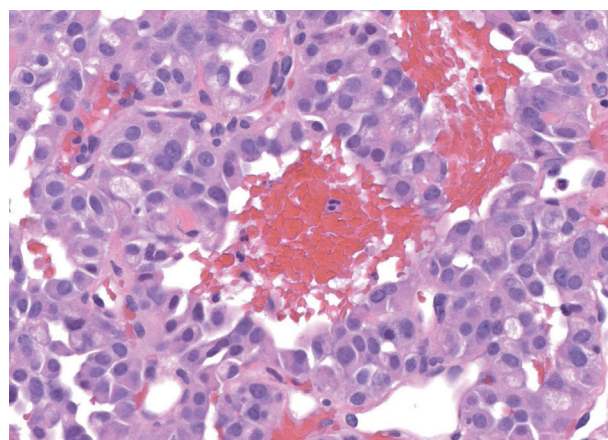


Fig. 2. Tissue fragments from needle rinsings or clotted tissue worms as illustrated in Fig. 1 should be processed as a cellblock, which provides readily available tissue for ancillary testing. This example of a well-differentiated neuroendocrine tumor resembles a solid-pseudopapillary neoplasm.

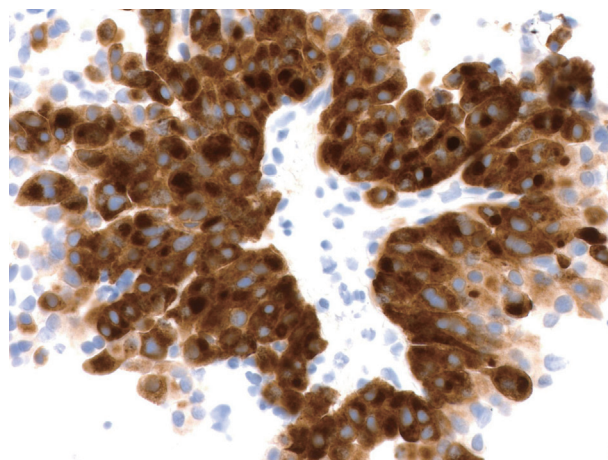


Fig. 3. The example of a well-differentiated neuroendocrine tumor resembling a solid-pseudopapillary neoplasm illustrated in Fig. 2 is tested with an immunohistochemical stain for synaptophysin, which shows diffuse strong staining supporting the diagnosis of a neuroendocrine tumor (peroxidase-anti-peroxidase).

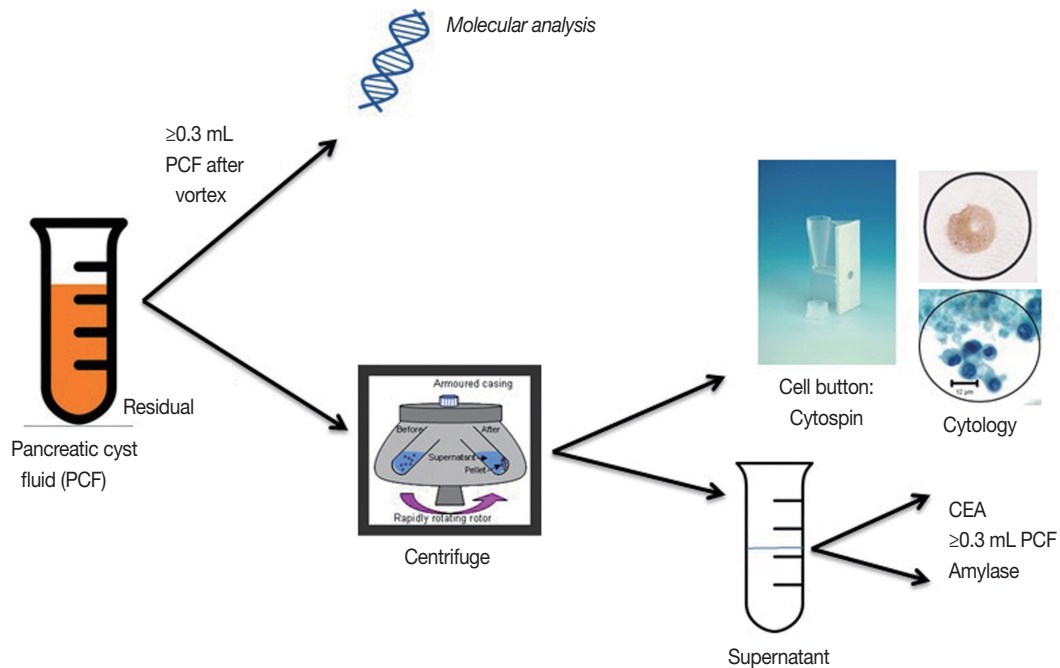


Fig. 4. Algorithm for PCF triage and ancillary testing at the Massachusetts General Hospital. CEA, carcinoembryonic antigen.

ed plasma from a blood bank. This method suspends the cells in a fibrin clot, which is wrapped in tissue paper and processed. Other methods include the HistoGel technique (Thermo Scientific Richard-Allan Scientific HistoGel, Kalamazoo, MI, USA) and the collodion bag technique (Mavidon, Nailsea, Somert, UK or Macron Fine Chemicals of Avantor Performance Materials Inc., Center Valley, PA, USA), both of which are more labor intensive, but which may be better for very scant specimens. An automated cellblock method is the Cellient Automated Cell Block System (Hologic Inc., Bedford, MA, USA) which creates a paraffin-embedded cell block by using vacuum filtration to deposit a layer of cells on a filter and then infiltrate those cells with processing reagents and paraffin.

Larger core biopsies which can be handled with forceps are processed using standard histotechnology techniques. All such core biopsies should be wrapped with tissue paper around a cardboard protector to prevent loss through the cassette during processing. If the core biopsy sample is small and fragmented, it should be handled as a cellblock. Having specimen fixed in formalin is an invaluable adjunct to cytological evaluation of a mass lesion. This is especially true for diseases dependent on some histologic architecture such as autoimmune pancreatitis, or morphologically similar tumors which are distinguished by immunohistochemical studies such as neuroendocrine neoplasms, acinar cell carcinoma and solid-pseudopapillary neoplasms. Secondarily cystic solid neoplasms, such as neuroendocrine tumors are de-

pendent on cytology, and in many cases on the immunohistochemical staining that supports the neuroendocrine nature of the cells, for a specific diagnosis since biochemical analysis and molecular analysis are noncontributory.^{23,24} So in addition to the simple hematoxylin and eosin stained sections from the cellblock, additional sections of the tissue can be used for ancillary testing including immunohistochemical stains and molecular analysis (Fig. 3).¹²

CYSTIC LESIONS

The triage of cyst fluid for testing is volume dependent. Cyst fluid should always remain fresh and unfixed and sent to the cytology lab for processing. Fig. 4 outlines the cyst fluid triage protocol developed at the Massachusetts General Hospital. Cyst fluid is triaged to address two specific clinical questions that directly impact patient management: (1) is the cyst mucinous? and (2) is the cyst high-risk by cytology?²⁵

Very small quantities of cyst fluid (< 0.5 mL) are typically too scant in cellularity to make cytology a meaningful test. However, if imaging features are characteristic of an intraductal papillary mucinous neoplasm (IPMN), then the remaining clinical question is whether there is cytological evidence of a high-risk lesion warranting resection. As such, all of the cyst fluid should be sent for cytological analysis. If, however, the primary question is whether the cyst is mucinous or non-mucinous, fluid should

be triaged to carcinoembryonic antigen (CEA) or, if prior testing demonstrated a non-elevated CEA, molecular analysis.²⁶

Cyst fluids measuring more than 0.5 mL offer sufficient volume for multiple ancillary tests (see below).

Cytospin

A cytospin is a cell concentration method of processing and is the best method for fresh cyst fluid and scantily cellular aspirates. High cellular samples need to be diluted. Cytospin preparations maintain the integrity of background elements such as mucin and necrosis. Once the pancreatic cyst fluid is centrifuged to create a cell button and the supernatant is sent for biochemical analysis, the cell button is resuspended and processed as a cytospin to create a cytological slide for routine staining.

BIOCHEMICAL ANALYSIS

The supernatant cyst fluid following centrifugation is submitted to the chemistry laboratory for CEA and/or amylase testing. At least 0.3 mL of fluid is usually needed for each assay. If volume is scant, CEA generally takes priority over amylase. If there is sufficient fluid, both assays are performed.

Carcinoembryonic antigen

CEA has been shown to be the most reliable and accurate test for a mucinous cyst compared to mucin stains and cytology.²⁷ The CEA immunoassay uses the sandwich antibody method. The measured CEA value of a patient's sample can vary depending on the testing procedure used so each laboratory must validate the assay for normal and abnormal ranges. Cut-off levels affect sensitivity and specificity. At a level of 192 ng/mL CEA has an overall accuracy of up to 80% (specificity of 84% and sensitivity of 75%).²⁸ Raising the cut off value improves specificity at the expense of sensitivity. At a level of 800 ng/mL, the specificity is 98% but sensitivity is 48%.²⁹ Serous cystadenomas and pseudocysts typically have CEA levels lower than 0.5 ng/mL. However, elevations of CEA may be seen in pseudocysts and other non-mucinous cysts such as lymphoepithelial cysts,³⁰ and non-neoplastic mucinous cysts such as gastrointestinal duplication cysts.³¹ In addition, CEA is not always elevated in a mucinous cyst so a low CEA level may be supportive of a non-mucinous cyst, but should not be interpreted as diagnostic of a non-mucinous cyst. CEA levels also do not correlate with malignancy.

Amylase

Amylase testing uses an enzymatic colorimetric assay to

quantify α -amylase. The utility of amylase analysis in cyst fluid is to support the clinical and cytological diagnosis of a pseudocyst or serous cystadenoma. Pseudocysts should always have a high amylase level, usually in the 1000's due to the destruction of pancreatic acinar tissue, and serous cystadenomas consistently demonstrate low amylase levels.³² A low amylase level (< 250 U/L) in a pseudocyst is very unlikely.²⁹ Amylase levels are highly variable in mucinous cysts and do not distinguish between IPMN and mucinous cystic neoplasm (MCN).^{27,33}

MOLECULAR ANALYSIS

Mutational analysis is not routinely used for diagnosis or prognosis of solid pancreatic masses, but is extremely valuable in the diagnosis of pancreatic cysts.^{26,34-38} Most epithelial neoplasms are readily diagnosed using routine cytology with or without immunohistochemical analysis. Molecular mutations are typically not sufficiently specific to establish a malignant diagnosis since precursor lesions such as pancreatic intraepithelial neoplasia (PanIN) demonstrate some of the same mutations as invasive adenocarcinoma. The model of progressive and cumulative mutations from normal pancreas to PanIN to carcinoma has been established with the sequential accumulation of alterations in the *KRAS* and *TP53* genes and loss of the *CDKN2A* and/or *SMAD4* tumor suppressor genes.³⁹ Immunohistochemical stains of tissue in cellblocks can analyze for upregulation of *P53* and loss of *SMAD4* by staining for the protein products of these genes.

For cysts, however, molecular analysis of DNA from the few cells or supernatant fluid is very valuable. Molecular testing is performed on a homogenized aliquot of cyst fluid typically at least 0.3 mL in volume. The DNA present in the sample may or may not be representative of the cells evaluated by cytology; in other words, the cytology may not demonstrate neoplastic cells, but the molecular analysis demonstrates a *KRAS* mutation.^{26,37,40,41} Whatever DNA is present in the sample is analyzed, whether it is from cells in the sample or free DNA in the cyst fluid. As such, the presence of a mutation is a true positive result, but the absence of a mutation may very likely represent a false-negative result. Detection of *KRAS/GNAS/RNF43* mutations are highly specific for determining that the cyst is mucinous, and may preclude the need for repeat testing if CEA is not elevated to support the clinical impression of a mucinous cyst from imaging.^{26,41} Detection of mutations late in the adenoma-carcinoma sequence such as in *TP53*, *p16/CDKN2A*, and *SMAD4* may add weight to an indeterminate (atypical or suspicious) cytological interpre-

Table 1. Molecular changes associated with the most common precursor and cystic lesions in the pancreas

Genetic change	Associated lesions
<i>KRAS</i> mutation	IPMN, MCN, and PanIN, all grades
<i>GNAS</i> mutation	IPMN, all grades
<i>RNF43</i> mutation	IPMN and MCN, all grades
<i>P16/CDKN2A</i> loss	IPMN, MCN, and PanIN, all grades
<i>TP53</i> mutation	IPMN, MCN, and PanIN, high-grade
<i>SMAD4</i> loss	IPMN, MCN, and PanIN, high-grade
<i>VHL</i> mutation	Serous cystadenoma
<i>CTNNB1</i> mutation	Solid-pseudopapillary neoplasm

IPMN, intraductal papillary mucinous neoplasm; MCN, mucinous cystic neoplasm; PanIN, pancreatic intraepithelial neoplasia.

Table 2. Standardized pancreaticobiliary terminology proposed by the Papanicolaou Society of Cytopathology

I. Nondiagnostic
II. Negative (for malignancy)
III. Atypical
IV. Neoplastic
A. Benign
Serous cystadenoma
Neuroendocrine microadenoma
Lymphangioma
B. Other
Intraductal papillary mucinous neoplasm (low, intermediate and high-grade dysplasia)
Mucinous cystic neoplasm (low, intermediate and high-grade dysplasia)
Well-differentiated neuroendocrine tumor
Solid-pseudopapillary neoplasm
V. Suspicious (for malignancy)
VI. Positive/Malignant
Ductal adenocarcinoma and variants
High-grade (G3) neuroendocrine carcinoma
Acinar cell carcinoma
Pancreatoblastoma
Lymphoma
Metastases

ation. Table 1 outlines the molecular profiles useful in the evaluation of pancreatic cysts.

STANDARDIZED REPORTING OF PANCREATICOBILIARY CYTOLOGY

The Papanicolaou Society of Cytopathology has proposed a standardized terminology scheme for reporting pancreaticobiliary cytology with six categories (Table 2).¹ New and somewhat controversial is the category “neoplastic” that is divided into clearly “benign” neoplasms and “other” neoplasms. The “other” category includes a wide variety of lesions ranging from premalignant mucinous cysts to low-grade potentially malignant and

low-grade malignant neoplasms. This standardized terminology and nomenclature system aims to provide intra- and interdepartmental guidance for diagnosis, and one that correlates the diagnosis to our current understanding of the lesion’s biological behavior and management recommendations.

Category I. Non-diagnostic

A cytology specimen is non-diagnostic when it fails to provide any diagnostic or useful information about the solid or cystic lesion sampled. The clinical and imaging context should be taken into consideration when assessing whether a sample is adequate. Thick extracellular mucin without epithelial cells is not non-diagnostic, for example. Thin cyst fluid with an elevated CEA level above a validated cut-off level supporting a mucinous cyst is also not non-diagnostic despite the absence of an epithelial cell component.²⁷⁻²⁹ In contrast, cyst fluid without lesional epithelium, scant thin extracellular mucin which could be gastrointestinal contamination, and a CEA level below the established cut-off level supporting a mucinous cyst is a nondiagnostic specimen.

Category II. Negative (for malignancy)

When an FNA contains adequate cellular and/or extracellular tissue to evaluate or define a lesion that is identified on imaging, it can be classified as negative (for malignancy). Whenever possible a specific diagnosis should be given, for example, chronic pancreatitis or lymphoepithelial cyst.⁴² Benign pancreaticobiliary tissue in the setting of vague fullness and no discrete mass also qualifies as a negative interpretation. A negative interpretation with a descriptive diagnosis implies that the sample is adequately cellular and that no cytological atypia is present.

Category III. Atypical

When cells display cellular changes inconsistent with normal or reactive cellular changes, and that are insufficiently atypical or characteristic to make a diagnosis of a neoplasm or to be suspicious for a high-grade malignancy, then the atypical category is appropriate. Aspirates with cytological findings suggestive but not diagnostic of a low-grade neoplasm such as a neuroendocrine tumor or solid-pseudopapillary neoplasm due to insufficient specimen for confirmation of a specific diagnosis belong in the atypical category. Brushing cytology yielding atypical biliary epithelium remains in this category since premalignant lesions of the biliary tract have not been as well defined with correlative management algorithms.

Category IV. Neoplastic

IVA. Neoplastic: benign

Aspirates diagnostic of a benign neoplasm belong in this interpretation category, for example, serous cystadenoma, neuroendocrine microadenoma, and lymphangioma.

IVB. Neoplastic: other

Pre-malignant neoplasms such as IPMN or MCN with low, intermediate, or high-grade dysplasia, and potentially malignant or low-grade malignant neoplasms such as well-differentiated pancreatic neuroendocrine tumors and solid-pseudopapillary neoplasms belong in this category.

The rationale for this proposed category relates the desire to standardize and correlate the cytological nomenclature with the 2010 World Health Organization (WHO) terminology classification that maintains the nomenclature for both neuroendocrine tumors and solid-pseudopapillary neoplasms as “neoplasms” rather than carcinomas, and to take into consideration the increasingly conservative management approaches for many of the lesions.⁴³

These “other” neoplasms are either pre-invasive, potentially malignant, or low-grade malignant neoplasms, which should be distinguished from aggressive, high-grade malignancies such as ductal adenocarcinoma. All of the tumors in this category are clearly neoplastic, and even though some are low-grade malignant, the heading “Neoplastic: other” is an accurate and reasonable generic term that accurately reflects the pre-operative cytological terminology and does not define the neoplasm as benign or malignant. The cytological categories of “atypical” and “suspicious for malignancy” connote an indeterminate interpretation and do not relate the detection of a neoplasm, which could lead to unnecessary repeat biopsy.

The cytological interpretation of a neuroendocrine tumor, not otherwise specified indicates a well-differentiated neoplasm. The term “carcinoma” is reserved for high-grade neoplasms (G3), typically with a small cell carcinoma or large cell undifferentiated carcinoma morphology. Although it is now widely accepted that well-differentiated neuroendocrine tumors have malignant potential,⁴⁴ many are very slow growing and even curable if caught at an early stage, and some are detected incidentally in asymptomatic, elderly patients who may be better served with conservative observation than surgical intervention. To distinguish these low-grade neoplasms from highly aggressive malignant neoplasms and to offer management flexibility in elderly patients with small, asymptomatic tumors where the risk to bene-

fit ratio of surgery is high compared to conservative management, neuroendocrine tumors are placed in this category rather than the malignant category. Convincing a patient with a malignant cytology report that conservative management of their incidental 1-cm-sized neuroendocrine tumor is the best option for them is virtually impossible.

Solid-pseudopapillary neoplasm is a low-grade malignancy but with a small local recurrence rate and low metastatic potential.⁴⁵ For these reasons coupled with the fact that the tumor is called a “neoplasm” and not carcinoma, it is included in this Neoplastic: other category.

The pre-malignant mucinous cysts of the pancreas, IPMNs and MCNs, are lined by low, intermediate, or high-grade dysplasia; malignancy requires an invasive component. Atypia less than overtly malignant is included in this category of ‘Neoplastic: other’. Distinguishing the atypia in these cysts is challenging using a four-tiered system, and it is not always possible to distinguish high-grade dysplasia from carcinoma, or intermediate-grade dysplasia from high-grade dysplasia. A two-tiered system of low-grade (low-grade and intermediate-grade dysplasia) and high-grade (high-grade dysplasia or adenocarcinoma) epithelial atypia provides the best information for clinical management.⁴⁶⁻⁴⁹

Category V. Suspicious (for malignancy)

A specimen is suspicious for malignancy when the quality and/or quantity of the cellular atypia are insufficient for a malignant interpretation. This category generally refers to pancreatic adenocarcinoma since most malignancies in the pancreas are ductal adenocarcinoma, but this category is used for all high-grade, aggressive malignancies. The suspicious category is also used for aspirates that include high-grade neoplasms in the differential diagnosis, e.g., acinar cell carcinoma or pancreatoblastoma, but insufficient tissue for confirmatory ancillary studies is not available.

Category VI. Positive or malignant

This category includes high-grade, aggressive tumors such as pancreatic ductal adenocarcinoma and its variants, cholangiocarcinoma, acinar cell carcinoma, high-grade neuroendocrine carcinoma (small cell and large cell), pancreatoblastoma, lymphomas, sarcomas and metastases to the pancreas.

SUMMARY

Pancreatic cytology is an accurate method of evaluating solid and cystic lesions in the pancreas. Accuracy, however, requires a

multidisciplinary and multimodal approach where the cytological features are interpreted in the context of the clinical, imaging and ancillary testing information available. Adequate tissue procurement, processing and triage are vital steps in ensuring that the tissue is sufficient for a diagnosis, and standardized terminology ensures that the language used to report the findings in a single coherent, integrated report is understood by all caregivers involved in the management of the patient.

Conflicts of Interest

No potential conflict of interest relevant to this article was reported.

REFERENCES

- Pitman MB, Centeno BA, Ali SZ, *et al.* Standardized terminology and nomenclature for pancreatobiliary cytology: the Papanicolaou Society of Cytopathology guidelines. *Diagn Cytopathol* 2014; 42: 338-50.
- Mekky MA, Abbas WA. Endoscopic ultrasound in gastroenterology: from diagnosis to therapeutic implications. *World J Gastroenterol* 2014; 20: 7801-7.
- Adler D, Max Schmidt C, Al-Haddad M, *et al.* Clinical evaluation, imaging studies, indications for cytologic study, and preprocedural requirements for duct brushing studies and pancreatic FNA: the Papanicolaou Society of Cytopathology recommendations for pancreatic and biliary cytology. *Diagn Cytopathol* 2014; 42: 325-32.
- Brugge W, Dewitt J, Klapman JB, *et al.* Techniques for cytologic sampling of pancreatic and bile duct lesions. *Diagn Cytopathol* 2014; 42: 333-7.
- Volmar KE, Vollmer RT, Jowell PS, Nelson RC, Xie HB. Pancreatic FNA in 1000 cases: a comparison of imaging modalities. *Gastrointest Endosc* 2005; 61: 854-61.
- Okasha HH, Naga MI, Esmat S, *et al.* Endoscopic ultrasound-guided fine needle aspiration versus percutaneous ultrasound-guided fine needle aspiration in diagnosis of focal pancreatic masses. *Endosc Ultrasound* 2013; 2: 190-3.
- Dumonceau JM, Polkowski M, Larghi A, *et al.* Indications, results, and clinical impact of endoscopic ultrasound (EUS)-guided sampling in gastroenterology: European Society of Gastrointestinal Endoscopy (ESGE) Clinical Guideline. *Endoscopy* 2011; 43: 897-912.
- Wiersema MJ, Vilmann P, Giovannini M, Chang KJ, Wiersema LM. Endosonography-guided fine-needle aspiration biopsy: diagnostic accuracy and complication assessment. *Gastroenterology* 1997; 112: 1087-95.
- Lee JH, Stewart J, Ross WA, Anandasabapathy S, Xiao L, Staerkel G. Blinded prospective comparison of the performance of 22-gauge and 25-gauge needles in endoscopic ultrasound-guided fine needle aspiration of the pancreas and peri-pancreatic lesions. *Dig Dis Sci* 2009; 54: 2274-81.
- Madhoun MF, Wani SB, Rastogi A, *et al.* The diagnostic accuracy of 22-gauge and 25-gauge needles in endoscopic ultrasound-guided fine needle aspiration of solid pancreatic lesions: a meta-analysis. *Endoscopy* 2013; 45: 86-92.
- Panic N, Larghi A. Techniques for endoscopic ultrasound-guided fine-needle biopsy. *Gastrointest Endosc Clin N Am* 2014; 24: 83-107.
- Layfield LJ, Ehya H, Filie AC, *et al.* Utilization of ancillary studies in the cytologic diagnosis of biliary and pancreatic lesions: the Papanicolaou Society of Cytopathology guidelines for pancreatobiliary cytology. *Diagn Cytopathol* 2014; 42: 351-62.
- Pitman M. Pancreas. In: Bibbo M, Wilbur DC, eds. *Comprehensive cytopathology*. London: Elsevier, 2014; 751-73.
- Bang JY, Magee SH, Ramesh J, Trevino JM, Varadarajulu S. Randomized trial comparing fanning with standard technique for endoscopic ultrasound-guided fine-needle aspiration of solid pancreatic mass lesions. *Endoscopy* 2013; 45: 445-50.
- Jenssen C, Dietrich CF. Endoscopic ultrasound-guided fine-needle aspiration biopsy and trucut biopsy in gastroenterology: an overview. *Best Pract Res Clin Gastroenterol* 2009; 23: 743-59.
- Brugge WR. The role of EUS in the diagnosis of cystic lesions of the pancreas. *Gastrointest Endosc* 2000; 52(6 Suppl): S18-22.
- Lee LS, Saltzman JR, Bounds BC, Poneros JM, Brugge WR, Thompson CC. EUS-guided fine needle aspiration of pancreatic cysts: a retrospective analysis of complications and their predictors. *Clin Gastroenterol Hepatol* 2005; 3: 231-6.
- Yoon WJ, Daglilar ES, Fernandez-del Castillo C, Mino-Kenudson M, Pitman MB, Brugge WR. Peritoneal seeding in intraductal papillary mucinous neoplasm of the pancreas patients who underwent endoscopic ultrasound-guided fine-needle aspiration: the PIPE Study. *Endoscopy* 2014; 46: 382-7.
- Olson MT, Ali SZ. Cytotechnologist on-site evaluation of pancreas fine needle aspiration adequacy: comparison with cytopathologists and correlation with the final interpretation. *Acta Cytol* 2012; 56: 340-6.
- Iglesias-Garcia J, Dominguez-Munoz JE, Abdulkader I, *et al.* Influence of on-site cytopathology evaluation on the diagnostic accuracy of endoscopic ultrasound-guided fine needle aspiration (EUS-FNA) of solid pancreatic masses. *Am J Gastroenterol* 2011; 106: 1705-10.
- Collins BT, Murad FM, Wang JF, Bernadt CT. Rapid on-site evaluation for endoscopic ultrasound-guided fine-needle biopsy of the pancreas decreases the incidence of repeat biopsy procedures. *Can-*

- cer Cytopathol 2013; 121: 518-24.
22. da Cunha Santos G, Ko HM, Saieg MA, Geddie WR. "The petals and thorns" of ROSE (rapid on-site evaluation). *Cancer Cytopathol* 2013; 121: 4-8.
 23. Yoon WJ, Daglilar ES, Pitman MB, Brugge WR. Cystic pancreatic neuroendocrine tumors: endoscopic ultrasound and fine-needle aspiration characteristics. *Endoscopy* 2013; 45: 189-94.
 24. Morales-Oyarvide V, Yoon WJ, Ingkakul T, *et al.* Cystic pancreatic neuroendocrine tumors: the value of cytology in preoperative diagnosis. *Cancer Cytopathol* 2014; 122: 435-44.
 25. Pitman MB. Pancreatic cyst fluid triage: a critical component of the preoperative evaluation of pancreatic cysts. *Cancer Cytopathol* 2013; 121: 57-60.
 26. Jones M, Zheng Z, Wang J, *et al.* Impact of next-generation sequencing on the clinical impression of pancreatic cysts. *Gastrointest Endosc* 2015 Aug 5 [Epub]. <http://dx.doi.org/10.1016/j.gie.2015.06.047>.
 27. Cizginer S, Turner BC, Bilge AR, Karaca C, Pitman MB, Brugge WR. Cyst fluid carcinoembryonic antigen is an accurate diagnostic marker of pancreatic mucinous cysts. *Pancreas* 2011; 40: 1024-8.
 28. Brugge WR, Lewandrowski K, Lee-Lewandrowski E, *et al.* Diagnosis of pancreatic cystic neoplasms: a report of the cooperative pancreatic cyst study. *Gastroenterology* 2004; 126: 1330-6.
 29. van der Waaij LA, van Dullemen HM, Porte RJ. Cyst fluid analysis in the differential diagnosis of pancreatic cystic lesions: a pooled analysis. *Gastrointest Endosc* 2005; 62: 383-9.
 30. Raval JS, Zeh HJ, Moser AJ, *et al.* Pancreatic lymphoepithelial cysts express CEA and can contain mucous cells: potential pitfalls in the preoperative diagnosis. *Mod Pathol* 2010; 23: 1467-76.
 31. Johnston J, Wheatley GH 3rd, El Sayed HF, Marsh WB, Ellison EC, Bloomston M. Gastric duplication cysts expressing carcinoembryonic antigen mimicking cystic pancreatic neoplasms in two adults. *Am Surg* 2008; 74: 91-4.
 32. Lewandrowski KB, Southern JF, Pins MR, Compton CC, Warshaw AL. Cyst fluid analysis in the differential diagnosis of pancreatic cysts. A comparison of pseudocysts, serous cystadenomas, mucinous cystic neoplasms, and mucinous cystadenocarcinoma. *Ann Surg* 1993; 217: 41-7.
 33. Moparty B, Pitman MB, Brugge WR. Pancreatic cyst fluid amylase is not a marker to differentiate IPMN from MCN. *Gastrointest Endosc* 2007; 65: AB303.
 34. Khalid A, Zahid M, Finkelstein SD, *et al.* Pancreatic cyst fluid DNA analysis in evaluating pancreatic cysts: a report of the PANDA study. *Gastrointest Endosc* 2009; 69: 1095-102.
 35. Shen J, Brugge WR, Dimaio CJ, Pitman MB. Molecular analysis of pancreatic cyst fluid: a comparative analysis with current practice of diagnosis. *Cancer* 2009; 117: 217-27.
 36. Wu J, Matthaei H, Maitra A, *et al.* Recurrent *GNAS* mutations define an unexpected pathway for pancreatic cyst development. *Sci Transl Med* 2011; 3: 92ra66.
 37. Nikiforova MN, Khalid A, Fasanella KE, *et al.* Integration of *KRAS* testing in the diagnosis of pancreatic cystic lesions: a clinical experience of 618 pancreatic cysts. *Mod Pathol* 2013; 26: 1478-87.
 38. Amato E, Molin MD, Mafficini A, *et al.* Targeted next-generation sequencing of cancer genes dissects the molecular profiles of intraductal papillary neoplasms of the pancreas. *J Pathol* 2014; 233: 217-27.
 39. Hruban RH, Goggins M, Parsons J, Kern SE. Progression model for pancreatic cancer. *Clin Cancer Res* 2000; 6: 2969-72.
 40. Finkelstein SD, Bibbo M, Loren DE, *et al.* Molecular analysis of centrifugation supernatant fluid from pancreaticobiliary duct samples can improve cancer detection. *Acta Cytol* 2012; 56: 439-47.
 41. Wu J, Jiao Y, Dal Molin M, *et al.* Whole-exome sequencing of neoplastic cysts of the pancreas reveals recurrent mutations in components of ubiquitin-dependent pathways. *Proc Natl Acad Sci U S A* 2011; 108: 21188-93.
 42. Pitman MB, Centeno BA, Ali SZ, *et al.* Standardized terminology and nomenclature for pancreatobiliary cytology: The Papanicolaou Society of Cytopathology Guidelines. *Cytojournal* 2014; 11(Suppl 1): 3.
 43. Kuo EJ, Salem RR. Population-level analysis of pancreatic neuroendocrine tumors 2 cm or less in size. *Ann Surg Oncol* 2013; 20: 2815-21.
 44. Klimstra DS. Pathology reporting of neuroendocrine tumors: essential elements for accurate diagnosis, classification, and staging. *Semin Oncol* 2013; 40: 23-36.
 45. Kloppel G, Hruban R, Klimstra D, *et al.* Solid-pseudopapillary neoplasm of the pancreas. In: Bosman FT, Carneiro F, Hruban RH, Theise ND, eds. *WHO classification of tumours of the digestive system*. 4th ed. Sterling: Stylus Publishing, 2010. p. 327-30.
 46. Pitman MB, Centeno BA, Daglilar ES, Brugge WR, Mino-Kenudson M. Cytological criteria of high-grade epithelial atypia in the cyst fluid of pancreatic intraductal papillary mucinous neoplasms. *Cancer Cytopathol* 2014; 122: 40-7.
 47. Pitman MB, Centeno BA, Genevay M, Fonseca R, Mino-Kenudson M. Grading epithelial atypia in endoscopic ultrasound-guided fine-needle aspiration of intraductal papillary mucinous neoplasms: an international interobserver concordance study. *Cancer Cytopathol* 2013; 121: 729-36.
 48. Pitman MB, Genevay M, Yaeger K, *et al.* High-grade atypical epithelial cells in pancreatic mucinous cysts are a more accurate predictor of malignancy than "positive" cytology. *Cancer Cytopathol* 2010; 118: 434-40.
 49. Pitman MB, Lewandrowski K, Shen J, Sahani D, Brugge W, Fernandez-del Castillo C. Pancreatic cysts: preoperative diagnosis and clinical management. *Cancer Cytopathol* 2010; 118: 1-13.

SALL4 Expression in Hepatocellular Carcinomas Is Associated with EpCAM-Positivity and a Poor Prognosis

Hyunjin Park · Hyejung Lee
An Na Seo¹ · Jai Young Cho²
Young Rok Choi² · Yoo-Seok Yoon²
Ho-Seong Han² · Young Nyun Park³
Haeryoung Kim

Department of Pathology, Seoul National University Bundang Hospital, Seoul National University College of Medicine, Seoul;

¹Department of Pathology, Kyungpook National University Medical Center, Kyungpook National University School of Medicine, Daegu;

²Department of Surgery, Seoul National University Bundang Hospital, Seoul National University College of Medicine, Seoul;

³Department of Pathology, Yonsei University College of Medicine, Seoul, Korea

Received: May 28, 2015

Revised: July 1, 2015

Accepted: July 8, 2015

Corresponding Author

Haeryoung Kim, MD, PhD
Department of Pathology, Seoul National University Bundang Hospital, Seoul National University College of Medicine, 82 Gumi-ro 173beon-gil, Bundang-gu, Seongnam 13620, Korea
Tel: +82-31-787-7715
Fax: +82-31-787-4012
E-mail: haeryoung.kim@snu.ac.kr

Young Nyun Park, MD, PhD
Department of Pathology, Yonsei University College of Medicine, 50-1 Yonsei-ro, Seodaemun-gu, Seoul 03722, Korea
Tel: +82-2-2228-1678
Fax: +82-2-362-0860
E-mail: young0608@yuhs.ac

Background: There is increasing interest in hepatocellular carcinomas (HCC) expressing “stemness”-related markers, as they have been associated with aggressive behavior and poor prognosis. In this study, we investigated the usefulness of Sal-like protein 4 (SALL4), a recently proposed candidate marker of “stemness.” **Methods:** Immunohistochemical stains were performed for SALL4, K19, and epithelial cellular adhesion molecule (EpCAM) on tissue microarrays constructed from 190 surgically resected HCCs, and the results were correlated with the clinicopathological features and patient survival data. **Results:** Nuclear SALL4 expression was observed in 39/190 HCCs (20.5%), while K19 and EpCAM were expressed in 30 (15.9%) and 92 (48.7%) HCCs, respectively. The nuclear expression was generally weak, punctate or clumped. SALL4 expression was significantly associated with a poor overall survival compared to SALL4-negative HCCs ($p = .014$) compared to SALL4-negative HCCs. On multivariate analysis adjusted for tumor size, multiplicity, vascular invasion, and pathological tumor stage, SALL4 remained as a significant independent predictor of decreased overall survival ($p = .004$). SALL4 expression was positively correlated with EpCAM expression ($p = .013$) but not with K19 expression. HCCs that expressed both SALL4 and EpCAM were associated with significantly decreased overall survival, compared to those cases which were negative for both of these markers ($p = .031$). **Conclusions:** Although SALL4 expression was not significantly correlated with other clinicopathological parameters suggestive of tumor aggressiveness, SALL4 expression was an independent predictor of poor overall survival in human HCCs, and was also positively correlated with EpCAM expression.

Key Words: Carcinoma, hepatocellular; SALL4; Immunohistochemistry; Prognosis

Hepatocellular carcinoma (HCC) is one of the leading causes of cancer mortality in the world, with a limited number of currently available therapeutic options. Recent advances in research have suggested various molecular classifications for HCC, for example the “hepatoblast signature,” “cholangiocarcinoma-like signature,” “epithelial cellular adhesion molecule (EpCAM)-positive signature,” and “5-gene score,” which help to identify subsets

of HCC with poor prognosis and aggressive biological behavior, and which also point to the heterogeneity of HCC.¹⁻⁴ Translating the molecular classifications into surgical pathology practice would potentially add more functionally and clinically relevant information in addition to the purely morphological diagnosis, and such endeavors have resulted in new classifications of various cancers, including HCC, which reflect the histopathologi-

cal, immunophenotypical and molecular features of the tumors.

Interestingly, a remarkable number of the proposed poor prognostic signatures for HCC are related to “stemness,” and the expression of hepatic stem/progenitor cell–related markers in HCCs have been associated with an aggressive clinical behavior, compared to conventional HCCs that do not express these markers.^{5,6} It may be speculated that HCCs with “stemness”-related marker expression result from the malignant transformation of hepatic stem/progenitor cells, or from the dedifferentiation of conventional HCCs that acquire “stemness”-related markers during tumor progression. Whatever the pathogenesis, these tumors show features of aggressive behavior, such as frequent vascular invasion, and poor prognosis, up-regulation of epithelial-mesenchymal transition-related genes, longer telomeres and increased resistance to chemotherapeutic agents.^{5,7,8}

It is still uncertain which marker is the best one for identifying this aggressive subgroup of HCCs; most of the recent literature has focused on K19, EpCAM, and CD133. Recent studies have proposed as a novel marker for the progenitor subclass of HCC Sal-like protein 4 (SALL4), which is known to be an important regulator of pluripotency in embryonic stem cells.^{9–12} In this study, we investigated the usefulness of SALL4 as a prognostic marker and a marker of “stemness” in HCC.

MATERIALS AND METHODS

Case selection and review

This study was approved by the Institutional Review Board of Seoul National University Bundang Hospital (B-1502-286-302). One hundred and ninety consecutive cases of surgically resected or explanted HCCs were enrolled in this study, and were retrieved from the surgical pathology files of Seoul National University Bundang Hospital from May 2003 to April 2010. The clinicopathological characteristics of the cases are summarized in Table 1. The electronic medical records, surgical pathology reports, and the hematoxylin and eosin-stained slides were reviewed for each case, and the clinicopathological variables noted included tumor size, multiplicity (including intrahepatic metastasis/satellite nodules and multicentric occurrences), histological differentiation according to the Edmondson-Steiner grade (the highest grade in tumors with heterogeneity), the presence of microvascular or major vascular invasion, the patient demographics (age and sex), and the presence of an underlying etiology (e.g., hepatitis B, C, alcohol). Follow-up data was also obtained from the medical records, including recurrences (including local recurrence and distant metastasis) and death. The median

Table 1. Clinicopathologic characteristics of the HCC patients (n = 190)

Characteristic	No. (%)
Age (yr)	58.1 ± 11.8
Sex	
Male	151 (79.5)
Female	39 (20.1)
Etiology	
Hepatitis B	136 (71.6)
Hepatitis C	17 (8.9)
Alcohol	8 (4.2)
Others	30 (15.8)
Serum alpha-fetoprotein (IU/mL)	1,634.6 ± 4,590.4
Serum PIVKA-II (AU/mL)	661.2 ± 1,528.9
Multiplicity	
Absent	106 (55.8)
Present	31 (16.3)
Tumor size (cm) ^a	4.6 ± 3.0
Edmondson-Steiner grade	
I	1 (0.5)
II	47 (24.7)
III	122 (64.2)
IV	20 (10.5)
Microvascular invasion	
Absent	116 (61.1)
Present	74 (38.9)
Major vessel invasion ^b	
Absent	168 (88.4)
Present	22 (11.6)
Follow-up	
Recurrence ^c	102 (53.7)
Deaths due to HCC	24 (12.6)

Values are presented as mean ± standard deviation or number (%).

HCC, hepatocellular carcinomas.

^aSize of largest tumor in case of multiple tumors; ^bMain or first order branches of portal vein and/or one or more of right, middle or left hepatic veins; ^cLocal recurrence or distant metastasis.

follow-up period was 52 months (range, 0 to 133 months). Overall survival was defined as the interval from initial surgical treatment for HCC to the date of death, and disease-free survival as the interval from initial treatment to local or distant recurrence.

Tissue microarray construction and immunohistochemistry

Tissue cores measuring 2 mm in diameter were sampled from formalin-fixed paraffin-embedded HCC tissues and arranged in recipient tissue array blocks using a trephine apparatus (Superbiochips Laboratories, Seoul, Korea). Two or three cores were sampled from each HCC, depending on the amount of histological heterogeneity present in the tumor. One core was sampled from the corresponding non-neoplastic liver for each case. Four μm-thick sections were obtained from the tissue microarray blocks and subjected to immunohistochemical staining for SALL4

(1:100, mouse monoclonal antibody, clone EE-30, Santa Cruz Technologies Inc., Santa Cruz, CA, USA), K19 (1:150, mouse monoclonal antibody, clone BA17, Dako, Glostrup, Denmark) and EpCAM (1:3,000, mouse monoclonal antibody, clone VU-1D9, Calbiochem, Darmstadt, Germany). Briefly, tissue sections were deparaffinized in xylene, rehydrated in graded alcohol, and antigen retrieval was performed using citrate buffer

(pH 6.0) for 15 minutes. Sections were incubated with the primary antibodies at room temperature for 30 minutes, and then incubated with secondary antibodies (EnVision Detection System, Dako). Counterstaining was performed using Mayer's hematoxylin and the stained slides were mounted.

SALL4 was expressed in the tumor cell nuclei, and positivity for SALL4 expression was defined as nuclear staining for the

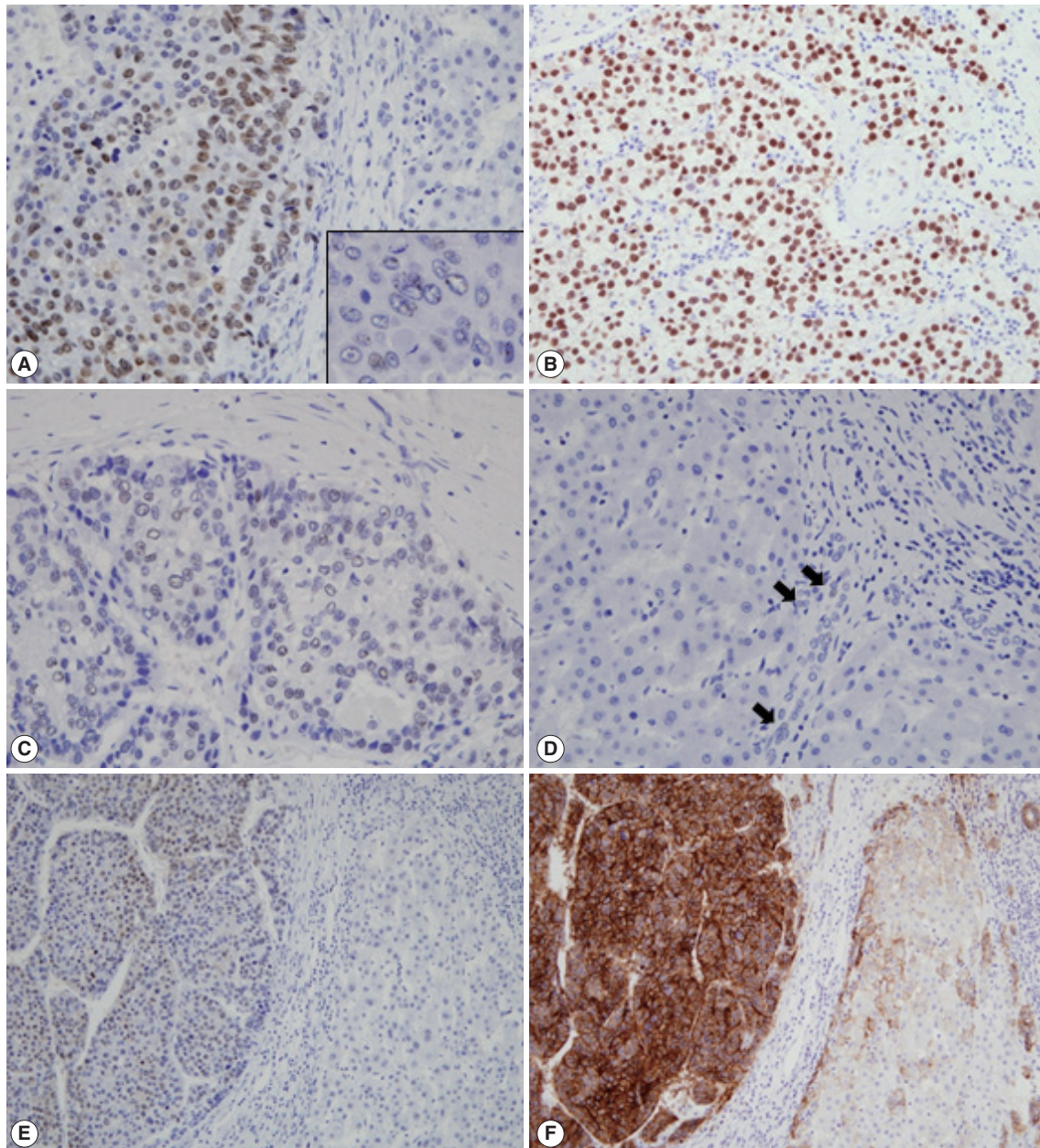


Fig. 1. Immunohistochemical stain results. Nuclear SALL4 staining is seen in a case of HCC (A), which is weaker and clumped (inset) compared to the strong nuclear staining seen in testicular seminoma (B). Clumped nuclear SALL4 expression is seen in another case of HCC with fibrous stroma (C). The non-neoplastic liver is negative for SALL4, except for occasional faintly positive cells in the ductular reactions (D, arrows). Nuclear SALL4 staining (E) is seen in an HCC with EpCAM expression (F). SALL4, Sal-like protein 4; HCC, hepatocellular carcinoma; EpCAM, epithelial cellular adhesion molecule.

protein in more than 10% of the tumor cells after calculating the SALL4-labeling index (a ratio of positive nuclei/total nuclei under the 400× field magnification) with the help of the Image J software (downloaded from <http://imagej.nih.gov/ij>). A testicular seminoma tissue sample was used as a positive control for SALL4. Membranous and/or cytoplasmic staining in the tumor cells were counted as positive for EpCAM and K19.

Statistical analysis

All statistical analyses were conducted using IBM SPSS ver. 21 (IBM Corp., Armonk, NY, USA). Chi-square, Fisher's exact and t tests were performed as deemed appropriate. Univariable analyses for overall survival and disease-free survival were performed using the Kaplan-Meier method and log-rank tests. Statistically significant variables from the univariable analysis were entered into the multivariable analyses using the Cox proportional hazard method. Statistical significance was defined as $p < .05$.

RESULTS

SALL4, K19, and EpCAM expression in HCC

The immunohistochemical stain results and the expression frequencies of SALL4, K19, and EpCAM are summarized in Figs. 1 and 2, respectively. The SALL4 nuclear labeling index ranged from 0% to 78.9% (mean ± standard deviation, $8.9 \pm 19.2\%$) in the 190 HCCs, and 39 cases (20.5%) were deemed positive for SALL4 expression (labeling index $\geq 10\%$). Although a definite nuclear staining was present in the tumor cells, the intensity of staining was generally not as strong as in the positive

control tissue (testicular seminoma) (Fig. 1A–C). In some areas, the nuclear staining was punctate and only identifiable at higher power magnification. SALL4 positivity was generally uniformly distributed in the HCCs without predilections for a particular morphological tumor cell: some SALL4-positive tumor cells were small with increased nuclear/cytoplasmic ratios reminiscent of the stem/progenitor cell phenotype, while others were more typical HCCs with various degrees of differentiation. In the adjacent non-neoplastic liver, the hepatocytes and bile ducts did not stain for SALL4, and interestingly, SALL4 positivity was seen in occasional ductular reactions, although the staining was very faint and barely visible (Fig. 1D).

K19 and EpCAM expression data were available for 189 cases (due to tissue core loss in 1 case). K19 and EpCAM were expressed in 30 (15.9%) and 92 (48.7%) cases, respectively, in the typical membranous/cytoplasmic pattern, and they were also expressed in the bile ducts and ductular reactions in the non-neoplastic livers. A significant positive correlation was seen between EpCAM and K19 expression: K19 positivity was seen in 27 out of 92 EpCAM-positive HCCs (29.3%) compared to 3 out of 97 EpCAM negative HCCs (3.1%) ($p < .001$). SALL4 expression was more frequently seen in EpCAM-positive HCCs (26/92, 28.3%) compared to EpCAM-negative HCCs (13/97, 13.4%) ($p = .013$) (Fig. 1E, F). However, there was no significant correlation between SALL4 and K19 expression: only 3.2% of the HCCs demonstrated positivity for both SALL4 and K19 (Fig. 2). The relationships between the expression of SALL4, K19, and EpCAM in HCCs are summarized in a Venn diagram in Fig. 2.

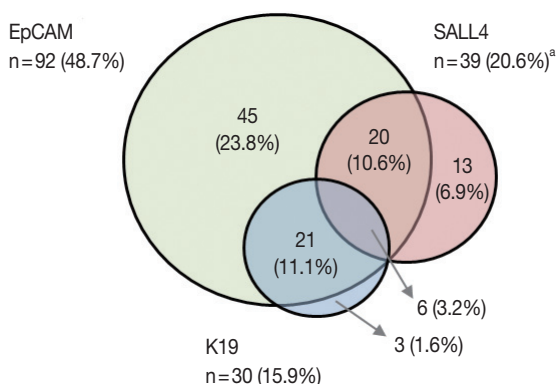


Fig. 2. Venn diagram summarizing the relationships between the expression of SALL4 (pink), K19 (blue), and EpCAM (green) in HCCs. While SALL4 expression is frequently co-expressed with EpCAM (26/39, 66.7%), K19 expression was only seen in 6 of SALL4-positive HCCs (15.4%). SALL4, Sal-like protein 4; EpCAM, epithelial cellular adhesion molecule; HCC, hepatocellular carcinoma. ^aTotal n = 189 with SALL4, EpCAM, and K19 data.

Correlation with clinicopathological variables and survival

Univariable analysis demonstrated that SALL4 expression was significantly associated with reduced overall survival ($p = .014$) (Fig. 3A). In addition to SALL4 expression, larger tumor size (> 3 cm, $p = .045$), multiplicity of tumor ($p = .001$), major vascular invasion ($p = .046$) and higher T stage (stage 3 or 4, $p < .001$) were significantly associated with decreased overall survival. In comparison, SALL4 expression was not significantly associated with disease-free survival (Fig. 3B), while larger size (> 3 cm, $p = .009$), multiplicity ($p = .002$) and higher T stage (stage 3 or 4, $p = .019$) were significantly associated with reduced disease-free survival. HCCs with K19 expression had a tendency for decreased overall survival, although this result was not statistically significant ($p = .063$), while disease-free survival was significantly decreased for K19 expressing HCCs ($p = .001$) (Fig. 3C, D). EpCAM expression was associated with a tendency for decreased

overall survival ($p = .053$); however, it was not associated with disease-free survival.

Interestingly, when we performed the survival analysis after combining EpCAM and SALL4 expression status, HCCs that expressed both SALL4 and EpCAM were associated with significantly decreased overall survival, compared to those cases which were negative for both these markers ($p = .031$) (Fig. 4). In addition, while EpCAM-negative HCCs were associated with a relatively favorable outcome compared to EpCAM-positive HCCs during the earlier follow-up period (< 5 years), EpCAM-negative HCCs with SALL4-positivity showed an abrupt decrease in over-

all survival after 5 years of follow-up.

On multivariable analysis, SALL4 ($p = .004$), multiplicity ($p = .016$) and higher T stage ($p = .004$) remained as significant independent predictors of decreased overall survival (Table 2). For disease-free survival, larger tumor size (> 3 cm, $p = .019$), and multiplicity ($p = .004$) were independent prognostic factors.

SALL4 expression was not significantly associated with other clinicopathological parameters of tumor aggressiveness, such as presence of vascular invasion, larger tumors, and multiplicity (Table 3). On the other hand, EpCAM expression in HCCs was more frequently associated with poor histological differentiation

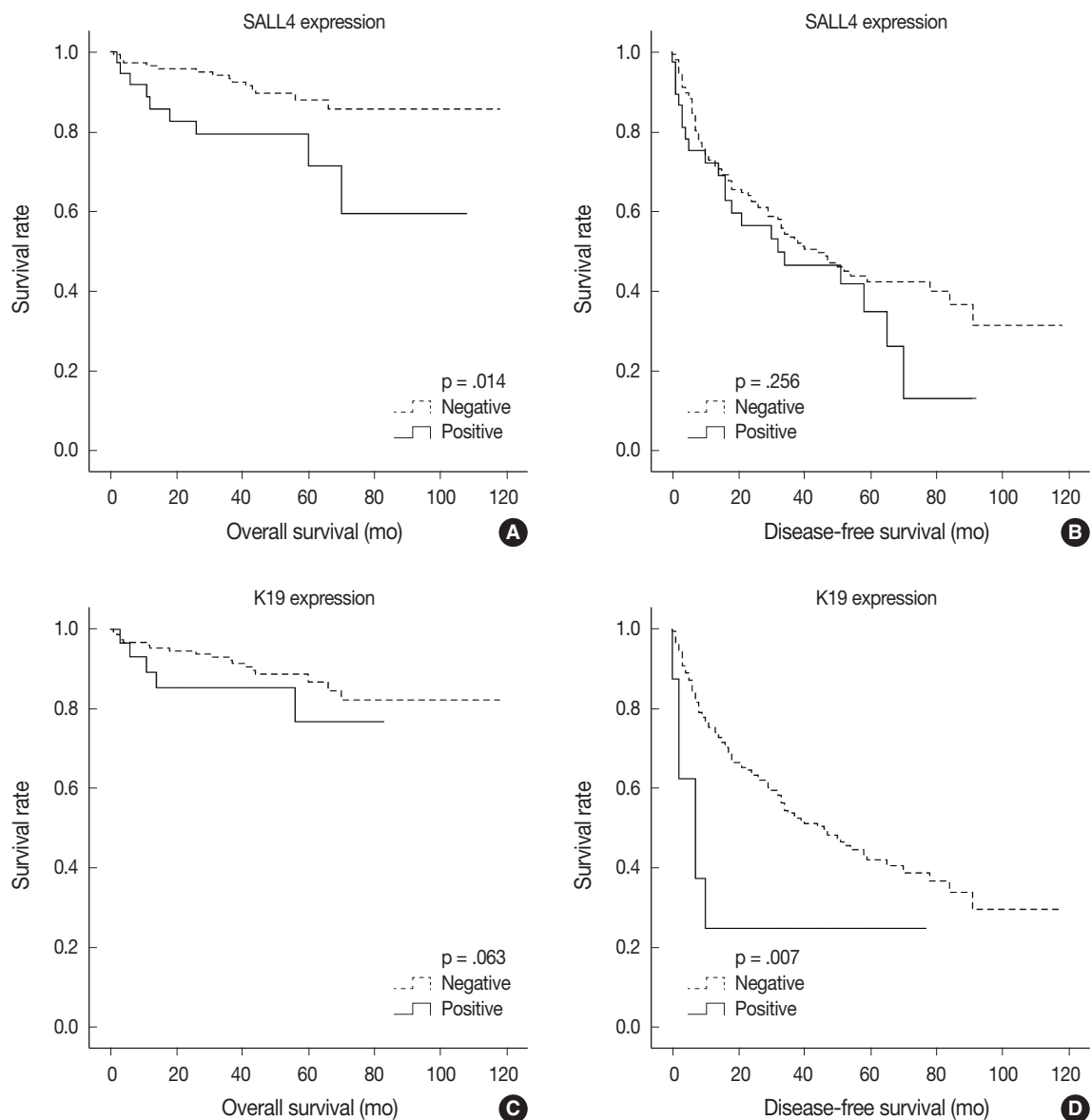


Fig. 3. Kaplan-Meier survival curves demonstrating decreased overall survival (A) and disease-free survival (B) in HCCs with SALL4 expression, and decreased overall survival (C) and disease-free survival (D) in HCCs with K19 expression. HCC, hepatocellular carcinoma; SALL4, Sal-like protein 4.

($p = .019$), microvascular invasion ($p = .011$), younger age ($p = .020$), B-viral etiology ($p = .010$), and high serum α -fetoprotein (AFP) levels ($p = .023$), and K19 expression was more frequently associated with higher serum AFP levels ($p = .032$), major vascular invasion ($p = .010$), and higher pathological T stage (3 or 4, $p = .011$). Increased tumor size was also more frequent in K19-positive HCCs, although not statistically significant ($p = .076$).

DISCUSSION

HCCs with “stemness”-related marker expression—those that have the histomorphological features of conventional HCCs but express markers related to stemness on immunohistochemistry—have been receiving increasing interest over the past several years, as there is accumulating evidence that they are associated with aggressive behavior and poor prognosis, compared to conventional HCCs that do not express these markers.^{5,6} The

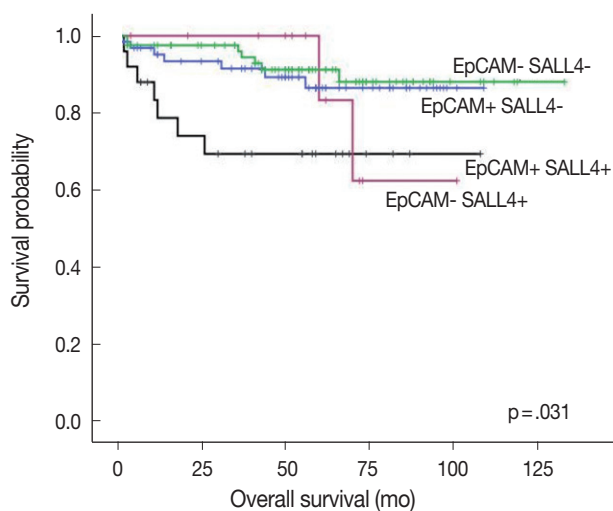


Fig. 4. Kaplan-Meier survival curves demonstrating the differences in overall survival in HCCs after combining EpCAM and SALL4 expression status. HCC, hepatocellular carcinoma; EpCAM, epithelial cellular adhesion molecule; SALL4, Sal-like protein 4.

more frequently discussed markers of stemness in HCCs include K19, EpCAM, and CD133; however, it is still uncertain which marker best represents stemness in HCCs, and there is still a growing number of putative markers of stemness in the literature, including the recently proposed SALL4, which need further validation.¹⁰ We were interested to see whether SALL4 expression in HCCs is indeed associated with the expression of other more established markers of stemness (K19 and EpCAM) and whether it has clinicopathological implications in our cohort of resected HCCs. Interestingly, we found SALL4 expression in 20.5% of HCCs, that SALL4 expression is positively correlated with EpCAM expression, and also that it has prognostic implications.

SALL4 is a zinc finger transcriptional activator located on chromosome 20q13.13-13.2 that is required for the maintenance of pluripotent embryonic stem cells, potentially through interactions with Oct3/4, Sox2, and Nanog.¹²⁻¹⁴ Mutation in SALL4 results in the Okihiro syndrome, a rare autosomal dominant disorder characterized by multiple organ defects.¹⁴ SALL4 has been found to be expressed in leukemias and hematopoietic stem cells, and also in solid tumors such as germ cell tumors and AFP-producing gastric cancers, suggesting that SALL4 may be a marker of embryonic stem cells and also cancer stem cells.¹⁵⁻¹⁸ In the fetal murine liver, SALL4 has been shown to be expressed in hepatic stem/progenitor cells, but the expression diminishes gradually during development and is not seen in adult hepatocytes.¹⁹ These findings suggest that SALL4 may be a good marker of hepatic stem/progenitor cells and HCC cancer stem cells.

Over the past two years, there has been increasing interest in SALL4 as a potential marker for identifying HCCs with features of “stemness,” aggressive behavior, and poor prognosis. Oikawa *et al.*⁹ demonstrated a decreased overall survival in their profiling analysis of 110 HCCs (from the microarray dataset published by Lee *et al.*¹), and also showed that the overexpression of SALL4 in liver cancer cells induced the expression of K19 and

Table 2. Multivariable analysis results: independent predictors of decreased overall survival and disease-free survival

	p-value	Hazard ratio	95% Confidence interval	
			Lower	Upper
Overall survival				
SALL4 positivity	.004	3.556	1.511	8.367
Multiplicity of tumor	.016	2.929	1.223	7.014
High T stage (T3 and 4)	.004	3.583	1.486	8.636
Disease-free survival				
Size (>3 cm)	.019	1.703	1.092	2.656
Multiplicity of tumor	.004	1.937	1.234	3.039

SALL4, Sal-like protein 4.

Table 3. Clinicopathologic characteristics and immunohistochemical stain results of 190 HCCs

	SALL4		p-value	K19 ^a		p-value	EpCAM ^a		p-value
	Negative	Positive		Negative	Positive		Negative	Positive	
Frequency	151 (79.5)	39 (20.5)		159 (84.1)	30 (15.9)		97 (51.3)	92 (48.7)	
Age (yr)			.858			.694			.020
< 60	81 (53.6)	20 (51.3)		83 (52.2)	17 (56.7)		43 (44.3)	57 (62.0)	
≥ 60	70 (46.4)	19 (48.7)		76 (47.8)	13 (43.3)		54 (55.7)	35 (38.0)	
Sex			1.000			.808			.113
Male	32 (21.2)	8 (20.5)		33 (20.8)	7 (23.3)		16 (16.5)	24 (26.1)	
Female	119 (78.8)	31 (79.5)		126 (79.2)	23 (76.7)		81 (83.5)	68 (73.9)	
Etiology			.319			.829			.010
Hepatitis B virus-related	40 (26.5)	14 (35.9)		45 (29.3)	9 (30.0)		36 (37.1)	18 (19.6)	
Non-hepatitis B virus-related	111 (73.5)	25 (64.1)		114 (71.7)	8 (70.0)		61 (62.9)	74 (80.3)	
Serum α -fetoprotein (IU/mL) (n = 132)			1.000			.032			.023
< 1,000	76 (76)	25 (78.1)		86 (80.4)	14 (58.3)		54 (85.7)	46 (79.3)	
≥ 1,000	24 (24)	7 (21.9)		21 (19.6)	10 (41.7)		9 (14.3)	22 (20.7)	
Multiplicity			.825			.328			.372
Absent	120 (79.5)	32 (82.1)		129 (81.1)	22 (73.3)		80 (82.5)	71 (77.2)	
Present	31 (20.5)	7 (17.9)		30 (18.9)	8 (26.7)		17 (17.5)	21 (22.8)	
Tumor size (cm) ^b			.432			.076			.873
< 5	105 (69.5)	30 (76.9)		118 (74.2)	17 (56.7)		70 (72.2)	65 (70.7)	
≥ 5	16 (30.5)	9 (23.1)		41 (25.8)	13 (43.3)		27 (27.8)	27 (29.3)	
Pathologic T stage			1.000			.011			.266
pT1/pT2	122 (80.8)	32 (82.1)		134 (84.3)	19 (63.3)		82 (84.5)	71 (77.2)	
pT3a/pT3b/pT4	29 (19.2)	7 (17.9)		25 (15.7)	11 (36.7)		15 (15.5)	21 (22.8)	
Edmondson-Steiner grade			.410			.648			.019
I/II	36 (23.8)	12 (30.8)		42 (26.4)	6 (20.0)		32 (33)	16 (17.4)	
III/IV	115 (76.2)	27 (69.2)		117 (73.6)	24 (80.0)		65 (67)	76 (82.6)	
Microvascular invasion			.581			.685			.011
Absent	94 (62.3)	22 (56.4)		98 (61.6)	17 (56.7)		68 (70.1)	47 (51.1)	
Present	57 (37.7)	17 (43.6)		61 (38.4)	13 (43.3)		29 (29.9)	45 (48.9)	
Major vessel invasion ^c			.781			.010			.366
Absent	134 (88.7)	34 (87.2)		145 (91.2)	22 (73.3)		88 (90.7)	79 (85.9)	
Present	17 (11.3)	5 (12.8)		14 (8.8)	8 (26.7)		9 (9.3)	13 (14.1)	

Values are presented as number (%).

HCC, hepatocellular carcinomas; SALL4, Sal-like protein 4; EpCAM, epithelial cellular adhesion molecule.

^an = 189 (tissue core loss in 1 case); ^bSize of largest tumor in case of multiple tumors; ^cMain or first order branches of portal vein and/or one or more of right, middle or left hepatic veins.

EpCAM, suggesting that SALL4 may be a marker of stem cells. Zeng *et al.*¹¹ demonstrated a decreased recurrence-free survival in SALL4-positive HCCs, and SALL4 activation in cell lines resulted in the up-regulation of hepatic stem cell markers KRT19, EPCAM, and CD44. Another extensive study showed a poor overall survival in SALL4-positive HCCs in two independent cohorts (Singapore, n = 179; Hong Kong, n = 228), in addition to an enrichment of progenitor-like gene signatures and overexpression of proliferative and metastatic genes on gene expression analysis.¹⁰ In another recent analysis of Western HCCs, higher tumor grade, more frequent lymphovascular invasion and shorter recurrence-free and overall survivals were seen in SALL4-positive HCCs, although the SALL4-positivity was only seen very rarely (1.3%), suggesting differences in SALL4 expres-

sion status according to the etiology of HCC.²⁰ The expression frequency of SALL4 in HCC has in fact varied widely in different reports, ranging from 1.3% to 85%.^{9-11,20,21} It is plausible that a higher prevalence of hepatitis B virus infection may account for the higher frequency of SALL4-positivity in Eastern HCCs; interestingly, SALL4-positivity has been shown to be more frequently associated with hepatitis B virus infection.¹¹ In addition, the differences in the antibodies, immunohistochemistry protocols, and the interpretation methods for defining “SALL4-positivity” are also likely to account for the wide range of SALL4-positivity reported in the literature.

As it has been previously demonstrated that nuclear labeling for SALL4 in liver tissues is seen with high pH antigen retrieval and not as clearly with the conventional citrate buffer,⁹ we also

stained the same tissue microarrays for SALL4 using a different antigen retrieval method (Tris-EDTA buffer; pH 9.0) to see if there were differences in the staining pattern or frequency; however, the results were identical (data not shown). Therefore, SALL4 immunostaining is feasible using the citrate buffer (pH 6.0) for antigen retrieval. We found that the nuclear staining for SALL4 in the testicular seminoma was very intense, diffuse and finely granular, in comparison to most SALL4-positive HCCs in which the nuclear staining was weaker and punctate or clumped, similar to a previous report.²¹ In practice, when faced with the occasional diagnostic challenge of discriminating between HCC and yolk sac tumor—which may have similar morphological features and also positivity for AFP and glypican-3—SALL4 immunohistochemistry may play a role, as the strong and diffuse staining for SALL4 is rarely seen in HCCs.²¹ However, as for the utility of SALL4 in HCCs as a prognostic marker and a marker of “stemness,” further validation in independent cohorts of HCC would be necessary, as the staining is not as intense, and there is likely to be interobserver variation in the interpretation of SALL4 positivity. Although we found a significantly decreased overall survival and a higher frequency of EpCAM positivity in SALL4-positive HCCs compared to SALL4-negative HCCs, we performed a semi-manual count of the SALL4-labeling index with the help of an image analysis software, which is not always a feasible method in routine pathology practice in comparison to the distinct cytoplasmic staining for K19 or EpCAM.

Our finding of a positive correlation between SALL4 and EpCAM expression in HCCs, poor overall survival in SALL4-positive HCCs, and positive (albeit weak and sporadic) staining in the ductular reactions support the recent literature that SALL4 may be a useful marker of “stemness” in hepatic stem/progenitor cells and HCCs. However, in contrast to K19 or EpCAM, the nuclear staining is not as easily appreciable by immunohistochemistry, and other than being a prognostic indicator of poor overall survival, there were no significant correlations between SALL4 positivity and the clinicopathological parameters suggestive of aggressiveness. Therefore, while SALL4 is an independent prognostic factor for decreased overall survival in HCC patients and may be a potential marker for identifying the aggressive subgroup of HCCs with “stemness” features, further validation in larger HCC cohorts is required prior to further consideration of SALL4 as a good marker of “stemness” in liver specimens.

Conflicts of Interest

No potential conflict of interest relevant to this article was reported.

Acknowledgments

This study was supported by grant number 14-2014-012 from the SNUBH Research Fund, and the Basic Science Research Program through NRF funded by the Ministry of Education (2013R1A1A2062320).

REFERENCES

1. Lee JS, Heo J, Libbrecht L, *et al.* A novel prognostic subtype of human hepatocellular carcinoma derived from hepatic progenitor cells. *Nat Med* 2006; 12: 410-6.
2. Nault JC, De Reynies A, Villanueva A, *et al.* A hepatocellular carcinoma 5-gene score associated with survival of patients after liver resection. *Gastroenterology* 2013; 145: 176-87.
3. Woo HG, Lee JH, Yoon JH, *et al.* Identification of a cholangiocarcinoma-like gene expression trait in hepatocellular carcinoma. *Cancer Res* 2010; 70: 3034-41.
4. Yamashita T, Forgues M, Wang W, *et al.* EpCAM and alpha-fetoprotein expression defines novel prognostic subtypes of hepatocellular carcinoma. *Cancer Res* 2008; 68: 1451-61.
5. Kim H, Choi GH, Na DC, *et al.* Human hepatocellular carcinomas with “Stemness”-related marker expression: keratin 19 expression and a poor prognosis. *Hepatology* 2011; 54: 1707-17.
6. Kim H, Park YN. Hepatocellular carcinomas expressing ‘stemness’-related markers: clinicopathological characteristics. *Dig Dis* 2014; 32: 778-85.
7. Govaere O, Komuta M, Berkers J, *et al.* Keratin 19: a key role player in the invasion of human hepatocellular carcinomas. *Gut* 2014; 63: 674-85.
8. Kim H, Yoo JE, Cho JY, *et al.* Telomere length, TERT and shelterin complex proteins in hepatocellular carcinomas expressing “stemness”-related markers. *J Hepatol* 2013; 59: 746-52.
9. Oikawa T, Kamiya A, Zeniya M, *et al.* Sal-like protein 4 (SALL4), a stem cell biomarker in liver cancers. *Hepatology* 2013; 57: 1469-83.
10. Yong KJ, Gao C, Lim JS, *et al.* Oncofetal gene SALL4 in aggressive hepatocellular carcinoma. *N Engl J Med* 2013; 368: 2266-76.
11. Zeng SS, Yamashita T, Kondo M, *et al.* The transcription factor SALL4 regulates stemness of EpCAM-positive hepatocellular carcinoma. *J Hepatol* 2014; 60: 127-34.
12. Zhang J, Tam WL, Tong GQ, *et al.* SALL4 modulates embryonic stem cell pluripotency and early embryonic development by the transcriptional regulation of Pou5f1. *Nat Cell Biol* 2006; 8: 1114-23.
13. Wu Q, Chen X, Zhang J, *et al.* SALL4 interacts with Nanog and occupies Nanog genomic sites in embryonic stem cells. *J Biol Chem* 2006; 281: 24090-4.
14. Kohlhasse J, Heinrich M, Schubert L, *et al.* Okihiro syndrome is

- caused by *SALL4* mutations. *Hum Mol Genet* 2002; 11: 2979-87.
15. Ikeda H, Sato Y, Yoneda N, *et al.* α -Fetoprotein-producing gastric carcinoma and combined hepatocellular and cholangiocarcinoma show similar morphology but different histogenesis with respect to *SALL4* expression. *Hum Pathol* 2012; 43: 1955-63.
 16. Ushiku T, Shinozaki A, Shibahara J, *et al.* *SALL4* represents fetal gut differentiation of gastric cancer, and is diagnostically useful in distinguishing hepatoid gastric carcinoma from hepatocellular carcinoma. *Am J Surg Pathol* 2010; 34: 533-40.
 17. Ma Y, Cui W, Yang J, *et al.* *SALL4*, a novel oncogene, is constitutively expressed in human acute myeloid leukemia (AML) and induces AML in transgenic mice. *Blood* 2006; 108: 2726-35.
 18. Cao D, Humphrey PA, Allan RW. *SALL4* is a novel sensitive and specific marker for metastatic germ cell tumors, with particular utility in detection of metastatic yolk sac tumors. *Cancer* 2009; 115: 2640-51.
 19. Oikawa T, Kamiya A, Kakinuma S, *et al.* *SALL4* regulates cell fate decision in fetal hepatic stem/progenitor cells. *Gastroenterology* 2009; 136: 1000-11.
 20. Liu TC, Vachharajani N, Chapman WC, Brunt EM. *SALL4* immunoreactivity predicts prognosis in Western hepatocellular carcinoma patients but is a rare event: a study of 236 cases. *Am J Surg Pathol* 2014; 38: 966-72.
 21. Gonzalez-Roibon N, Katz B, Chau A, *et al.* Immunohistochemical expression of *SALL4* in hepatocellular carcinoma, a potential pitfall in the differential diagnosis of yolk sac tumors. *Hum Pathol* 2013; 44: 1293-9.

Membranous Insulin-like Growth Factor-1 Receptor (IGF1R) Expression Is Predictive of Poor Prognosis in Patients with Epidermal Growth Factor Receptor (*EGFR*)-Mutant Lung Adenocarcinoma

Eunhyang Park^{1*} · Soo Young Park^{2*}
Hyojin Kim¹ · Ping-Li Sun²
Yan Jin² · Suk Ki Cho³
Kwhanmien Kim³ · Choon-Taek Lee⁴
Jin-Haeng Chung^{1,2}

¹Department of Pathology, Seoul National University College of Medicine, Seoul; Departments of ²Pathology, ³Thoracic and Cardiovascular Surgery, and ⁴Internal Medicine, Seoul National University Bundang Hospital, Seoul National University College of Medicine, Seongnam, Korea

Received: July 7, 2015

Revised: July 7, 2015

Accepted: July 9, 2015

Corresponding Author

Jin-Haeng Chung, MD, PhD
Department of Pathology, Seoul National University Bundang Hospital, 82 Gumi-ro 173beon-gil, Bundang-gu, Seongnam 13620, Korea
Tel: +82-31-787-7713
Fax: +82-31-787-4012
E-mail: chungjh@snu.ac.kr

*Eunhyang Park and Soo Young Park contributed equally to this work.

Background: Insulin-like growth factor-1 receptor (IGF1R) is a membrane receptor-type tyrosine kinase that has attracted considerable attention as a potential therapeutic target, although its clinical significance in non-small cell lung cancer (NSCLC) is controversial. This study aimed to clarify the clinical significance of IGF1R expression in human NSCLC. **Methods:** IGF1R protein expression was evaluated using immunohistochemistry in 372 patients with NSCLC who underwent curative surgical resection (146 squamous cell carcinomas [SqCCs] and 226 adenocarcinomas [ADCs]). We then analyzed correlations between expression of IGF1R and clinicopathological and molecular features and prognostic significance. **Results:** Membranous and cytoplasmic IGF1R expression were significantly higher in SqCCs than in ADCs. In patients with SqCC, membranous IGF1R expression was associated with absence of vascular, lymphatic, and perineural invasion; lower stage; and better progression-free survival (PFS) (hazard ratio [HR], 0.586; $p = .040$). In patients with ADC, IGF1R expression did not have a significant prognostic value; however, in the subgroup of epidermal growth factor receptor (*EGFR*)-mutant ADC, membranous IGF1R expression was associated with lymphatic and perineural invasion, solid predominant histology, and higher cancer stage and was significantly associated with worse PFS (HR, 2.582; $p = .009$). **Conclusions:** Lung ADC and SqCC showed distinct IGF1R expression profiles that demonstrated prognostic significance. High membranous IGF1R expression was predictive of poor PFS in *EGFR*-mutant lung ADC, while it was predictive of better PFS in SqCC. These findings will help improve study design for subsequent investigations and select patients for future anti-IGF1R therapy.

Key Words: Carcinoma, non-small-cell lung; Insulin-like growth factor-1 receptor; Receptor, epidermal growth factor; Immunohistochemistry; Membranous expression

Epidermal growth factor receptor (EGFR)-tyrosine kinase inhibitors (TKIs) have been used to treat non-small cell lung cancer (NSCLC), and a better response and prolonged survival have been observed in patients who harbor *EGFR* mutations.^{1,2} However, despite a dramatic response, most NSCLC patients experience drug resistance and tumor progression. Two major resistance mechanisms of a secondary point mutation of T790M and *MET* gene amplification have been reported.^{3,4} However, the resistance mechanism remains largely unknown.

Insulin-like growth factor-1 receptor (IGF1R) is a membrane receptor-type tyrosine kinase that plays a crucial role in cancer cell proliferation, inhibition of apoptosis, angiogenesis, and anchorage-independent growth via the phosphatidylinositol 3-ki-

nase-AKT and RAS/RAF/mitogen activated protein kinase signaling pathways.^{5,6} In addition, both *in vitro* and *in vivo* studies have revealed extensive crosstalk between EGFR and IGF1R signaling on multiple levels.⁷⁻¹⁰ These data indicate that IGF1R can lead to acquired resistance against *EGFR*-targeted drugs, and targeting both receptors could provide better efficacy in cancer treatment by overcoming drug resistance.^{11,12}

Despite extensive research to clarify the clinical significance of IGF1R in NSCLC, the characteristics and implicated prognostic value remain controversial. Cappuzzo *et al.*¹⁰ have suggested that patients who have high IGF1R expression and are receiving gefitinib therapy might have improved outcomes compared with those with lower expression. In addition, Kikuchi *et al.*¹³ reported

that low IGF1R expression was associated with poor prognosis in lung adenocarcinomas (ADCs). In contrast, Tsuta *et al.*¹⁴ revealed that, in surgically treated patients, IGF1R protein expression, copy number and IGF1R bright-field *in-situ* hybridization positivity did not correlate with overall survival. These discrepancies might partly be attributable to the heterogeneity of the study groups including ethnicity, histologic subtypes, and molecular subtypes. To address these differences, we investigated the expression and clinical significance of IGF1R expression in histologically and genotypically specified subgroups of NSCLC.

MATERIALS AND METHODS

Patients

We collected tumor samples from 372 patients who underwent curative surgical resection for NSCLC at Seoul National University Bundang Hospital in Korea, between May 2003 and December 2008. Patients who did not undergo curative resection and those who had a history of malignancy, preoperative chemotherapy, or radiotherapy were excluded. Smoking status was defined as never-smoker (< 100 lifetime cigarettes) or smoker. Tumors were staged using the American Joint Committee on Cancer (AJCC) TNM classification of malignant tumors seventh edition criteria, and the histological type and grade of differentiation of tumors were determined according to the classification system developed by the World Health Organization fourth edition.^{15,16} Overall survival (OS) was measured from the date of lung cancer surgery until the time of death, and progression-free survival (PFS) was measured from the date of surgery until recurrence or death. Clinicopathological characteristics of the patients are summarized in Table 1. All patients provided written informed consent, and this study was approved by the Institutional Review Board (IRB) of Seoul National University Bundang Hospital.

IGF1R expression according to immunohistochemistry

Formalin-fixed paraffin-embedded tissues were sectioned at a thickness of 4 μ m and stained with rabbit monoclonal antibody against human IGF1R (G11, Ventana Medical Systems, Tucson, AZ, USA) using an automated immunostainer (Ventana Medical Systems). Placental tissue was used as a positive control, and non-immune serum was used as a negative control instead of the

Table 1. Patient characteristics

Characteristic	No. (%) (n=372)
Median age (range, yr)	66 (39–83)
Sex	
Male	249 (66.9)
Female	123 (33.1)
Histology	
SqCC	146 (39.2)
ADC	226 (60.8)
Smoking history	
Never	146 (39.2)
Former/current	226 (60.8)
Tumor size (cm)	
≤ 3	143 (38.4)
> 3	229 (61.6)
Pleural invasion	
Absent	219 (58.9)
Present	153 (41.1)
Vascular invasion	
Absent	313 (84.1)
Present	59 (15.9)
Lymphatic invasion	
Absent	209 (56.2)
Present	163 (43.8)
Perineural invasion	
Absent	342 (91.9)
Present	30 (8.1)
Pathological stage	
I	165 (42.7)
II	99 (25.6)
III	108 (28.0)

SqCC, squamous cell carcinoma; ADC, adenocarcinoma.

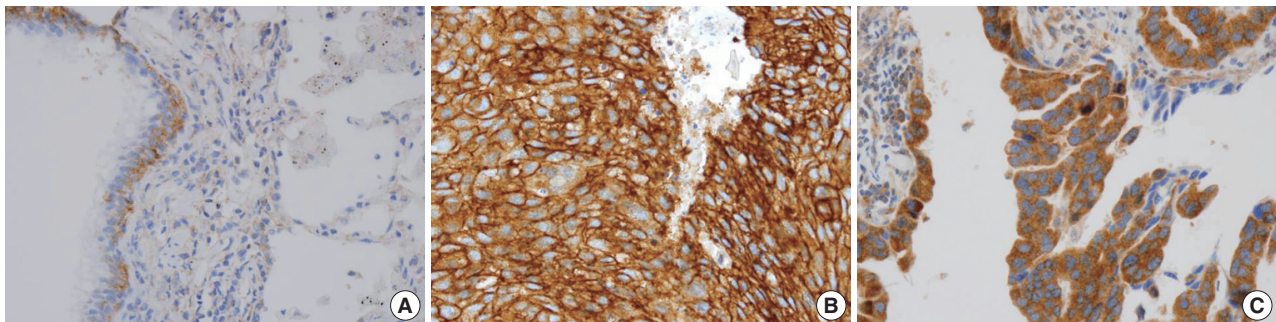


Fig. 1. Representative immunohistochemistry examples of membranous insulin-like growth factor-1 receptor (IGF1R) expression. IGF1R expression in non-neoplastic lung tissue (A), membranous IGF1R expression in squamous cell carcinoma (B), membranous IGF1R expression of adenocarcinoma (C).

primary antibody. Adjacent normal-appearing bronchial epithelium within each tissue section served as an internal reference.

The H-score (semiquantitative system with a total score range of 0–300) was used to evaluate immunohistochemical staining, and membranous and cytoplasmic staining were evaluated separately. The percentage of positive cells (0%–100%) was multiplied by the dominant intensity score of staining. The intensity score was defined as follows: 0, no appreciable staining; 1, barely detectable staining; 2, distinct brown staining; and 3, strong dark brown staining. A total score range of 0 to 300 was generated for each sample, where median score was used as a cutoff value. All of the slides were evaluated by two pathologists (E.P. and H.K.) in a blinded manner. If discrepancies occurred, a consensus score was reached.

Study of *EGFR*, *KRAS*, *ALK*, *ROS1*, and *MET* mutations

Samples were analyzed for *EGFR* mutations within exons 18 to 21 and *KRAS* exon 2 (codons 12, 13, and 61) using polymerase chain reaction and direct DNA sequencing or pyrosequencing methods.¹⁷ *In situ* hybridization was performed for *ALK* and *ROS1* rearrangement and *MET* amplification.^{18–20}

Statistical analyses

Statistical analyses were performed using IBM SPSS ver. 19.0 (SPSS Inc., Chicago, IL, USA). All of the values were based on two-sided statistical analysis, and a p-value of < 0.05 was determined to indicate a statistically significant difference.

RESULTS

IGF1R expression according to immunohistochemistry

In non-neoplastic lung tissue, the distribution of IGF1R expression was different among cell types. Bronchial basal cells showed constant weak membranous and distinct cytoplasmic expression of IGF1R. Alveolar pneumocytes and alveolar macrophages showed negative to negligible cytoplasmic positivity. In NSCLC, the prevalence of IGF1R expression was significantly higher in squamous cell carcinoma (SqCC) compared with ADC ($p = .000$), and representative examples are shown in Fig. 1.

IGF1R expression and clinical outcomes in SqCC

Membranous and cytoplasmic IGF1R expression were evident in the 146 patients with SqCC. Membranous IGF1R expression was identified in 100 of 146 patients (68.5%) and was significantly associated with absence of vascular invasion ($p = .039$), absence of lymphatic invasion ($p = .047$), absence of perineural in-

vasion ($p = .027$), lower stage ($p = .011$), and better PFS ($p = .011$) and OS ($p = .034$) compared to the negative subgroup (Table 2, Fig. 2A, B). Multivariate analysis indicated that membranous IGF1R expression was an independent prognostic factor for better PFS (hazard ratio [HR], 0.586; 95% confidence interval [CI], 0.352 to 0.975; $p = .040$) but not OS (HR, 0.550; 95% CI, 0.302 to 1.002; $p = .051$). Cytoplasmic IGF1R expression was identified in 107 of 146 patients (73.3%) and tended to correlate with younger age ($p = .021$) and absence of pleural invasion ($p = .013$). Patients were additionally divided into four groups: group I that was positive for both membranous and cytoplasmic expression (M+/C+), group II that was membranous expression-positive and cytoplasmic expression-negative (M+/C-), group III that was membranous expression-negative and cyto-

Table 2. Clinicopathological characteristics in relation to expression of IGF1R in SqCC

Characteristic	Membranous IGF1R staining		p-value
	Positive	Negative	
Age (yr)			
<65	57 (69.5)	25 (30.5)	.451
≥65	43 (67.2)	21 (32.8)	
Sex			
Male	93 (68.4)	43 (31.6)	.611
Female	7 (70.0)	3 (30.0)	
Smoking history			
Never	7 (63.6)	4 (36.4)	.476
Former/current	93 (68.9)	42 (31.1)	
Tumor size (cm)			
≤3	32 (74.4)	11 (25.6)	.213
>3	68 (66.0)	35 (34.0)	
Differentiation			
Well	7 (70.0)	3 (30.0)	.453
Moderately	80 (70.8)	33 (29.2)	
Poorly	11 (61.1)	7 (38.9)	
Pleural invasion			
Absent	71 (72.4)	27 (27.6)	.101
Present	29 (60.4)	19 (39.6)	
Vascular invasion			
Absent	84 (72.4)	32 (27.6)	.039
Present	16 (53.3)	14 (46.7)	
Lymphatic invasion			
Absent	62 (74.7)	21 (25.3)	.047
Present	38 (60.3)	25 (39.7)	
Perineural invasion			
Absent	93 (71.5)	37 (28.5)	.027
Present	7 (43.8)	9 (56.3)	
Pathological stage			
I	34 (75.6)	11 (24.4)	.011
II	48 (75.0)	16 (25.0)	
III	18 (48.6)	19 (51.4)	

Values are presented as number (%).

IGF1R, insulin-like growth factor-1 receptor; SqCC, squamous cell carcinoma.

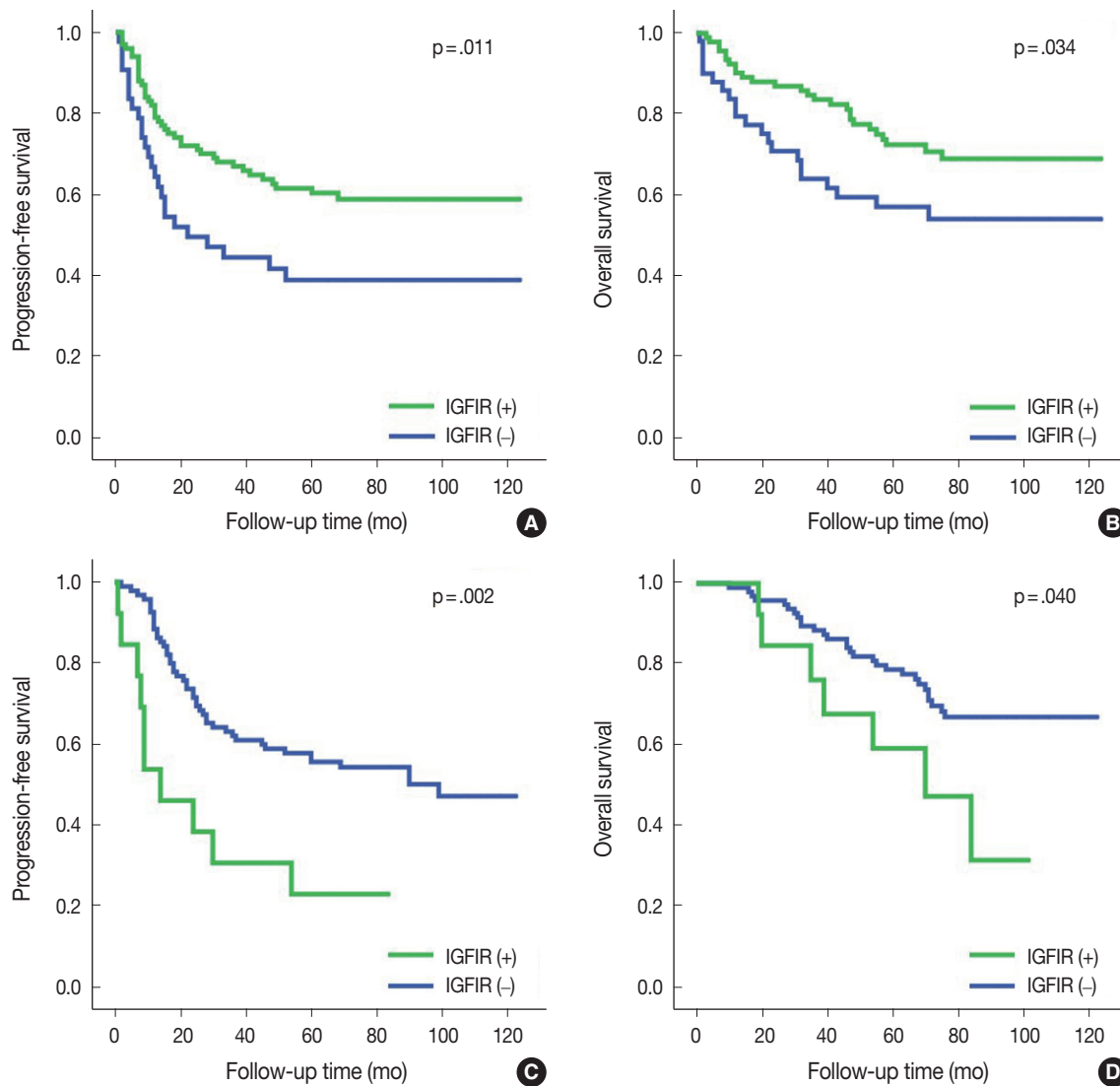


Fig. 2. Kaplan-Meier survival analysis of progression-free survival and overall survival curves based on membranous insulin-like growth factor-1 receptor (IGF1R) expression. Membranous IGF1R expression had significantly better progression-free survival (A) and overall survival (B) in squamous cell carcinoma. Membranous IGF1R expression in epidermal growth factor receptor (*EGFR*)-mutant adenocarcinoma had significantly poor progression-free survival (C) and a trend toward poor overall survival (D).

plasmic expression-positive (M-/C+), and group IV that was negative for both membranous and cytoplasmic expression (M-/C-). The groups included 85, 16, 24, and 21 patients, respectively. On univariate analysis, group II that was membranous expression-positive and cytoplasmic expression-negative (M+/C-) showed the best PFS ($p = .021$) and OS ($p = .028$), followed by group I (M+/C+), group IV (M-/C-), and group III (M-/C+).

IGF1R expression and clinical outcomes in ADC

In ADC patients, IGF1R expression was predominantly cytoplasmic with weak membranous staining. Positive membranous IGF1R expression was identified in 31 of 226 patients (13.7%)

and was significantly associated with perineural invasion ($p = .040$), although the measure had no significant prognostic value. Cytoplasmic expression was identified in 141 of 226 patients (62.4%) and correlated with smaller tumor size ($p = .002$) and absence of vascular invasion ($p = .046$), but these results were not statistically significant for PFS or OS.

IGF1R expression and clinical outcomes in *EGFR*-mutant ADC

EGFR mutation was found in 108 of 226 patients (47.8%). The most common mutation was in-frame deletion in exon 19 (57 of 108, 52.8%), followed by missense mutation (L858R) in

exon 21 (35 of 108, 32.4%). When ADC samples were stratified into *EGFR*-mutant and *EGFR*-wild type subgroups, membranous IGF1R expression was identified in 13 of 108 patients (12.0%) in the *EGFR*-mutant ADC subgroup. Membranous IGF1R expression was associated with lymphatic invasion ($p = .039$), perineural invasion ($p = .004$), solid predominant histology ($p = .037$), and higher cancer stage ($p = .030$) and showed a significantly worse PFS ($p = .002$) and OS ($p = .040$) compared with those without membranous expression (Table 3, Fig. 2C, D). Multivariate analysis revealed that membranous IGF1R expression was an independent prognostic factor for worse PFS (HR, 2.582; 95% CI, 1.265 to 5.271; $p = .009$) but not for OS (HR, 1.369; 95% CI, 0.558 to 3.359; $p = .492$) in patients with *EGFR*-mutant ADC. Cytoplasmic IGF1R expression was not associated with any clinicopathological parameters in PFS or OS.

In *EGFR*-wild type ADC, membranous IGF1R expression was identified in 23 of 118 patients (19.5%) and was not correlated with clinicopathological parameters. In contrast, cytoplasmic IGF1R expression was observed in 86 patients (73.5%) who showed significantly better PFS ($p = .033$) and OS ($p = .05$) compared to the negative subgroup. No positive membranous IGF1R expression was observed for TKI-treated *EGFR*-mutant ADC ($n = 36$). Positive IGF1R cytoplasmic expression was seen in 15 of 36 patients (41.7%) but was not associated with PFS or OS. In addition, IGF1R expression was not correlated with *ALK*, *KRAS*, *ROS1*, or *MET* mutation ($p > .05$).

DISCUSSION

We determined the possible clinical significance of IGF1R expression in NSCLC. The main findings of this study are as follows: (1) the prevalence of IGF1R expression was significantly higher in SqCC compared with ADC; (2) in SqCC, membranous IGF1R expression was associated with significantly better PFS compared with those without membranous expression; (3) in ADC, membranous and cytoplasmic IGF1R expression had no significant prognostic value; (4) in the *EGFR*-mutant ADC subgroup, membranous IGF1R expression was significantly associated with worse PFS.

In SqCC, membranous IGF1R expression was associated with several good prognostic clinicopathological parameters and showed a linear relationship with PFS. Several previous studies have delineated the association between IGF1R expression and better OS, although the biologic mechanism is unclear.^{9,21} One possible explanation is that, because IGF1R is expressed in normal bronchial basal cells, the progenitors of SqCC tumor cells,

Table 3. Clinicopathological characteristics in relation to expression of IGF1R in *EGFR*-mutant ADC

Characteristic	Membranous IGF1R staining		p-value
	Positive	Negative	
Age (yr)			
<65	8 (11.0)	65 (89.0)	.417
≥65	5 (14.3)	30 (85.7)	
Sex			
Male	5 (11.6)	38 (88.4)	.583
Female	8 (12.3)	57 (87.7)	
Smoking history			
Never	8 (11.0)	65 (89.0)	.417
Former/current	5 (14.3)	30 (85.7)	
Tumor size (cm)			
≤3	3 (6.1)	46 (93.9)	.075
>3	10 (16.9)	49 (83.1)	
Pleural invasion			
Absent	7 (11.9)	52 (88.1)	.590
Present	6 (12.2)	43 (87.8)	
Vascular invasion			
Absent	9 (9.6)	85 (90.4)	.064
Present	4 (28.6)	10 (71.4)	
Lymphatic invasion			
Absent	4 (6.5)	58 (93.5)	.039
Present	9 (19.6)	37 (80.4)	
Perineural invasion			
Absent	9 (8.9)	92 (91.1)	.004
Present	4 (57.1)	3 (42.9)	
Predominant pattern			
Acinar	7 (9.2)	69 (90.8)	.303
Papillary	3 (21.4)	11 (78.6)	
Solid	2 (28.6)	5 (71.4)	
Lepidic	1 (9.1)	10 (90.9)	
Presence of lepidic			
Positive	3 (5.9)	48 (94.1)	.057
Negative	10 (17.5)	47 (82.5)	
Presence of solid			
Positive	4 (33.3)	8 (66.7)	.037
Negative	9 (9.4)	87 (90.6)	
Pathological stage			
I	3 (4.9)	58 (95.1)	.030
II	2 (16.7)	10 (83.3)	
III	8 (22.9)	27 (77.1)	

Values are presented as number (%).

IGF1R, insulin-like growth factor-1 receptor; EGFR, epidermal growth factor receptor; ADC, adenocarcinoma.

membranous IGF1R expression on tumor cells could be interpreted as an activated and overexpressed form of the physiological function of the receptor.²² If the tumor cell displays higher IGF1R expression, it is a more mature and well-differentiated cell that still depends on the normal IGF1R pathway and can be expected to become indolent during the course of the disease. An alternative explanation, based on the fact that the degree of re-

ceptor expression would reflect the level of its ligands, is that, if the level of the ligand is higher, more receptors would be occupied and internalized for signaling, while low circulating ligand level would result in receptor overexpression as a compensatory mechanism. Therefore, positive membranous IGF1R expression could be interpreted as a level of IGF1 or IGF2 within or lower than the normal range, which could imply that the tumor has low proliferative activity.

Not only was membranous IGF1R expression significantly associated with better survival in SqCC, but the membranous-positive and cytoplasmic-negative subgroup (M+/C-) had the best PFS and OS in SqCC. This result suggests opposing effects of IGF1R protein expression based on its location. This is the first study to evaluate the cellular location of IGF1R expression in NSCLC and provides better understanding of the relevance of pattern of IGF1R staining in NSCLC.

In ADC patients, IGF1R expression did not affect clinical outcome. However, when we classified these patients on the basis of *EGFR*-mutation status, the *EGFR*-mutant ADC subgroup showed strong correlations with several negative prognostic clinicopathological parameters and worse survival. Therefore, IGF1R was identified as a poor prognostic factor in *EGFR*-mutant ADC, which is opposite the result seen in the SqCC group.

This difference prompted speculation that the role of the IGF1R pathway in ADC might differ according to the presence of *EGFR* mutations. We assume that, in the *EGFR*-mutant ADC subgroup, the IGF1R pathway would activate downstream targets on the EGFR, which could promote cellular proliferation, inhibition of apoptosis, angiogenesis, and anchorage-independent growth. In NSCLC, experimental studies have demonstrated that IGF1R activation can underlie resistance to *EGFR*-targeted therapies, and several clinical trials have indicated that co-expression of EGFR and IGF1R correlates with poor survival.^{8,23} Furthermore, Yeo *et al.*²⁴ recently reported that IGF1R expression was a negative predictive factor for response to *EGFR*-TKI treatment in *EGFR*-mutant ADC patients. Although these data indicate that IGF1R leads to acquired resistance against *EGFR*-targeted drugs, none of the patients in the *EGFR*-TKI treated group showed membranous IGF1R expression.

In summary, the implication of IGF1R expression in NSCLC differs according to subtype, and the clinical significance of IGF1R expression should be interpreted after considering the histology and genotype of the tumor. High membranous IGF1R expression might be a biomarker of better PFS in SqCC and of poor PFS in *EGFR*-mutant lung ADC. These findings will serve to improve study design for subsequent investigations into IGF1R and NSCLC and to select patients for future anti-IGF1R therapy.

F1R and NSCLC and to select patients for future anti-IGF1R therapy.

Conflicts of Interest

No potential conflict of interest relevant to this article was reported.

Acknowledgments

This work was supported by the Basic Science Research Program through the National Research Foundation of Korea funded by the Ministry of Education, Science and Technology (2013-059757) and partly by a grant from the Korea Healthcare Technology R&D Project, Ministry of Health and Welfare, Republic of Korea (HI14C1907). The authors thank J. Patrick Barron, Professor Emeritus, Tokyo Medical University and Adjunct Professor, Seoul National University Bundang Hospital for his pro bono editing of this manuscript.

REFERENCES

1. Mok TS, Wu YL, Thongprasert S, *et al.* Gefitinib or carboplatin-paclitaxel in pulmonary adenocarcinoma. *N Engl J Med* 2009; 361: 947-57.
2. Fukuoka M, Wu YL, Thongprasert S, *et al.* Biomarker analyses and final overall survival results from a phase III, randomized, open-label, first-line study of gefitinib versus carboplatin/paclitaxel in clinically selected patients with advanced non-small-cell lung cancer in Asia (IPASS). *J Clin Oncol* 2011; 29: 2866-74.
3. Yun CH, Mengwasser KE, Toms AV, *et al.* The T790M mutation in *EGFR* kinase causes drug resistance by increasing the affinity for ATP. *Proc Natl Acad Sci U S A* 2008; 105: 2070-5.
4. Engelman JA, Zejnullahu K, Mitsudomi T, *et al.* *MET* amplification leads to gefitinib resistance in lung cancer by activating ERBB3 signaling. *Science* 2007; 316: 1039-43.
5. Ward CW, Garrett TP, McKern NM, *et al.* The three dimensional structure of the type I insulin-like growth factor receptor. *Mol Pathol* 2001; 54: 125-32.
6. Blakesley VA, Stannard BS, Kalebic T, Helman LJ, LeRoith D. Role of the IGF-I receptor in mutagenesis and tumor promotion. *J Endocrinol* 1997; 152: 339-44.
7. Bianconi F, Baldelli E, Ludovini V, Crino L, Flacco A, Valigi P. Computational model of EGFR and IGF1R pathways in lung cancer: a systems biology approach for translational oncology. *Biotechnol Adv* 2012; 30: 142-53.
8. Ludovini V, Bellezza G, Pistola L, *et al.* High coexpression of both insulin-like growth factor receptor-1 (IGFR-1) and epidermal

- growth factor receptor (EGFR) is associated with shorter disease-free survival in resected non-small-cell lung cancer patients. *Ann Oncol* 2009; 20: 842-9.
9. Dziadziuszko R, Merrick DT, Witta SE, *et al.* Insulin-like growth factor receptor 1 (IGF1R) gene copy number is associated with survival in operable non-small-cell lung cancer: a comparison between IGF1R fluorescent in situ hybridization, protein expression, and mRNA expression. *J Clin Oncol* 2010; 28: 2174-80.
 10. Cappuzzo F, Tallini G, Finocchiaro G, *et al.* Insulin-like growth factor receptor 1 (IGF1R) expression and survival in surgically resected non-small-cell lung cancer (NSCLC) patients. *Ann Oncol* 2010; 21: 562-7.
 11. van der Veecken J, Oliveira S, Schifflers RM, Storm G, van Bergen En Henegouwen PM, Roovers RC. Crosstalk between epidermal growth factor receptor- and insulin-like growth factor-1 receptor signaling: implications for cancer therapy. *Curr Cancer Drug Targets* 2009; 9: 748-60.
 12. Morgillo F, Hong WK, Lee H. Insulin-like growth factor-1 receptor/epidermal growth factor receptor (EGFR) heterodimerization and resistance to epidermal growth factor receptor tyrosine kinase inhibitors in non-small-cell lung cancer. *J Clin Oncol* 2006; 24: 13032.
 13. Kikuchi R, Sonobe M, Kobayashi M, *et al.* Expression of IGF1R is associated with tumor differentiation and survival in patients with lung adenocarcinoma. *Ann Surg Oncol* 2012; 19 Suppl 3: S412-20.
 14. Tsuta K, Mimae T, Nitta H, *et al.* Insulin-like growth factor-1 receptor protein expression and gene copy number alterations in non-small cell lung carcinomas. *Hum Pathol* 2013; 44: 975-82.
 15. Edge S, Byrd DR, Compton CC, Fritz AG, Greene FL, Trotti A. *AJCC cancer staging manual*. 7th ed. New York: Springer, 2010.
 16. Travis WD, Brambilla E, Burke AP, Marx A, Nicholson AG. WHO classification of tumours of the lung, pleura, thymus and heart. 4th ed. Lyon: IARC Press, 2015.
 17. Lee HJ, Xu X, Kim H, *et al.* Comparison of direct sequencing, PNA clamping-real time polymerase chain reaction, and pyrosequencing methods for the detection of *EGFR* mutations in non-small cell lung carcinoma and the correlation with clinical responses to EGFR tyrosine kinase inhibitor treatment. *Korean J Pathol* 2013; 47: 52-60.
 18. Kim H, Yoo SB, Choe JY, *et al.* Detection of *ALK* gene rearrangement in non-small cell lung cancer: a comparison of fluorescence *in situ* hybridization and chromogenic *in situ* hybridization with correlation of ALK protein expression. *J Thorac Oncol* 2011; 6: 1359-66.
 19. Jin Y, Sun PL, Kim H, *et al.* *MET* gene copy number gain is an independent poor prognostic marker in Korean stage I lung adenocarcinomas. *Ann Surg Oncol* 2014; 21: 621-8.
 20. Jin Y, Sun PL, Kim H, *et al.* *ROS1* gene rearrangement and copy number gain in non-small cell lung cancer. *Virchows Arch* 2015; 466: 45-52.
 21. Reinmuth N, Kloos S, Warth A, *et al.* Insulin-like growth factor 1 pathway mutations and protein expression in resected non-small cell lung cancer. *Hum Pathol* 2014; 45: 1162-8.
 22. Sutherland KD, Berns A. Cell of origin of lung cancer. *Mol Oncol* 2010; 4: 397-403.
 23. Gately K, Forde L, Cuffe S, *et al.* High coexpression of both EGFR and IGF1R correlates with poor patient prognosis in resected non-small-cell lung cancer. *Clin Lung Cancer* 2014; 15: 58-66.
 24. Yeo CD, Park KH, Park CK, *et al.* Expression of insulin-like growth factor 1 receptor (IGF-1R) predicts poor responses to epidermal growth factor receptor (EGFR) tyrosine kinase inhibitors in non-small cell lung cancer patients harboring activating *EGFR* mutations. *Lung Cancer* 2015; 87: 311-7.

Parafibromin Staining Characteristics in Urothelial Carcinomas and Relationship with Prognostic Parameters

Serap Karaarslan · Banu Yaman¹
Hakan Ozturk²
Banu Sarsik Kumbaraci¹

Department of Pathology, Sifa University
Faculty of Medicine, Izmir;
¹Department of Pathology, Ege University
Faculty of Medicine, Izmir;
²Department of Urology, Sifa University
Faculty of Medicine, Izmir, Turkey

Received: February 26, 2015
Revised: August 5, 2015
Accepted: August 10, 2015

Corresponding Author

Serap Karaarslan, MD
Department of Pathology,
Sifa University Faculty of Medicine,
Sanayi Caddesi No. 7, Bornova, Izmir 35100, Turkey
Tel: +90-232-343-4445
Fax: +90-232-343-5656
E-mail: serapkaraarslan@gmail.com

Background: Parafibromin is a recently defined tumor suppressor gene. The aim of our study was to determine the relationships of parafibromin expression in urothelial carcinomas (UCs) with prognostic parameters and to evaluate the use of parafibromin as a potential marker of UC. **Methods:** Parafibromin expression was assessed in 49 UC specimens using immunohistochemistry. The correlations between parafibromin expression and clinical and pathologic parameters were investigated. **Results:** Of the patients, 42 (85.7%) were male, and the mean age was 69.6 ± 8.2 years (range, 54 to 88 years). Morphologically, the UCs were divided into two groups: papillary (n = 27) and non-papillary (n = 22). There were seven low-grade (14.3%) and 42 high-grade (85.7%) tumors. Parafibromin was negative in 13 tumors (26.5%), partially positive in 19 tumors (38.8%), and positive in 17 tumors (34.7%). Parafibromin expression was more negative in UCs from upper urinary locations (n = 17) and with muscularis propria invasion (n = 28), which was statistically significant (p = .009 and p = .007, respectively). There was no statistically significant relationship between parafibromin expression and gender, age, tumor grade, survival, or disease-free survival. **Conclusions:** We found that UC cases with parafibromin positivity had less of a tendency to show muscularis propria invasion and were more commonly located in the lower urinary system. These results need to be confirmed with studies based on larger case series.

Key Words: Parafibromin; Urothelial carcinoma; Muscularis propria; Papillary; Non-papillary

Urothelial neoplasms are the most common urinary tract cancers and can be located in the lower (bladder and urethra) or upper (pelvocalyceal cavities and ureter) urinary tract. Bladder tumors make up 90%–95% of all urothelial malignancies,¹ while upper urinary tract urothelial carcinomas (UUTUCs) are uncommon and make up only 5%.^{2–4} The natural history of bladder tumors and UUTUCs differ; 60% of UUTUCs, but only 15% of bladder tumors, are found to be invasive at the time of diagnosis.^{5–7} Tumor stage, histological grade, lymph node involvement, and type of surgical procedure used have been shown to be significant prognostic factors for urothelial carcinomas.^{8–10} Several classical clinicopathological, morphometric, cytometric, immunohistochemical, and molecular markers have also been shown to have prognostic significance, but the search for markers that affect patient outcome continues.

Parafibromin is a protein encoded by the hyperparathyroidism 2 (*HRPT2*) tumor suppressor gene. Mutations of this protein lead to autosomal dominant hyperparathyroidism-jaw tumor syndrome with parathyroid adenoma or carcinoma, mandibular or

maxillary fibro-osseous tumors, and renal neoplastic and non-neoplastic abnormalities such as Wilms' tumor, hamartoma, or cystic renal disease.^{11–13} The *HRPT2* gene, located in human chromosome 1q31.2, consists of 17 exons and spans 18.5 kb in the genome. The 2.7-kb transcript that it encodes is translated into a 531-amino acid parafibromin protein with a molecular weight of 60 kD.^{14,15} This gene might function as a tumor suppressor gene as *HRPT2*-inactivating mutations have been reported in various malignancies.^{16–21} These findings suggest a potential role of parafibromin in the pathogenesis and progression of malignancy.

The role of the newly discovered tumor suppressor gene parafibromin in urothelial carcinoma has not been investigated. We evaluated the immunohistochemistry of parafibromin expression in urothelial carcinoma and paired benign urothelium from patients undergoing transurethral resection, radical cystectomy (RC), and nephroureterectomy. The aim was to investigate the expression of parafibromin in urothelial carcinoma and to determine its role in tumor behavior and prognosis in urothelial carcinoma (UC) patients.

MATERIALS AND METHODS

Patient and tissue selection

The study cohort consisted of 49 cases diagnosed as urothelial carcinoma at a single center between January 2006 and December 2013. A total of 49 surgical specimens from 21 transurethral resections, 11 radical cystectomies, and 17 nephroureterectomies were retrospectively reviewed. Survival periods were calculated based on patient demographics. All patients provided consent for use of their tumor tissue for clinical research, and the Sifa University Ethics Committee approved the research protocol. We assessed patient medical charts for clinical features such as progression, recurrence, and presence and number of near and distant metastases.

Histopathological evaluation

All surgical specimens were processed according to standard pathology procedures and were histologically confirmed to be urothelial carcinoma. Tumor grading was performed according to the 2004 World Health Organization–International Society of Urological Pathology Consensus Classification.²² Tumor architecture was defined as papillary or non-papillary based on

the predominant feature of the index lesion.

Immunohistochemical evaluation of parafibromin

Formalin-fixed and paraffin-embedded tissue specimens were prepared for immunohistochemical (IHC) staining for all patients. A demonstrative block containing benign urothelium tissue adjacent to the tumor was selected for IHC evaluation. Sections 4–5- μ m-thick were prepared from the paraffin-embedded tissues and were placed on electrostatic-charged slides (X-tra, Surgipath Medical Industries, Richmond, IL, USA). Sections were deparaffinized and dehydrated through a graded ethanol series using routine protocols. The IHC study was performed using parafibromin (1:100, HRPT2, Santa Cruz Biotechnology, Santa Cruz, CA, USA). Slides from parathyroid adenoma cases were used as positive controls. The IHC staining process, including deparaffinization and antigen retrieval, was performed on a Dako LV-1 automated immunostaining system (Dako, Glostrup, Denmark). Scoring was performed separately by two pathologists who were blinded to patient characteristics. Nuclear staining was accepted as positive for parafibromin. The staining pattern was classified as diffusely and strongly positive when there was nuclear staining in all or nearly all (i.e., >95%) of the tumor cells regardless of staining intensity, negative when there

Table 1. Clinical and histopathological features of the patients

Clinical and histopathological features	No. of cases (%)
Gender	
Male	42 (85.7)
Female	7 (14.3)
Tumor type	
Papillary UC	27 (55.1)
Non-papillary UC	22 (44.9)
Tumor grade	
Low	7 (14.3)
High	42 (85.7)
Muscularis propria invasion	
Present	21 (42.8)
Absent	28 (57.2)
Latest health status	
Alive	46 (93.9)
Dead	3 (6.1)
Recurrences	
Present	20 (40.8)
One	14 (28.6)
More	6 (12.2)
Absent	29 (59.2)
Progression ^a	
Absent	30 (61.2)
Present	19 (38.8)

UC, urothelial carcinoma.

^aProgression is accepted when the tumor developed invasive features/ deep invasion/lymph node metastasis/distant organ metastasis.

Table 2. The relationship between tumor subtype and clinico-pathologic parameters

Clinico-pathologic parameters	Papillary subtype (n=27)	Non-papillary subtype (n=22)	p-value
Gender			
Male	3	4	.385
Female	24	18	
Tumor grade			
Low	7	0	.01
High	20	22	
Muscularis propria invasion			
Absent	19	2	.001
Present	8	20	
Tumor localization			
Upper urinary system	7	10	.153
Lower urinary system	20	12	
Latest health status			
Alive	27	19	.071
Dead	0	3	
Recurrences			
Present			.110
One	5	9	
More	5	1	
Absent	17	12	
Progression			
Absent	17	13	.683
Present	10	9	

was almost no staining (< 1%) of tumor nuclei, and partially positive in all other cases.¹⁷ A negative result was reported only if there was an internal positive control. There was no difference between the grades of the two pathologists.

Statistical data analysis

The SPSS ver. 18.0 (SPSS Inc., Chicago, IL, USA) software program was used for statistical analyses. In addition to descriptive statistical methods, the chi square test and Fisher exact test were used for the comparison of categorical variables. Binary numerical data were compared with the Mann-Whitney U test. Survival data were obtained with Kaplan-Meier, log rank, and Cox regression analyses. A p-value of < .05 was accepted as statistically significant.

RESULTS

Clinical and pathological parameters

The mean age was 69.55 ± 8.2 years (range, 54 to 88 years),

and men made up 85.7% ($n = 42$) of the group. Table 1 presents the clinicopathological features of the subjects. The follow-up range was 3 to 96 months. There were three deaths due to tumor during follow-up. Tumor progression (including development of invasive features, deep invasion, lymph node metastasis, and distant organ metastasis) was seen in 19 cases. Mean survival duration was 37.88 ± 29.6 months. Mean disease-free progression in the recurrence-free cases was 26.98 ± 26.2 months. There was a statistically significant relationship between tumor subtype and tumor grade and muscularis propria invasion ($p = .01$ and $p = .001$, respectively) (Table 2). All low-grade non-invasive tumors were of the papillary subtype, while high-grade tumors were mainly of the non-papillary subtype. Invasion was found in five of six high-grade UCs with squamous differentiation. There was no statistically significant relationship between tumor subtype and tumor localization, gender, age, presence or number of recurrences, presence of progression, survival, or disease-free survival (Table 2).

Table 3. The relationship between parafibromin expression and clinicopathologic parameters

Clinicopathologic parameter	Parafibromin expression			p-value
	Negative	Partially positive	Positive	
Gender				.569
Male	10	17	15	
Female	3	2	2	
Tumor type				.111
Papillary UC	6	14	7	
Non-papillary UC	7	5	10	
Tumor grade				.105
Low	0	5	2	
High	13	14	15	
Muscularis propria invasion				.007
Absent	1	12	8	
Present	12	7	9	
Tumor localization				.009
Upper urinary system	9	4	4	
Lower urinary system	4	15	13	
Latest health status				.353
Alive	13	19	14	
Dead	0	0	3	
Disease-free survival	13	19	17	.311
Recurrences				.573
Present				
One	2	6	6	
More	1	2	3	
Absent	10	11	8	
Progression ^a				.183
Absent	10	12	8	
Present	3	7	9	

UC, urothelial carcinoma.

^aProgression is accepted when the tumor developed invasive features/deep invasion/lymph node metastasis/distant organ metastasis.

The relationship between parafibromin expression and urothelial carcinoma

Parafibromin expression was negative in 13 cases (26.5%), partially positive in 19 cases (38.8%), and positive in 17 cases (34.7%) (Table 3, Figs. 1–3). There was a statistically significant relationship between parafibromin expression and muscularis propria invasion and tumor location (upper/lower urinary system). It was interesting that parafibromin was more negative in UCs with muscularis propria invasion than in tumors that did not invade muscle ($p = .007$). Parafibromin expression was higher in tumors of the lower urinary system than in upper urinary system tumors ($p = .009$). There was no statistically significant relationship between parafibromin expression and gender, age, tumor grade, presence and number of recurrences, presence of progression, survival, or disease-free survival (Table 3). Parafibromin positivity in the normal urothelial epithelium adjacent to

the tumor was seen in nine cases (Fig. 4). The positivity rate in normal urothelial epithelium was 50% to 90%.

DISCUSSION

Parafibromin is a tumor suppressor gene that has attracted interest for its potential prognostic value in some tumor types, especially parathyroid tumors. Its use as a potential indicator of tumor aggressiveness has been reported in other organs (e.g., colon, stomach, and breast).^{18,20,21} To the best of our knowledge, there has not been a study on parafibromin staining in UCs in the English literature. The main aim of this study was to contribute to establishing criteria that can predict the behavior of tumors in suspect cases. We also evaluated the presence of statistically significant relationships between parafibromin staining and other prognostic parameters. Parafibromin expression was

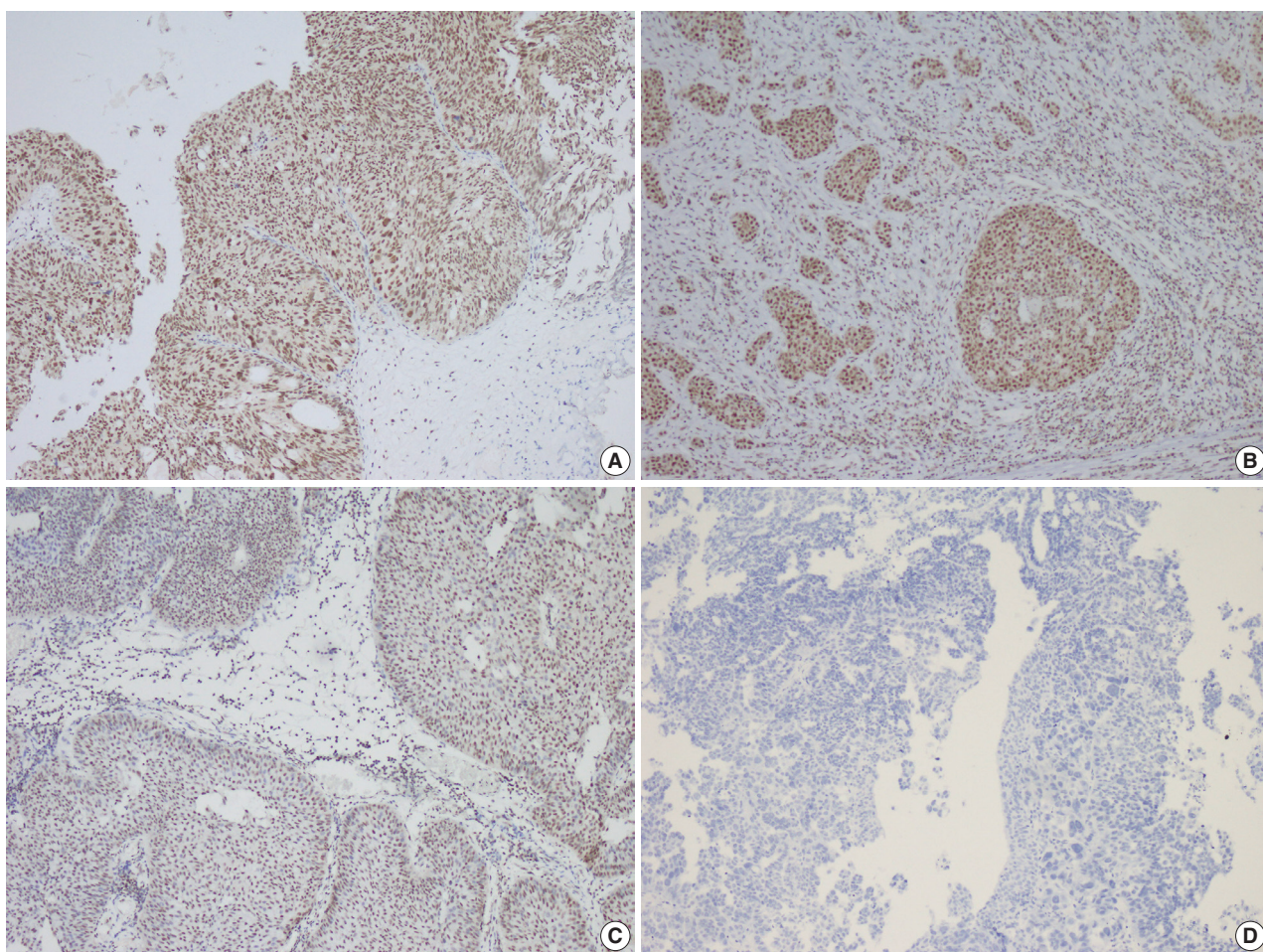


Fig. 1. Parafibromin staining in different types of urothelial carcinomas. (A) Parafibromin positivity on immunohistochemical evaluation of non-invasive high-grade papillary urothelial carcinoma. (B) Parafibromin positivity in the invasive areas of high-grade urothelial carcinoma of the bladder. (C) Partial parafibromin positivity in non-invasive low-grade papillary urothelial carcinoma. (D) Parafibromin negativity in non-invasive high-grade papillary urothelial carcinoma.

weaker in UCs with muscularis propria invasion than in those without invasion of the muscle. Parafibromin staining was more common in lower urinary system UCs than in those of the upper urinary system. The parafibromin staining data in our study correlates with that of previous parafibromin staining studies of malignancies of other systems. Selvarajan *et al.*¹⁸ observed an inverse correlation between tumor size and parafibromin expression in 163 breast carcinoma cases ($p = .05$). Zheng *et al.*²⁰ observed that lymph node metastasis and prognosis are related to parafibromin expression in colorectal carcinoma. Compared with the non-neoplastic colorectal mucosa, adenomas and carcinomas had decreased nuclear expression of parafibromin messenger RNA level. Zheng *et al.*²¹ also reported that parafibromin expression gradually decreased in carcinoma areas compared to the normal gastric mucosa areas, and statistically significant

relationships between parafibromin and lymphatic invasion, invasion depth, lymph node metastasis, and tumor stage were observed. The rate of muscularis propria invasion in bladder carcinomas is estimated to be 20%–30% at the time of diagnosis. Muscularis propria invasion results in progression in 20%–50% of cases, even if the tumor is diagnosed early.^{23,24} We found a statistically significant relationship between parafibromin expression and muscularis propria invasion, which suggests that this biomarker can function as an indicator of progression.

The rate of upper urinary system recurrence (UUSR) following RC is low (0.7% and 7.4%) but indicates a worse prognosis. The most important independent factors predicting UUSR following RC are number of metastatic lymph nodes and presence of local recurrence in the renal pelvis.²⁵ We did not find a statistically significant relationship between parafibromin ex-

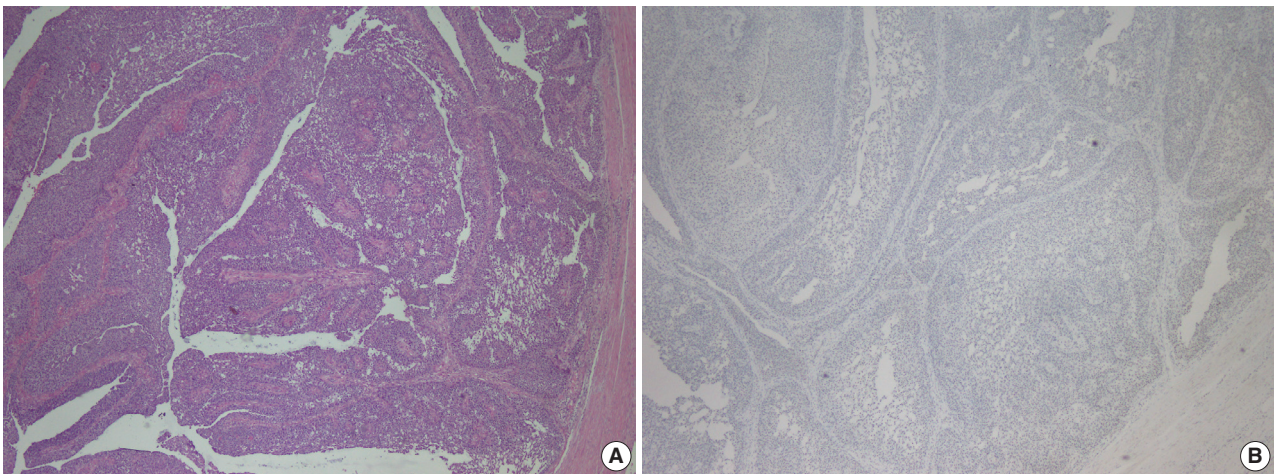


Fig. 2. Parafibromin negativity in minimally invasive high-grade papillary urothelial carcinoma of the ureter. (A) Morphological features of urothelial carcinoma. (B) Parafibromin negativity in the same tumor.

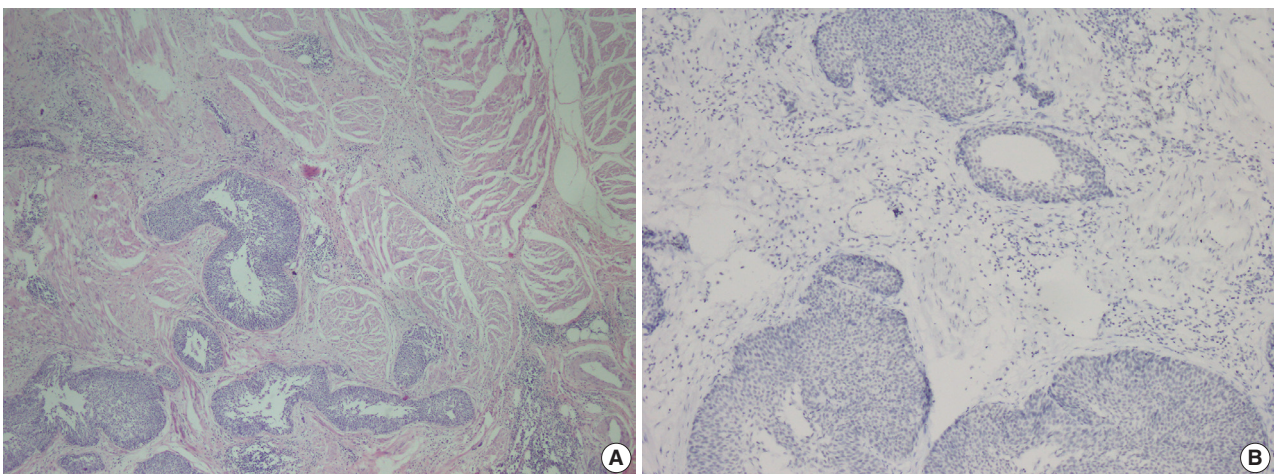


Fig. 3. Parafibromin negativity in invasive high-grade papillary urothelial carcinoma of the bladder. (A) Morphological features of urothelial carcinoma. (B) Parafibromin negativity in areas of muscularis propria invasion of the same tumor.

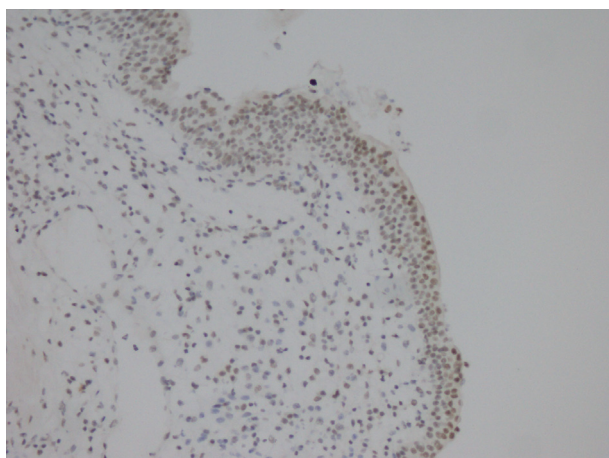


Fig. 4. Parafibromin positivity in normal urothelial epithelium.

pression and recurrence or progression in tumors that were removed by cystectomy, but parafibromin negativity was relatively prominent in recurring and progressive cases.

Urothelial carcinomas with squamous differentiation are known to have a poor prognosis. Their clinical course depends on the extension of the tumor to adjacent tissue and lymph nodes, requiring prompt radical surgery. Studies on the development mechanism and postoperative treatment of these tumors are ongoing.²⁶ We did not find a marked difference in the diffuseness or intensity of parafibromin staining in the six tumors of this group (three were strongly positive, one was positive, and two were negative). However, two patients died (one with a tumor in the ureter, and the other with a tumor in the renal pelvis), which is consistent with data from the literature.

Although our study focused on UC, we also took into account the transition areas with normal urothelial epithelium during sample selection. All nine cases of normal urothelial epithelium in the observed areas were positive for parafibromin. Porzionato *et al.*²⁷ have evaluated parafibromin staining in human and mouse tissues and reported that human bladder epithelium did not stain with parafibromin. However, the normal epithelium showed positive parafibromin staining in our cases. We are not sure of the cause of this discrepancy, but it could be related to differences in the parafibromin stain.

We found that the infiltration rate of the muscularis propria decreased in parafibromin-positive urinary system carcinomas. The parafibromin positivity rate was higher in carcinomas of the papillary type and in those of the lower urinary system. The question remains whether these features can be used as guiding parameters in tumor subgroups where the follow-up criteria have not been fully standardized, such as with papillary UCs. Pa-

rafibromin expression was lower in higher-grade tumors, although this difference from lower-grade tumors was not statistically significant. Parafibromin negativity might provide guidance on adjuvant therapy in cases with poor prognostic parameters such as urothelial carcinoma with squamous differentiation. All of these statements require support from studies based on larger groups with longer follow-up periods.

Conflicts of Interest

No potential conflict of interest relevant to this article was reported.

REFERENCES

1. Ploeg M, Aben KK, Kiemeny LA. The present and future burden of urinary bladder cancer in the world. *World J Urol* 2009; 27: 289-93.
2. Jemal A, Siegel R, Ward E, Hao Y, Xu J, Thun MJ. Cancer statistics, 2009. *CA Cancer J Clin* 2009; 59: 225-49.
3. Margulis V, Shariat SF, Matin SF, *et al.* Outcomes of radical nephroureterectomy: a series from the Upper Tract Urothelial Carcinoma Collaboration. *Cancer* 2009; 115: 1224-33.
4. Oldbring J, Glifberg I, Mikulowski P, Hellsten S. Carcinoma of the renal pelvis and ureter following bladder carcinoma: frequency, risk factors and clinicopathological findings. *J Urol* 1989; 141: 1311-3.
5. Babjuk M, Oosterlinck W, Sylvester R, *et al.* EAU guidelines on non-muscle-invasive urothelial carcinoma of the bladder. *Eur Urol* 2008; 54: 303-14.
6. Hall MC, Womack S, Sagalowsky AI, Carmody T, Erickstad MD, Roehrborn CG. Prognostic factors, recurrence, and survival in transitional cell carcinoma of the upper urinary tract: a 30-year experience in 252 patients. *Urology* 1998; 52: 594-601.
7. Olgac S, Mazumdar M, Dalbagni G, Reuter VE. Urothelial carcinoma of the renal pelvis: a clinicopathologic study of 130 cases. *Am J Surg Pathol* 2004; 28: 1545-52.
8. Faraj SF, Chau A, Gonzalez-Roibon N, *et al.* ARID1A immunohistochemistry improves outcome prediction in invasive urothelial carcinoma of urinary bladder. *Hum Pathol* 2014; 45: 2233-9.
9. Ramos Soler D, Ferrer Lozano J, Navarro Fos S, Llobart-Bosch A. Multiple analysis of morphologic factors with prognostic value in transitional cell papillary carcinoma of the bladder. Retrospective study of 571 cases. *Actas Urol Esp* 1999; 23: 119-26.
10. Schapers RF, Pauwels RP, Wijnen JT, *et al.* A simplified grading method of transitional cell carcinoma of the urinary bladder: reproducibility, clinical significance and comparison with other prognostic parameters. *Br J Urol* 1994; 73: 625-31.
11. Aldred MJ, Talacko AA, Savarirayan R, *et al.* Dental findings in a

- family with hyperparathyroidism-jaw tumor syndrome and a novel *HRPT2* gene mutation. *Oral Surg Oral Med Oral Pathol Oral Radiol Endod* 2006; 101: 212-8.
12. Pimenta FJ, Gontijo Silveira LF, Tavares GC, *et al.* *HRPT2* gene alterations in ossifying fibroma of the jaws. *Oral Oncol* 2006; 42: 735-9.
 13. Shattuck TM, Välimäki S, Obara T, *et al.* Somatic and germ-line mutations of the *HRPT2* gene in sporadic parathyroid carcinoma. *N Engl J Med* 2003; 349: 1722-9.
 14. Carpten JD, Robbins CM, Villablanca A, *et al.* *HRPT2*, encoding parafibromin, is mutated in hyperparathyroidism-jaw tumor syndrome. *Nat Genet* 2002; 32: 676-80.
 15. Wang PF, Tan MH, Zhang C, Morreau H, Teh BT. *HRPT2*, a tumor suppressor gene for hyperparathyroidism-jaw tumor syndrome. *Horm Metab Res* 2005; 37: 380-3.
 16. Cetani F, Ambrogini E, Viacava P, *et al.* Should parafibromin staining replace *HRPT2* gene analysis as an additional tool for histologic diagnosis of parathyroid carcinoma? *Eur J Endocrinol* 2007; 156: 547-54.
 17. Gill AJ, Clarkson A, Gimm O, *et al.* Loss of nuclear expression of parafibromin distinguishes parathyroid carcinomas and hyperparathyroidism-jaw tumor (HPT-JT) syndrome-related adenomas from sporadic parathyroid adenomas and hyperplasias. *Am J Surg Pathol* 2006; 30: 1140-9.
 18. Selvarajan S, Sii LH, Lee A, *et al.* Parafibromin expression in breast cancer: a novel marker for prognostication? *J Clin Pathol* 2008; 61: 64-7.
 19. Tan MH, Morrison C, Wang P, *et al.* Loss of parafibromin immunoreactivity is a distinguishing feature of parathyroid carcinoma. *Clin Cancer Res* 2004; 10: 6629-37.
 20. Zheng HC, Wei ZL, Xu XY, *et al.* Parafibromin expression is an independent prognostic factor for colorectal carcinomas. *Hum Pathol* 2011; 42: 1089-102.
 21. Zheng HC, Takahashi H, Li XH, *et al.* Downregulated parafibromin expression is a promising marker for pathogenesis, invasion, metastasis and prognosis of gastric carcinomas. *Virchows Arch* 2008; 452: 147-55.
 22. Eble JN, Sauter G, Epstein JI, Sesterhenn IA. World Health Organization classification of tumours: pathology and genetics of tumours of the urinary system and male genital organs. Lyon: IARC Press, 2004; 90.
 23. Quek ML, Stein JP, Clark PE, *et al.* Natural history of surgically treated bladder carcinoma with extravesical tumor extension. *Cancer* 2003; 98: 955-61.
 24. Tilki D, Reich O, Svatek RS, *et al.* Characteristics and outcomes of patients with clinical carcinoma in situ only treated with radical cystectomy: an international study of 243 patients. *J Urol* 2010; 183: 1757-63.
 25. Kim SH, Yang HK, Lee JH, Lee ES. A retrospective analysis of incidence and its associated risk factors of upper urinary tract recurrence following radical cystectomy for bladder cancer with transitional cell carcinoma: the significance of local pelvic recurrence and positive lymph node. *PLoS One* 2014; 9: e96467.
 26. Rausch S, Hofmann R, von Knobloch R. Nonbilharzial squamous cell carcinoma and transitional cell carcinoma with squamous differentiation of the lower and upper urinary tract. *Urol Ann* 2012; 4: 14-8.
 27. Porzionato A, Macchi V, Barzon L, *et al.* Immunohistochemical assessment of parafibromin in mouse and human tissues. *J Anat* 2006; 209: 817-27.

Comparison of Cytologic Characteristics between Adenoid Cystic Carcinoma and Adenoid Basal Carcinoma in the Uterine Cervix

Juhyeon Jeong · Seung Yeon Ha
Hyun Yee Cho · Dong Hae Chung
Jungsuk An

Department of Pathology, Gachon University
Gil Medical Center, Incheon, Korea

Received: May 20, 2015
Revised: June 26, 2015
Accepted: July 8, 2015

Corresponding Author

Seung Yeon Ha, MD, PhD
Department of Pathology, Gachon University
Gil Medical Center, 21 Namdong-daero
774beon-gil, Namdong-gu, Incheon 21565, Korea
Tel: +82-32-460-3073
Fax: +82-32-460-2394
E-mail: syha@gilhospital.com

Background: Adenoid cystic carcinoma (ACC) and adenoid basal carcinoma (ABC) are rare in the uterine cervix. ACC is more aggressive than ABC, thus accurate differential diagnosis is important. In this study, we identified cytologic features useful in distinguishing these two tumors for diagnosis. **Methods:** Three cases of ACC and five cases of ABC were selected for this study. Cervicovaginal smear slides were reviewed retrospectively, and the area, circumference, major axis, and minor axis of nuclei were measured using an image analyzer. **Results:** ACC displayed three-dimensional clusters with a small acini pattern. ABC displayed peripheral palisading without an acini pattern. The nuclei of ACC were more irregular and angulated than those of ABC, and the former showed a coarsely granular chromatin pattern. The nucleic area, circumference, major axis, and minor axis were $18.556 \pm 8.665 \mu\text{m}^2$, $23.320 \pm 11.412 \mu\text{m}$, $5.664 \pm 1.537 \mu\text{m}$, and $4.127 \pm 1.107 \mu\text{m}$ in ACC and $11.017 \pm 4.440 \mu\text{m}^2$, $15.920 \pm 5.664 \mu\text{m}$, $4.612 \pm 1.025 \mu\text{m}$, and $3.088 \pm 0.762 \mu\text{m}$ in the cases of ABC. All measured values showed statistically significant difference ($p < .001$). **Conclusions:** Although the nuclei of both of these tumor types were oval shaped, inferred from the ratio of minor axis to major axis (0.728 in ACC and 0.669 in ABC), the area of nuclei was approximately 1.7 times larger in ACC than in ABC. Distinguishing nucleic features, including area, morphology, and chromatin pattern, may be helpful in making a correct diagnosis.

Key Words: Adenoid cystic carcinoma; Adenoid basal carcinoma; Vaginal smears; Papanicolaou test

The World Health Organization (WHO) classifies malignant tumors of the uterine cervix into three categories: squamous tumors, glandular tumors, and “other epithelial tumors.”¹ The category of “other epithelial tumors” is composed of five different tumor types: adenosquamous carcinoma, adenoid cystic carcinoma (ACC), adenoid basal carcinoma (ABC), neuroendocrine tumors, and undifferentiated carcinoma.¹ Both ACC and ABC are rare tumors, accounting for less than 1% of all cervical adenocarcinomas and are usually found in postmenopausal women over the age of 60.² In spite of the fact that the cytologic features of these two malignant tumors of the uterine cervix can be very confusing, an accurate diagnosis of ACCs and ABCs is important because their clinical and biological behaviors are quite different; ACCs have worse prognosis than ABCs.¹

The Papanicolaou test, the most useful screening method for detecting precursor lesions of the uterine cervix, has been used universally with very high diagnostic accuracy. We have been using the Bethesda System revised in 2001 for diagnostic terminology. For evaluation of precancerous and malignant lesions, the diagnostic terms are grouped into squamous cells and glandular

cells. However, the system does not classify glandular cell lesions more specifically. Because the incidence of both malignant lesions is very low, distinguishing ACCs and ABCs from other malignancies usually relies on cytology. These tumors are occasionally associated with conventional squamous cell carcinoma, and cytologic findings are similar to those of endometrial cells and masquerade as squamous cell carcinoma. In addition, the diagnostic cytology of ACC is usually negative because of intact overlying mucosa.³

In this study, we evaluated the cytological differences between ACC and ABC in order to identify useful cytologic features that can distinguish the two.

MATERIALS AND METHODS

Cytologic and surgical specimens were obtained from nine patients diagnosed with ACC or ABC from 1998 to 2014 at Gachon University Gil Medical Center. Of the 2,229 cases of uterine cervix carcinomas during this period, there were four cases of ACC (0.17%) and five cases of ABC (0.22%). All cytology

specimens were obtained by the routine Papanicolaou cervicovaginal smear and the cases were confirmed by surgical specimens obtained from punch biopsy, conization or hysterectomy. Of the four of ACC cases, one case that coexisted with squamous cell carcinoma. The age range of these ACC cases was 45 to 76 years old at the time of diagnosis. One ACC case was excluded because there were no visible malignant cells on the reviewed cytologic slide. Of the five cases diagnosed as ABCs, four cases coexisted with squamous cell carcinoma. The age range of these ABC cases was 56 to 78 years old at the time of diagnosis (Table 1).

All patients underwent several cervicovaginal smear tests before and after surgical treatment. Conventional Papanicolaou smear and liquid based preparation methods were used. Of the ACC patients, three had undergone conventional smears, and the one case that was excluded had undergone a liquid based preparation. All patients with ABC, had undergone conventional smear. Cytologic diagnosis was made based on the Bethesda system. After cytological diagnosis, patients underwent surgical procedure for definitive diagnosis or treatment. Punch biopsy, curettage, conization or hysterectomy were performed. We retrospectively reviewed the cervicovaginal smear slides obtained before surgery after histological confirmation.

In all cytology slides, selected individually dispersed representative tumor cells were measured using an image analyzer. A DP70 digital camera (Olympus, Tokyo, Japan) was used to take pictures of tumor cells. I-Solution ver. 8.4 (IMT i-Solution, Coquitlam, BC, Canada) was used for measurement of the area, circumference, major axis, and minor axis of nuclei. These parameters were then used to compare the morphological differentiation of the nuclei of the ACC and ABC in cytology specimens.

Data analysis was performed using SPSS ver. 21.0 (IBM Corp., Armonk, NY, USA). Mann-Whitney U-test was used for comparison of numeric data of area, circumference, major axis, and minor axis of the nuclei of ACC and ABC. Differences between ACC and ABC were considered statistically significant

when p-values were less than .05.

RESULTS

Cytologic characteristics of ACC

Three cases in this study were ACC. Initial cytologic diagnoses varied, including squamous cell carcinoma, adenocarcinoma, and other malignancies (Table 1). The overall cytologic features of the three cases included large amount of necrotic debris and tumor diathesis as well as numerous orangeophilic globules in the background. Most tumor cells were arranged in three-dimensional overlapping tumor cell clusters, consisting of 40 to 50 tumor cells. The tumor cells occasionally formed glandular structures (Fig. 1A). Rarely, opaque orangeophilic contents were observed in the center of the glandular pattern (Fig. 1B). A few tumor cells were scattered individually. Tumor cells were small and round to oval shape with moderate size variation. Each cell had an indistinct cell border and scant eosinophilic cytoplasm. The nuclei were angulated and hyperchromatic, with coarse granular chromatin pattern. They also had inconspicuous nucleoli (Table 2, Fig. 1C).

Diagnoses of ACCs were confirmed by surgical specimens. One case was cervical punch biopsy, while the others were radical hysterectomy specimens. All cases showed typical histologic findings. There were numerous well circumscribed cellular nests of various sizes in the cervical stroma. Tumors were composed of basaloid cells with indistinct nucleoli arranged in nests with a cribriform appearance, which sometimes had a palisading arrangement in the periphery (Fig. 1D).

Cytologic characteristics of ABC

There were four cases of ABC in this study. All four cases (cases Nos. 4–6 and 8) coexisted with squamous cell carcinomas confirmed by surgical specimens. All but one case (case No. 8) were diagnosed as squamous cell carcinoma in cytologic exami-

Table 1. Clinical summary of adenoid cystic carcinoma and adenoid basal carcinoma

Case No.	Age (yr)	Cytologic diagnosis	Surgical procedure	Histologic diagnosis	Combined lesion
1	76	SCC	Punch biopsy	ACC	-
2	45	AC	Hysterectomy	ACC	-
3	68	MN	Hysterectomy	ACC	SD
4	78	SCC, AC	Punch biopsy	ABC	SCC
5	62	SCC	Hysterectomy	ABC	SCC
6	56	SCC	Hysterectomy	ABC	SCC
7	62	SCC	Hysterectomy	ABC	-
8	68	ASCUS	Hysterectomy	ABC	SCC

SCC, squamous cell carcinoma; ACC, adenoid cystic carcinoma; AC, adenocarcinoma; MN, other malignant neoplasm; SD, squamous differentiation; ABC, adenoid basal carcinoma; ASCUS, atypical squamous cells of undetermined significance.

nations. The cytologic diagnosis of case No. 4 was combined carcinoma, i.e., squamous cell carcinoma and adenocarcinoma. Case No. 8 was diagnosed as atypical squamous cells of undetermined significance (Table 1). In reviewed cytology slides of

five cases, some clusters of malignant cells showed distinctive features different from those of pure squamous cell carcinoma. Tumor diathesis was prominent in the background. Tumor cells occasionally presented as single cells, but mostly as three-di-

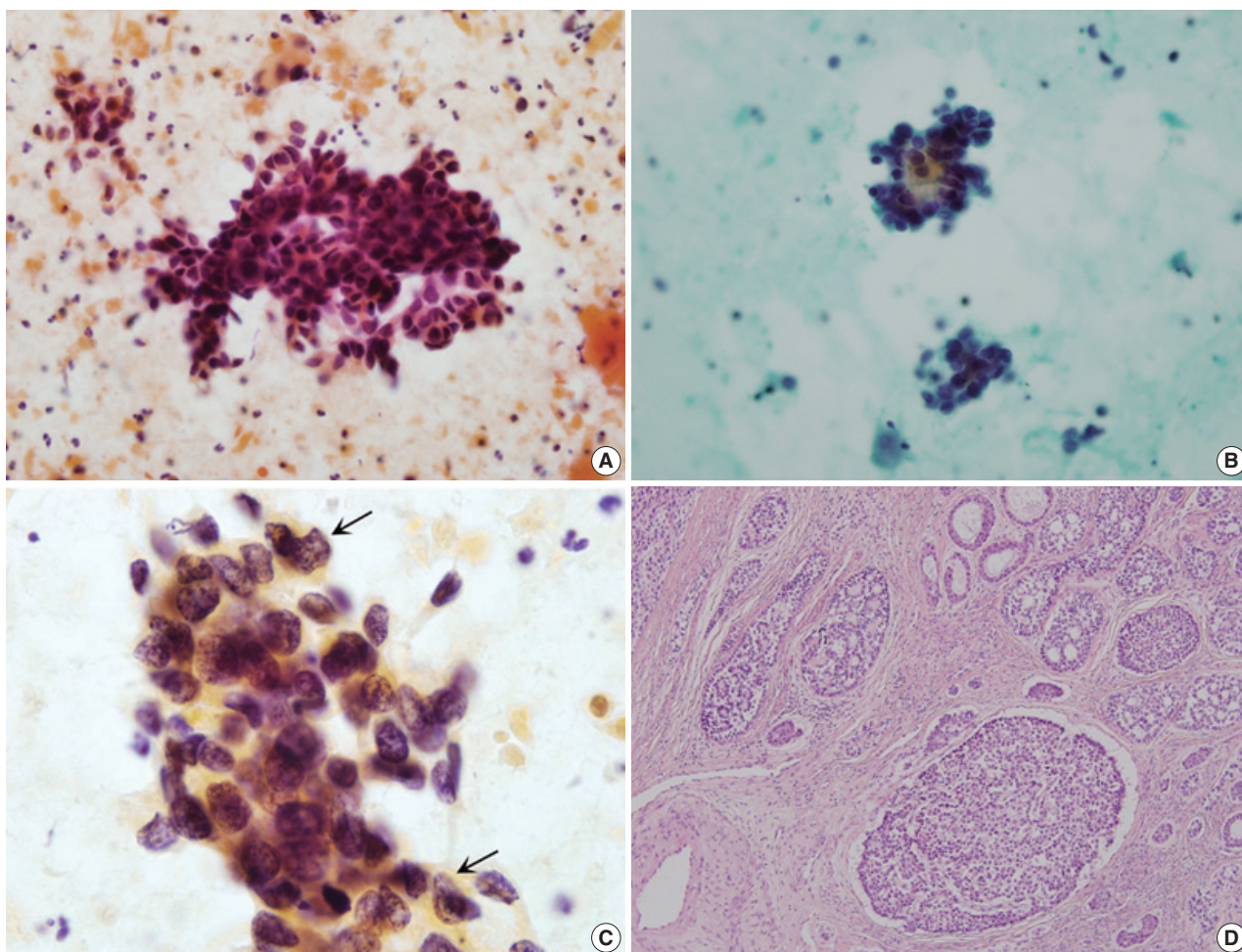


Fig. 1. Cytologic and histopathologic features of adenoid cystic carcinoma. (A) Tumor cells display three-dimensional clusters forming small acini or glandular pattern in necrotic background. (B) Some glandular structures contain opaque orangeophilic contents in the center. (C) The size of nuclei is variable. The nuclei have irregular and angulated membrane with coarsely granular chromatin pattern (arrows). (D) On histologic section, tumor nests consist of basaloid cells forming a cribriform appearance with palisading arrangement in the periphery.

Table 2. Summary of the cytologic features of adenoid cystic carcinoma and adenoid basal carcinoma of the cervix

Cytologic features	Adenoid cystic carcinoma	Adenoid basal carcinoma
Background	Bloody and necrotic; orangeophilic globules	Necrotic, mostly
Architecture	Three-dimensional clusters; occasionally glandular structures; opaque materials in the center of the glands	Three-dimensional clusters of sheets; nuclear overlapping; rarely peripheral palisading
N/C ratio	Moderate to high	High
Nuclear shape	Round to oval	Round to oval
Nuclear size (μm)	5–7 ^a	3–4 ^a
Nuclear size variation	Mild to moderate ^b	Mild ^b
Mitotic counts (/100–150 cells)	2–3	0–1
Chromatin pattern	Hyperchromatic; coarse granular chromatin pattern	Hyperchromatic; finely granular chromatin pattern
Nucleoli	Rarely seen; indistinct, mostly	Rarely seen; small nucleoli, occasionally

^aEstimate based on major axis in our cases; ^bEstimate based on major axis with standard deviation in our cases.

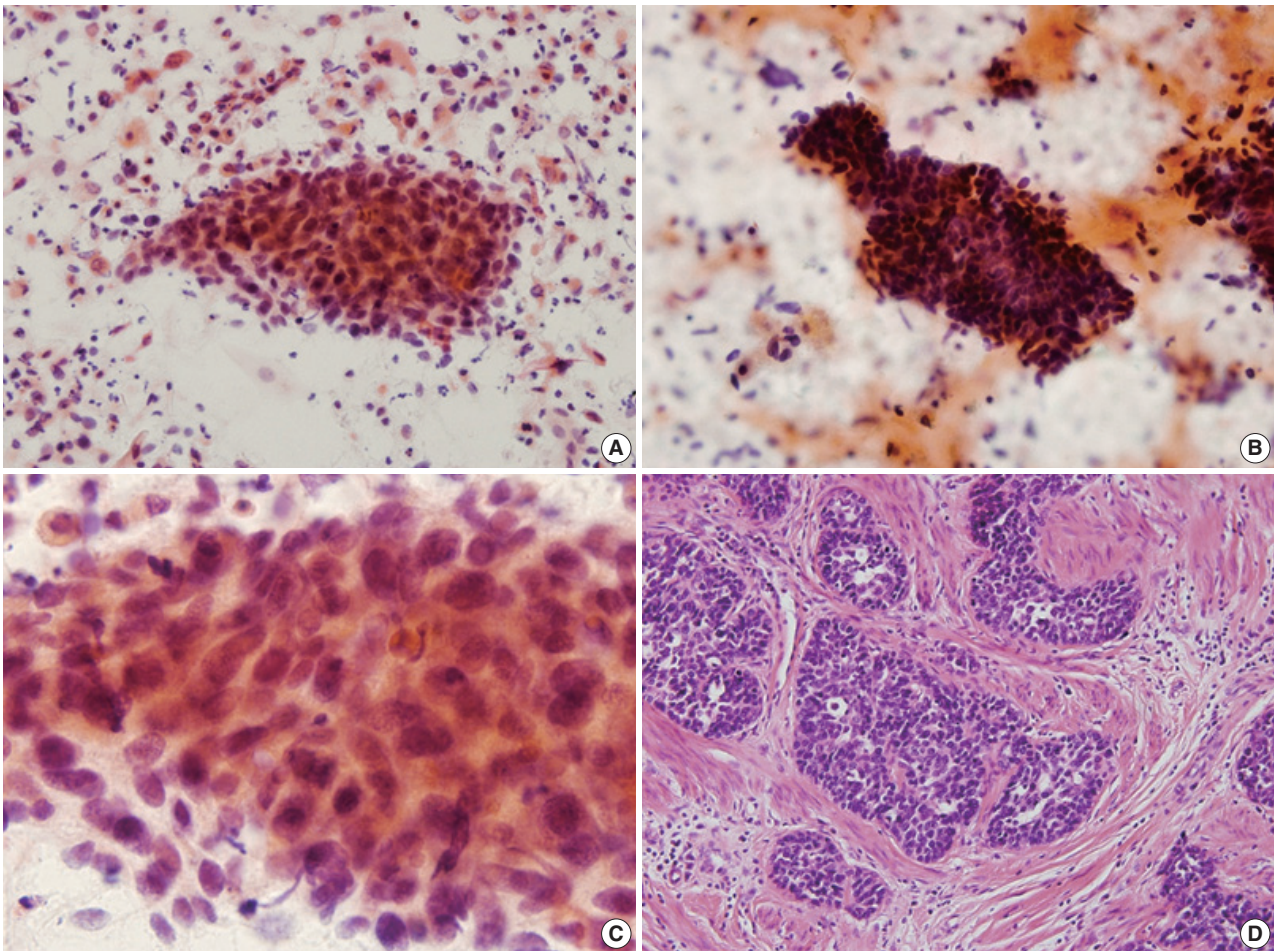


Fig. 2. Cytologic and histopathologic features of adenoid basal carcinoma. (A) Clusters consist of small round basaloid cells in the necrotic background. (B) Tumor cells display three-dimensional clusters with peripheral palisading without glandular pattern. (C) The size of nuclei shows mild variation. The nucleic membrane is smooth with a finely granular chromatin pattern. (D) On histologic section, basaloid cells forming tumor nests display peripheral palisading deep in cervical stroma.

mensional clusters. Rarely, the tumor cell clusters displayed peripheral palisading; however, there was no glandular structure formation (Fig. 2A, B). Individual cells were small and showed slight variation in size with a variable amount of eosinophilic cytoplasm. Nuclei were dense basophilic, hyperchromatic, and sometimes had a fine granular chromatin pattern. Inconspicuous nucleoli were seen (Table 2, Fig. 2C).

Punch biopsy was performed in one case, and radical hysterectomy was performed for cure in the others. Squamous cell carcinomas were also found in four of five cases. All cases showed cervical ulceration grossly, without formation of a mass-like lesion. The tumors had similar histology. ABC was not exposed to the surface. These tumors showed solid tumor cell nests with peripheral palisading or cord like arrangement, and they sometimes formed acini structures without hyaline material. Tumor cells had small basophilic nuclei, with inconspicuous nucleoli

(Fig. 2D).

Analysis of tumor cell nuclear morphology

The mean ACC nuclear area was $18.556 \pm 8.655 \mu\text{m}^2$, and $11.017 \pm 4.440 \mu\text{m}^2$ in ABC. The mean nuclear perimeter was $23.320 \pm 11.412 \mu\text{m}$ in ACC, and $15.920 \pm 5.664 \mu\text{m}$ in ABC. The major axis was $5.664 \pm 1.537 \mu\text{m}$ and $4.612 \pm 1.025 \mu\text{m}$ in ACC and ABC, respectively. The minor axis was $4.127 \pm 1.107 \mu\text{m}$ in ACC, and $3.088 \pm 0.762 \mu\text{m}$ in ABC. Thus, ACC and ABC differed significantly in mean nuclear area, circumference, major axis, and minor axis ($p < .001$) (Table 3).

DISCUSSION

ACC and ABC are rare, accounting for less than 1% of all tumors of the uterine cervix.² ACC of the cervix was first de-

Table 3. Comparison of nuclear features between adenoid cystic carcinoma and adenoid basal carcinoma

	ACC (n=117)	ABC (n=218)	p-value ^a
Area (μm^2)	18.556 \pm 8.655	11.017 \pm 4.440	<.001
Circumference (μm)	23.320 \pm 11.412	15.920 \pm 5.664	<.001
Major axis (μm)	5.664 \pm 1.537	4.612 \pm 1.025	<.001
Minor axis (μm)	4.127 \pm 1.107	3.088 \pm 0.762	<.001

Values are presented as mean \pm standard deviation.

ACC, adenoid cystic carcinoma; ABC, adenoid basal carcinoma.

^aStatistical significance was determined by Mann-Whitney U-test.

Table 4. Differential diagnosis of adenoid cystic carcinoma and adenoid basal carcinoma^{7,13}

Differential diagnosis	Nuclear features	Cytologic features	Structures
SCC, keratinizing	Marked variation in size and shape; irregular nuclear membrane; coarsely granular and irregularly distributed chromatin	Dense orangiophilic	Low cellularity; single cells and less commonly in aggregates
SCC, nonkeratinizing	Smaller than HSIL; markedly irregular distributed chromatin	Basophilic	Single or aggregated cells
Small cell carcinoma	Small, relatively uniform cells; hyperchromatic with granular or stippled chromatin; frequent mitosis; inconspicuous nucleoli	Scant cyanophilic cytoplasm	Singly and in groups with nuclear molding
Endocervical adenocarcinoma	Columnar configuration enlarged, pleomorphic nuclei; irregular nuclear membrane; macronucleoli	Usually finely vacuolated	Abundant abnormal cells; single cells or two-/three-dimensional sheets; discohesive groups
Endometrial carcinoma	Variation of nuclear size; loss of nuclear polarity; moderate hyperchromasia; large with clumped chromatin; small to prominent nucleoli	Scant, cyanophilic, often vacuolated; commonly intracytoplasmic neutrophil	Single or small, tight clusters
Benign endometrial stromal cells	Small round to oval shape; inconspicuous nucleoli	Scant, basophilic, or occasionally vacuolated	Three-dimensional ball-like clusters; double-contoured cluster (the first half of the menstrual cycle)
Atrophy	Intermediate cells with normochromatin; elongated nuclei; mild hyperchromasia	-	Flat, monolayer sheets

SCC, squamous cell carcinoma; HSIL, high grade intraepithelial lesion.

scribed by Paalman and Counseller in 1949,⁴ while ABC of the cervix was first reported as a separate entity in 1966 by Baggish and Woodruff.⁵ While there have been many single or multiple case reports of ACCs and ABCs, few have been reported on the cytologic characteristics of these two rare malignant tumors of the cervix.^{3,6-10} While some have posited that these tumors share origin from pluripotent reserve cells,¹¹ their biologic behavior is quite different: whereas ABCs are low-grade tumors with good prognosis, ACCs are aggressive, with frequent local recurrences or metastasis. Therefore, accurate differential diagnosis of these two tumors on cervicovaginal smear is very important. However, to date, there are no reports describing the morphologic differences between ACC and ABC that allow for sufficient diagnosis by cytology.

All reviewed cervicovaginal smear specimens have numerous three-dimensional overlapping tumor cell clusters. These patterns were described in a report by Grafton *et al.*,⁸ in which three cases were found, and these overlapping tumor cells were said to resemble endometrial adenocarcinoma cells. In the present

study, we found that tumor cells in cases of ACC display typical glandular structures, which are hardly seen in cases of ABC.⁹ This feature was previously mentioned as acinus formation, cribriform pattern, or rosette-like group.^{3,6,8,10} The cytologic diagnosis of four of the five ABC cases in this study was squamous cell carcinoma. This is not surprising because squamous cell carcinoma or squamous intraepithelial lesions are commonly associated with ABC. One case was diagnosed as atypical squamous cells of undetermined significance. In some reported ABC cases, the cytologic diagnosis was negative or squamous intraepithelial lesion because of the intact surface epithelium with or without dysplasia or no connection with the epithelium.⁹ While necrosis has not been reported as a feature of ABC,⁹ necrosis was frequently seen in the cervicovaginal smears of our ABC cases, which can be explained by the coexisting squamous cell carcinoma. Tumor cell clusters showing peripheral palisading in ABC was a characteristic finding in our cases and other reports.¹² Glandular structures were found more often in ACC, which have also been mentioned in previous reports as specific find-

ings of ACC.^{3,6,7,9,10} While these features are meaningful findings in the two different tumor groups, because ACC and ABC may show similar findings in the histology of surgical specimens, these are not significantly distinguishing points. In our ACC cases, glandular structures had opaque orangeophilic content in the lumina, which may be a helpful feature in making a diagnosis of ACC on the cervicovaginal smear.

The two different tumors in this study showed similar nucleic characteristics including hyperchromasia and indistinct nucleoli. However, we noted that ACC and ABC have different chromatin patterns. Whereas ACC had a coarsely granular chromatin pattern, ABC was more finely granular. In addition, ACC shows a more irregular and angulated nuclear outline than ABC (Figs. 1C, 2C).¹⁴ Importantly, the nucleic characteristics in ACC and ABC were significantly different in area, perimeter, major axis, and minor axis. The ratio of minor axis to major axis was approximately 0.728 in ACC and 0.669 in ABC, which suggests that the shape of the nuclei is very similar (i.e., oval rather than spherical in both tumors). However, the nucleic area of ACC was 1.684 times larger than that of ABC. Therefore, careful observation of nuclear size, outline, and chromatin pattern may be useful in reaching correct diagnosis when pathologists confuse ACC with ABC.

The differential diagnosis of uterine cervix tumor is very important. Because ACC and ABC are rare tumors, it is difficult to consider these tumors as part of a differential diagnosis. The most misdiagnosed tumor is squamous cell carcinoma, which commonly occurs in the cervix and is coexistent with ABC in many cases. In our institution, the initial cytologic diagnosis was squamous cell carcinoma for five of the eight cases in this study. Three of these five were ABC associated with squamous cell carcinoma. The cytologic characteristics of squamous cell carcinoma are tumor diathesis in the background, low cellularity with single cells or less commonly aggregated cells. The nuclei show marked variation in size and shape with irregular nuclear membrane and coarsely granular chromatin pattern. However, ACC and ABC commonly show three-dimensional tumor cell clusters and have relatively small, uniform tumor cells. These distinct features could aid pathologists in making a correct diagnosis of ACC or ABC. Other lesions to consider in differential diagnosis are summarized in Table 4. These include small cell carcinoma, endocervical adenocarcinoma, endometrial adenocarcinoma, benign endometrial cells, and benign cervical lesion such as atrophy (Table 4).

The purpose of this study was to provide comprehensive information on the cytologic characteristics of ACC and ABC of

the cervix, so that pathologists may consider these two malignant tumors when the cervicovaginal smear shows small round cell clusters. Although they show significant difference in nuclear area, circumference, major axis, and minor axis, such difference is not of practical use. However, the size difference of nuclei may be useful. In order to distinguish ACC from ABC, to summarize, pathologists will need to make careful observation on structure of tumor cell cluster, nuclear size, irregularity of nuclear membrane, and nuclear chromatin pattern, with a possibility of combined lesions in mind.

Conflicts of Interest

No potential conflict of interest relevant to this article was reported.

REFERENCES

1. Kurman RJ, Carcangiu ML, Herrington CS, Young RH. WHO classification of tumours of female reproductive organs. 4th ed. Lyon: IARC Press, 2014.
2. Kurman RJ, Ellenson LH, Ronnett BM. Blaustein's pathology of the female genital tract. 6th ed. Chicago: Springer, 2010; 288-9.
3. Ha SY, Cho H, Oh YH, Lyu GS. The cytologic features of adenoid cystic carcinoma of the uterine cervix: a case report. *Korean J Cytopathol* 1998; 9: 207-12.
4. Paalman RJ, Counsellor VS. Clyindroma of the cervix with proclendia. *Am J Obstet Gynecol* 1949; 58: 184-7.
5. Baggish MS, Woodruff JD. Adenoid-basal carcinoma of the cervix. *Obstet Gynecol* 1966; 28: 213-8.
6. Barisic A, Mahovlic V, Ovanin-Rakic A, *et al*. Cytologic characteristics of adenoid cystic carcinoma of the cervix uteri: case report. *Coll Antropol* 2010; 34: 233-5.
7. Dayton V, Henry M, Stanley MW, Carson L, Taber E. Adenoid cystic carcinoma of the uterine cervix: cytologic features. *Acta Cytol* 1990; 34: 125-8.
8. Grafton WD, Kamm RC, Cowley LH. Cytologic characteristics of adenoid cystic carcinoma of the cervix uteri. *Acta Cytol* 1976; 20: 164-6.
9. Powers CN, Stastny JF, Frable WJ. Adenoid basal carcinoma of the cervix: a potential pitfall in cervicovaginal cytology. *Diagn Cytopathol* 1996; 14: 172-7.
10. Ravinsky E, Safneck JR, Chantziantoniou N. Cytologic features of primary adenoid cystic carcinoma of the uterine cervix: a case report. *Acta Cytol* 1996; 40: 1304-8.
11. Grayson W, Taylor LF, Cooper K. Adenoid cystic and adenoid basal carcinoma of the uterine cervix: comparative morphologic, mucin,

- and immunohistochemical profile of two rare neoplasms of putative 'reserve cell' origin. *Am J Surg Pathol* 1999; 23: 448-58.
12. Peterson LS, Neumann AA. Cytologic features of adenoid basal carcinoma of the uterine cervix: a case report. *Acta Cytol* 1995; 39: 563-8.
 13. Solomon D, Nayer R. The Bethesda system for reporting cervical cytology: definitions, criteria, and explanatory notes. 2nd ed. New York: Springer, 2003.
 14. Russell MJ, Fadare O. Adenoid basal lesions of the uterine cervix: evolving terminology and clinicopathological concepts. *Diagn Pathol* 2006; 1: 18.

Paediatric Primary Pachymeningeal Xanthogranuloma with Scattered Foci Displaying Reticulohistiocytoma-like Features

Miguel Fdo. Salazar^{1,2}
María del Rocío Estrada Hernández¹
Erick Gómez Apo²
Laura G. Chávez Macías²
Carlos Alfonso Rodríguez Álvarez³

¹Anatomical Pathology Division, "Dr. Manuel Gea González" General Hospital, Mexico City;
²Pathology Unit, Neuropathology Service, Mexico General Hospital, Mexico City;
³Paediatric Neurosurgery, "Legaria" Paediatric Hospital, Mexico City, Mexico

Received: February 15, 2015
Revised: April 27, 2015
Accepted: May 28, 2015

Corresponding Author

Miguel Fdo. Salazar, MD
División de Anatomía Patológica, Hospital General
"Dr. Manuel Gea González", Calzada de Tlalpan
4800, Col. Sección XVI, Delegación Tlalpan, C.P.
14080, México D.F.
Tel: +52-4000-3000 (ext. 3302)
E-mail: k7nigricans@hotmail.com

We report a unique case of a 4-year-old girl with an intriguing fibrohistiocytic tumour. Magnetic resonance imaging scans showed a dural mass of variegated intensity compressing the left occipital pole and apparently extending toward the superior sagittal sinus. Grossly, the cut surface of the surgical specimen was yellow, pale, and soft with reddish kernel-like crusts. Histologically, the yellow areas resembled cholesterol granulomas with widespread coagulative necrosis, cholesterol clefts, powdery calcification, foreign body-type giant cells, and foamy macrophages, while the scattered red spots contained numerous multinucleated giant cells of foreign-body and Touton types, the former with amphophilic to slightly eosinophilic cytoplasm. Immunoperoxidase reactions confirmed the expression of histiocytic markers and vimentin. As far as we know, no tumour displaying these peculiar morphological features has yet been described.

Key Words: CNS fibrohistiocytic tumour; Dural tumour; Cholesterol granuloma; Solitary reticulohistiocytoma; Fibroxanthoma

Fibrohistiocytic tumours are well-recognized histopathological entities that usually occur in subcutaneous and soft tissues. Nevertheless, such lesions can also involve the neural axis. We recently encountered a particularly curious example arising from the pachymeninx; thus, we present this unique case along with its singular morphological traits.

CASE REPORT

A 4-year, 7-month-old girl presented for medical consultation with her parents. They complained about a lump in the back of the child's head that made it difficult to comb and plait the girl's hair. The child was entirely asymptomatic, and there was no relevant medical history, such as systemic ailment or associated long-bone disease. Haematological and biochemical tests were unremarkable, and no lipid abnormality was detected. Magnetic

resonance imaging scans showed an occipital dural-based tumour of heterogeneous intensity slightly compressing the left occipital pole and apparently extending toward the superior sagittal sinus (Fig. 1A, B). Resection was performed, and the surgical specimen was submitted for histopathological evaluation.

The outer surface of the fixed specimen (6 × 6 × 2 cm) was gray tan, smooth, and hard, yet the transverse cut surface contained yellow, pale, and pasty material with reddish kernel-like crusts, resulting in an overall appearance similar to a slice of butter-covered raspberry bread (Fig. 1C). Under light microscopy, the pale yellow areas contained widespread coagulative necrosis, powdery calcification, numerous cholesterol clefts, foreign body-type giant cells, and foamy macrophages, while the red nodules were populated by giant cells (Fig. 2A–C). The entire lesion was demarcated by a thin fibrous wall consistent with compacted dura mater. Closer examination of the nodular areas

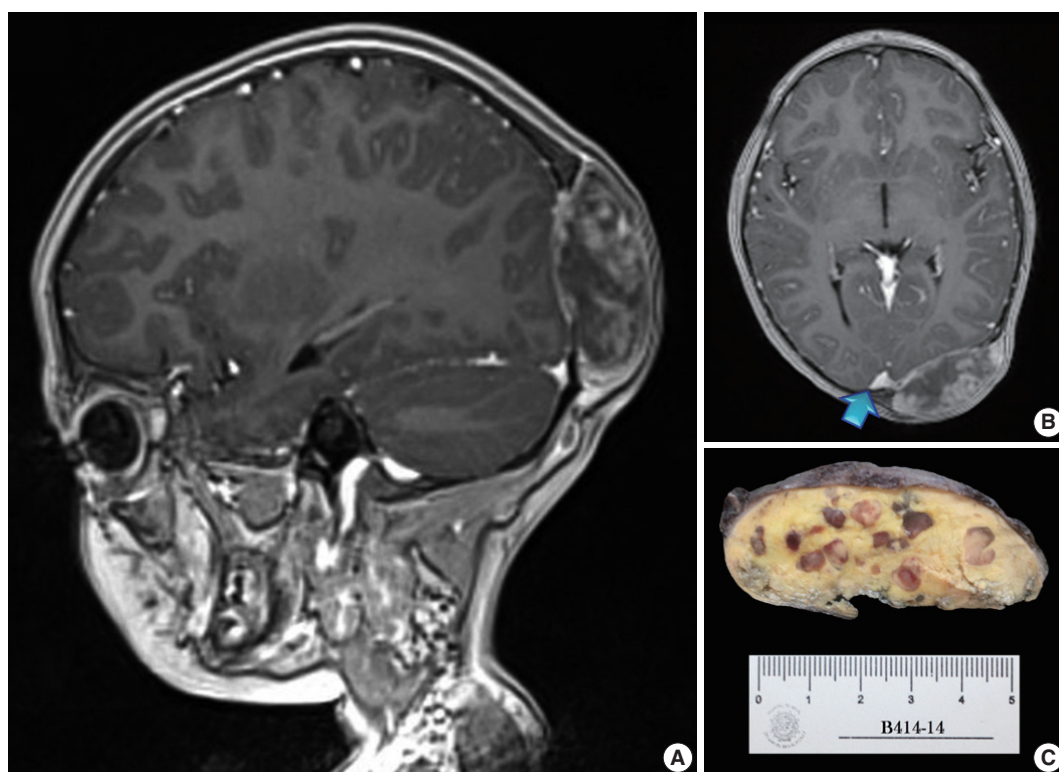


Fig. 1. Magnetic resonance imaging scans and gross surgical resection specimen. (A) T1-weighted sagittal scan demonstrating a tumour of heterogeneous intensity attached to the dura mater. (B) T1-weighted axial image. The arrow points to an area probably invaded by the tumour. (C) Transverse cut surface with a butter-covered raspberry slice of bread appearance.

detailed a miscellaneous group of giant cells including mononucleated as well as multinucleated forms of foreign-body and Touton types, the former with ground-glass amphophilic to flamboyantly eosinophilic cytoplasm and occasional empty vacuoles (Fig. 2C–G). At times, foci of a mixed inflammatory cell population could be recognized, including lymphocytes, neutrophils, and scarce eosinophils. Intriguingly, some giant cells demonstrated phagocytosis of related tumoural elements (cell cannibalism) and uptake of inflammatory cells (Fig. 2E). Disturbing bizarre nuclei were also present in some of these giant cells; however, mitotic activity was not identified (Fig. 2G). The immunoperoxidase-coupled reactions revealed a fibrohistiocytic immunophenotype with CD68, α_1 -antitrypsin (data not shown), α_1 -antichymotrypsin (data not shown), and vimentin positivity (Fig. 3A, B). CD34 immunostaining was negative but highlighted the delicate vascular branching, whereas the epithelial membrane antigen (EMA) unexpectedly delineated the giant cell borders (Fig. 3C, D). Likewise, staining for PS100, CD1a, CD207, FXIIIa, smooth-muscle actin (SMA), muscle-specific actin (MSA), podoplanin (D2-40), microphthalmia transcription factor (MITF), and glial fibrillary acidic protein (GFAP) was also negative. Ancillary histochemical stains were also requested

(Ziehl-Neelsen, auramine-rhodamine, Fite-Faraco, periodic acid-Schiff, Brown-Hopps and Grocott) and did not detect either conventional or atypical mycobacteria. An additional dural fragment labeled as “implant attached to the superior sagittal sinus” was received. It had yellow macules constituted microscopically of foamy histiocytes and multinucleated foreign-body type giant cells engulfing cholesterol crystals.

According to the aforementioned findings, the lesion was diagnosed as dural xanthogranuloma (cholesterol granuloma with broad areas of coagulative necrosis and foci of giant cells). To date the patient is healthy and without any complaints.

All procedures performed in this study were in accordance with the ethical standards of the institutional and/or national research committee and with the 1964 Helsinki Declaration and its later amendments or comparable ethical standards. Informed consent was obtained from the patient’s legal guardian, and anonymity of the patient was preserved.

DISCUSSION

Lesions of fibrohistiocytic origin seem to be quite rare among central nervous system (CNS) tumours.^{1–3} Accumulation of foamy

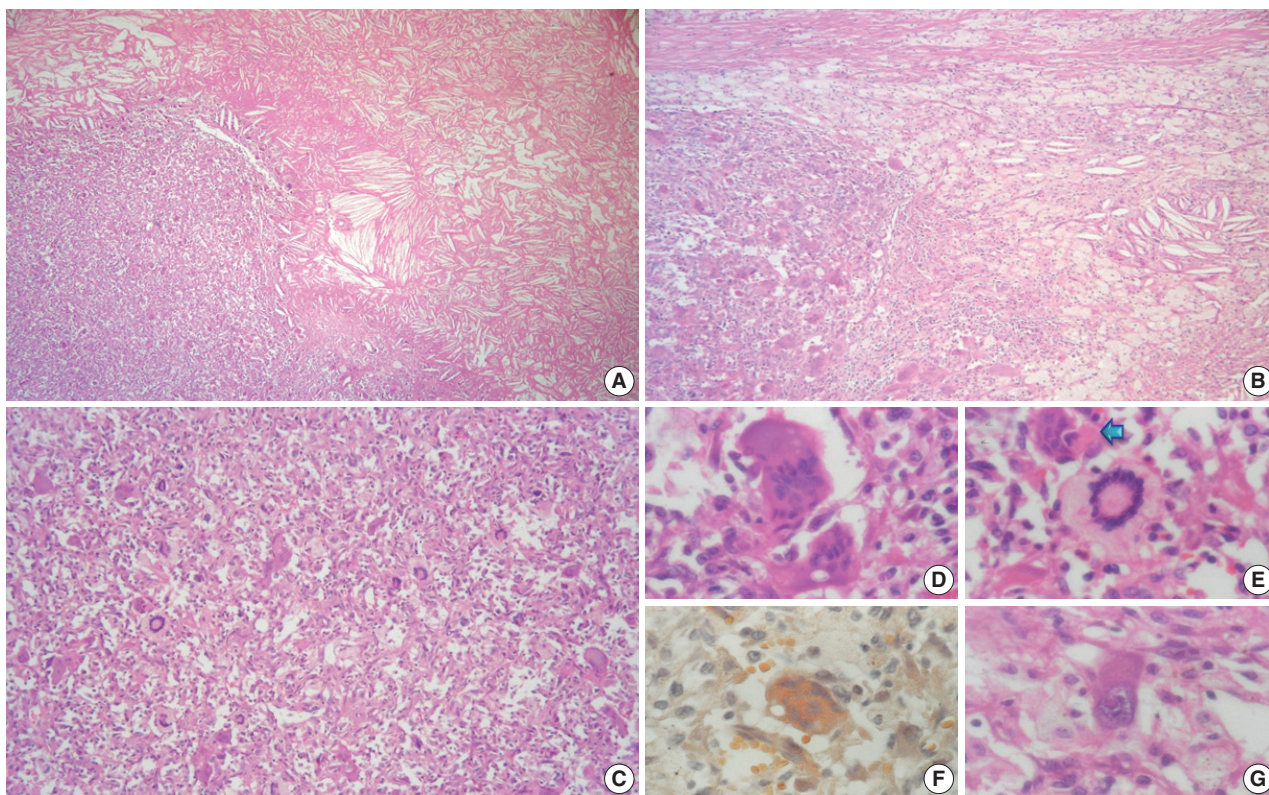


Fig. 2. Microscopic features. (A) Panoramic photomicrograph showing the boundary zone between the cholesterol granuloma area (right field) and one of the reticulohistiocytoma-like nodules (left field). (B) Boundary zone at higher magnification. Cholesterol clefts, xanthocytes, multinucleated foreign-body type giant cells, and strands of thin fibrous tissue can be identified. (C) Panoramic view of one of the reticulohistiocytoma-like nodules: "chaotic pattern" of lipidized and amphophilic multinucleated giant cells. (D) Multinucleated giant cells with amphophilic cytoplasm and empty vacuoles. (E) Touton-type giant cell next to a cannibal cell (arrow). (F) Amphophilic multinucleated giant cell with a finely granular cytoplasm filled with lipids (Oil Red). (G) Mononucleated giant cell with nuclear atypia.

macrophages in the neural axis can arise from known metabolic/storage disorders or serum lipid disturbances (secondary CNS involvement) but can also occur without an exact cause or triggering factor (primary CNS involvement).⁴⁻⁷ At present, the pathogenesis of the latter remains poorly understood. Nonetheless, two hypothetical pathways have been proposed to explain their formation:⁵⁻⁷ (1) local trauma or haemorrhage with overstimulation of mesenchymal cells from dura mater or vascular adventitia and (2) synthesis of lipotropic factors that cause undifferentiated mesenchymal cells to undergo xanthomatous transformation. These primary CNS, lipidized fibrohistiocytic tumours have been traditionally dichotomized as intraventricular (i.e., affecting *plexi choroidei*) or meningeal (dural-associated).⁴⁻⁷ This classification can be further expanded to include some other topographies, such as leptomeningeal or parenchymatous (intracerebral or intracerebellar).⁸⁻¹⁰

Although *plexi choroideorum* xanthomas have been described since the beginning of the 20th century,¹¹ the first observations of a non-ventricular fibrous xanthoma were presented in the 1973

work of Kepes *et al.*¹⁰ It was not until 1979 that Lam and Colah¹² reported the first dural-associated lesion of this kind. In contrast, CNS cholesterol granulomas (xanthogranulomas) are uncommon lesions usually found incidentally in *plexi choroidei* during postmortem examination (1.6% to 7% of autopsies). They are thought to occur either because of desquamation of choroidal epithelial cells or from local histiocytes recruited, perhaps, as formerly described.¹³ They feature needle-like cholesterol clefts flanked by foreign-body type giant cells, foamy histiocytes, chronic inflammatory cells, and scattered haemosiderin granules.^{1,2} Also, varying amounts of fibrosis can be present, becoming most marked in long-standing lesions. Otherwise, solitary reticulohistiocytoma is a distinctive but rare lesion in adults.^{1,14,15} Such tumours are seen as a yellow-brown to dark-red papule consisting of dense circumscribed nodules of deeply eosinophilic histiocytes often exhibiting multinucleation with no Touton giant cells. Some degree of nuclear atypia and occasional mitotic figures might be present. Immunoperoxidase reactions reveal expression of CD163, CD68, and vimentin, along with variable

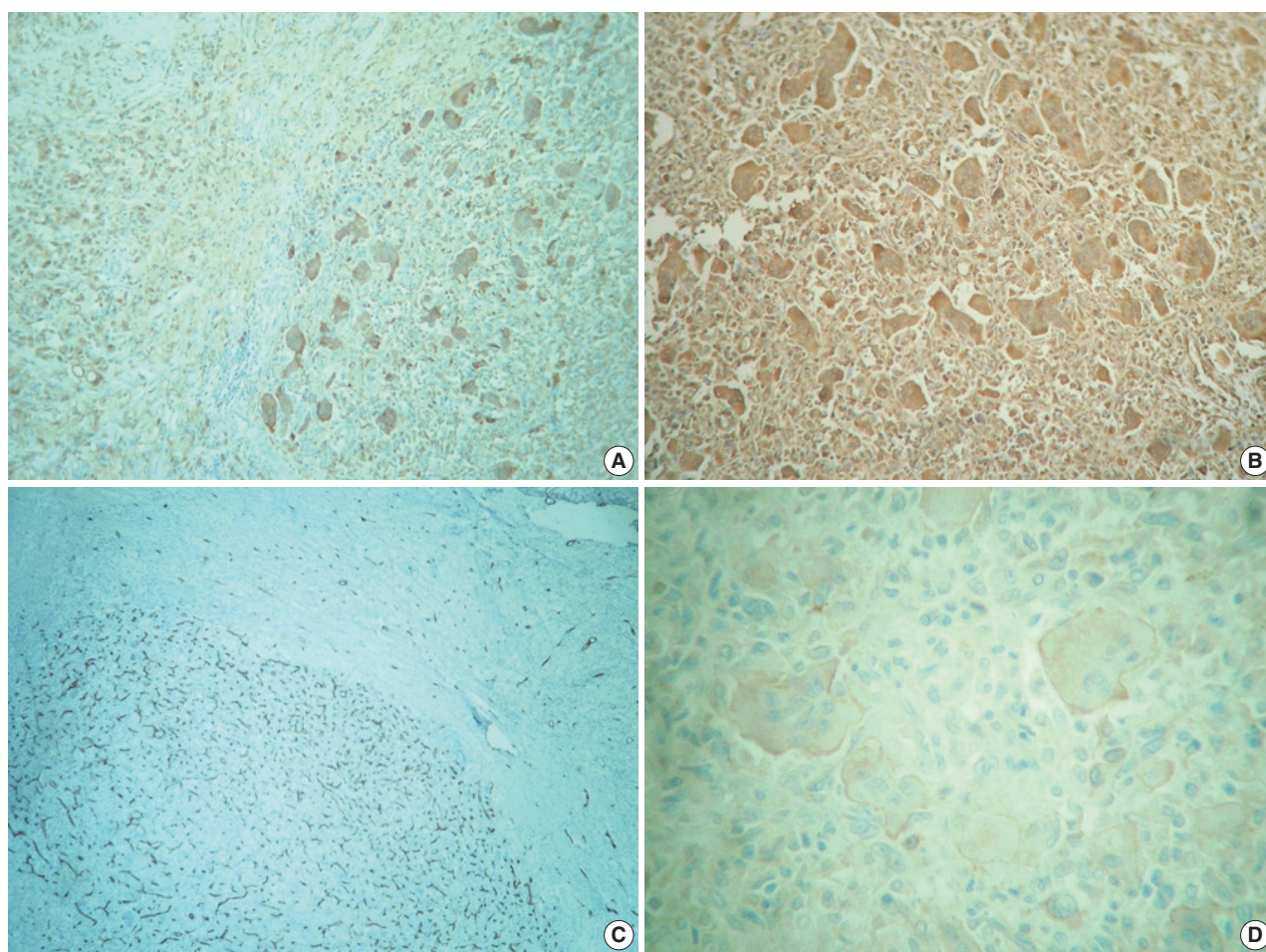


Fig. 3. Immunohistochemistry panel. (A) CD68 immunolabeling of foamy macrophages (left) and multinucleated giant cells (right). (B) Ubiquitous vimentin expression. (C) Delicate intranodal capillary branching unveiled by CD34. (D) Multinucleated giant cells' circumference immunostained with epithelial membrane antigen.

reactivity for HAM56, α_1 -antitrypsin, lysozyme, FXIIIa, PS100, MSA, and MITF. A multicentric variant has also been described, but it is associated with autoimmune disorders and internal malignancies. Interestingly, it has been suggested that the solitary form is similar to adult xanthogranuloma, with the distinction being largely based on predominance of multinucleated eosinophilic histiocytes.¹ Reports of solitary reticulohistiocytoma involving the neuroaxis are currently non-existent in the global medical literature.

There were various differential diagnoses to consider in our case, such as xanthoma, fibrous histiocytoma (fibroxanthoma), atypical fibrous histiocytoma, solitary (juvenile) xanthogranuloma, and Erdheim-Chester disease. As conveyed by Weiss and Enzinger, xanthomas are just collections of tissue histiocytes filled with lipids.^{1,5,7} These foamy macrophages are embedded within a loose stroma and organise in uniform sheets, occasionally divided into smaller nests by delicate fibrous bands. They

are thought to be closely related to cholesterol granulomas, probably in an earlier stage. Nevertheless, a comparative clinicopathological analysis of both lesions in *plexi choroidei* revealed some differences.¹⁶ Intense siderosis and a higher male-to-female ratio were noted in cholesterol granulomas (14:3 vs 13:8), while xanthomas were more frequently associated with dyslipidaemia. Histologically, benign fibrous histiocytomas are characterized by a mixture of spindle fibroblast-like cells arranged in short fascicles, with or without focal storiform profiles, and plump histiocyte-like cells accompanied by variable numbers of foamy histiocytes, haemosiderin-laden macrophages, multinucleated giant cells of foreign-body or Touton types, lymphocytes, plasma cells, and bundles of collagen.¹⁻³ The immunohistochemical profile shows an admixture of CD68, FXIIIa, CD34, PS100, SMA, and D2-40 cells, in variable proportions.^{1,3} A subset of fibrous histiocytomas exhibits borderline histologic signs of malignancy, including significantly greater cellular atypia and increased mitot-

ic activity.¹ In spite of the nuclear pleomorphism focally detected in our case, mitotic activity was not present; thus, the bizarre nuclei observed were considered a degenerative phenomenon such as that seen in ancient neurilemmoma or giant cell ependymoma. We also interpreted the small implant attached to the superior sagittal sinus as an additional lesion rather than direct extension from the larger one (i.e., an early multifocal process). Juvenile (solitary) xanthogranuloma demonstrates a wavering time-dependent appearance and is a challenging diagnosis to eliminate.^{1-3,17} Despite its classic morphology showing foamy histiocytes accompanied by Touton-type giant cells, early lesions tend to possess less intracytoplasmic lipid droplets. Hence, mononuclear cells display a plump eosinophilic cytoplasm. Conversely, longstanding lesions usually develop interstitial fibrosis and even assume a vague storiform pattern. Additionally, the existence of transitional cases with or without xanthomatous features, with or without interspersed spindle cells, and containing multinucleated giant cells with or without Touton configuration is also possible. Usually, a modest number of acute and chronic inflammatory cells are also present, especially eosinophils. Regardless of morphology, macrophages and Touton cells show immunoreactivity for CD68, α_1 -antitrypsin, α_1 -antichymotrypsin, lysozyme, CD31, and FXIIIa. Langerhans and non-Langerhans cell histiocytoses are also worth considering.² The former can be ruled out by means of an appropriate immunohistochemistry panel (PS100, CD1a, and CD207) in a suitable clinical setting (localized vs multiple sites of involvement). On the other hand, the latter can be troublesome, particularly when Erdheim-Chester disease is suspected, which is a rare disorder that most often becomes apparent in middle age and is typically seen in the context of long-bone and systemic disease. It is characterized by lipid-laden CD68+, CD1a-, and PS100- macrophages and Touton-type multinucleated giant cells accompanied by scarce eosinophils. Indeed, the reddish nodules described in our case displayed some of these features; however, considering the lack of multiple organ involvement, we considered the multinucleated foreign-body type giant cells to represent a trait more akin to solitary reticulohistiocytoma than to Erdheim-Chester disease. Tuberculosis was also a consideration; however, the gross appearance of the lesion was not consistent with a tuberculoma, which is usually hard and chalky-white rather than soft, and pale-yellow. Also, tuberculosis tends to be infratentorial in the paediatric population. Furthermore, there was no Heubner arteritis or typical epithelioid granulomas of tuberculosis with caseous necrosis and Langhan type giant cells. One might argue that it can be entirely feasible in an immunodeficient patient;

however, as previously stated, our patient was a completely healthy girl who had already received her bacillus Calmette-Guérin vaccine (which only provides protection against the leptomeningeal form). Other non-fibrohistiocytic neoplasms can show extensive xanthomatous changes, such as glioblastoma, pleomorphic xanthoastrocytoma, and metaplastic meningioma.^{10,18} Nonetheless, immunoperoxidase-coupled assays for GFAP and EMA can be useful to achieve a diagnosis in these settings. Though a dull peripheral rim was observed in the multinucleated giant cells through EMA immunostaining, it was uncertain whether to dismiss it as an artifact. Indeed, EMA expression has been demonstrated in normal plasma cells, monoblasts, and in some hematological malignancies.¹⁹

Xanthogranuloma and solitary reticulohistiocytoma are conditions grouped among the pathogenetically diverse category of fibrohistiocytic tumours.¹ Interestingly, these miscellaneous lesions sometimes show stunning overlapping morphological or immunophenotypic traits, which might be explained on the basis of the “facultative fibroblast” concept proposed by Ozzello in 1963.^{12,20} This concept features a cell with an inherent capacity to transdifferentiate to another morphologic and functional state, an assumption that could be true for the present case. Nonetheless, it can simply represent a time-dependent phenomenon (i.e., evolving stages of the same process). Hence, we report a lipidized fibrohistiocytic lesion arising in the dural coat of the CNS with peculiar and unconventional traits that, as far as we know, have not been previously described.

Conflicts of Interest

No potential conflict of interest relevant to this article was reported.

REFERENCES

1. Goldblum JR, Folpe AL, Weiss SW. Benign fibrohistiocytic and histiocytic tumors. In: Goldblum JR, Folpe AL, Weiss SW, eds. *Enzinger and Weiss's soft tissue tumors*. 6th ed. Philadelphia: Elsevier-Saunders, 2014; 341-86.
2. Paulus W, Perry A. Histiocytic tumours. In: Louis DN, Ohgaki H, Wiestler OD, Cavenee WK, eds. *WHO classification of tumours of the central nervous system*. 4th ed. Lyon: IARC Press, 2007; 193-6.
3. Black J, Coffin CM, Dehner LP. Fibrohistiocytic tumors and related neoplasms in children and adolescents. *Pediatr Dev Pathol* 2012; 15(1 Suppl): 181-210.
4. Chung IH, Lee YS, Myong NH, Lee MJ, Lee SK, Ko JH. Intracranial fibroxanthoma in an infant: a case report. *Korean J Radiol* 2009; 10:

- 402-6.
5. Kim DS, Kim TS, Choi JU. Intradural extramedullary xanthoma of the spine: a rare lesion arising from the dura mater of the spine: case report. *Neurosurgery* 1996; 39: 182-5.
 6. Miyazono M, Nishio S, Morioka T, Hamada Y, Fukui M, Yanai S. Fibroxanthoma arising from the cranial dura mater. *Neurosurg Rev* 1999; 22: 215-8.
 7. Usul H, Kuzeyli K, Cakir E, *et al.* Giant cranial extradural primary fibroxanthoma: a case report. *Surg Neurol* 2005; 63: 281-4.
 8. Pimentel J, Fernandes A, Távora L, Miguéns J, Lobo Antunes J. Benign isolated fibrohistiocytic tumor arising from the central nervous system: considerations about two cases. *Clin Neuropathol* 2002; 21: 93-8.
 9. Harries AM, Mitchell R. Haemorrhagic cerebellar fibrous histiocytoma: case report and literature review. *Br J Neurosurg* 2011; 25: 120-1.
 10. Kepes JJ, Kepes M, Slowik F. Fibrous xanthomas and xanthosarcomas of the meninges and the brain. *Acta Neuropathol* 1973; 23: 187-99.
 11. Blumer G. Bilateral cholesteatomatous endothelioma of the choroid plexus. *Johns Hopkins Hosp Rep* 1900; 9: 279-90.
 12. Lam RM, Colah SA. Atypical fibrous histiocytoma with myxoid stroma: a rare lesion arising from dura mater of the brain. *Cancer* 1979; 43: 237-45.
 13. Pear BL. Xanthogranuloma of the choroid plexus. *AJR Am J Roentgenol* 1984; 143: 401-2.
 14. Berti E, Zelger B, Caputo R. Reticulohistiocytosis. In: LeBoit PE, Burg G, Weedon D, Sarasin A, eds. *World Health Organization classification of tumours: pathology and genetics of skin tumours*. Lyon: IARC Press, 2006; 224-5.
 15. Miettinen M, Fetsch JF. Reticulohistiocytoma (solitary epithelioid histiocytoma): a clinicopathologic and immunohistochemical study of 44 cases. *Am J Surg Pathol* 2006; 30: 521-8.
 16. Muenchau A, Laas R. Xanthogranuloma and xanthoma of the choroid plexus: evidence for different etiology and pathogenesis. *Clin Neuropathol* 1997; 16: 72-6.
 17. Perry A, Dehner LP. Meningeal tumors of childhood and infancy. An update and literature review. *Brain Pathol* 2003; 13: 386-408.
 18. Sarkar C, Roy S, Bhatia S. Xanthomatous change in tumours of glial origin. *Indian J Med Res* 1990; 92: 324-31.
 19. Leong CF, Raudhawati O, Cheong SK, Sivagengei K, Noor Hamidah H. Epithelial membrane antigen (EMA) or MUC1 expression in monocytes and monoblasts. *Pathology* 2003; 35: 422-7.
 20. Ozzello L, Stout AP, Murray MR. Cultural characteristics of malignant histiocytomas and fibrous xanthomas. *Cancer* 1963; 16: 331-44.

Human Herpesvirus 8-Negative and Epstein-Barr Virus-Positive Effusion-Based Lymphoma in a Patient with Human Immunodeficiency Virus

Jung-Woo Choi · Younghye Kim
Ju-Han Lee · Young-Sik Kim

Department of Pathology, Korea University Ansan Hospital, Korea University College of Medicine, Ansan, Korea

Received: May 12, 2015
Revised: June 2, 2015
Accepted: June 3, 2015

Corresponding Author

Young-Sik Kim, MD, PhD
Department of Pathology, Korea University Ansan Hospital, Korea University College of Medicine, 123 Jeokgeum-ro, Danwon-gu, Ansan 15355, Korea
Tel: +82-31-412-5321
Fax: +82-31-412-5324
E-mail: apysk@korea.ac.kr

A 39-year-old man infected with human immunodeficiency virus (HIV) was admitted to our hospital because of sudden onset of chest pain. Chest radiography revealed pneumothorax of the right lung. Computed tomographic scans disclosed a 5.8-cm-sized emphysematous bulla in the right middle lobe of the lung. Histologically, the wedge-resected lung showed medium to large atypical cells within the bullous cavity of the *Pneumocystis jirovecii* pneumonia, without solid mass formation. These atypical cells were confirmed to be large B-cell lymphoma, Epstein-Barr virus-positive and human herpesvirus 8-negative. Therefore, this case was not diagnosed as primary effusion lymphoma, but effusion-based lymphoma arising in an emphysematous cavity of an HIV-infected patient. This type of effusion-based lymphoma has never been reported, and, although rare, it should be noted in order to clinically diagnose this lymphoma.

Key Words: Effusion-based lymphoma; Human herpesvirus 8; Epstein-Barr virus; HIV

Primary effusion lymphoma (PEL) is the only subtype of effusion-based lymphoma (EBL) listed on the 2008 World Health Organization (WHO) classification, and it is specified as a large B-cell lymphoma that presents as serous effusions without a detectable tumor mass.¹ PEL represents one of the specific lymphomas that occur in human immunodeficiency virus (HIV)-positive patients, accounting for less than 3% of all HIV-related lymphomas.² PEL cells are usually negative for pan-B-cell markers and often reveal a consistent dual herpesvirus infection with both human herpesvirus 8 (HHV8) and Epstein-Barr virus (EBV). Recently, HHV8-negative EBL has emerged as a distinct entity, often associated with older patient age, clinical history of fluid overload, and a universal expression of pan-B-cell markers.^{3,4} Patients with HHV8-negative EBL tend to be positive for the hepatitis C virus, but negative for HIV and EBV infection. Meanwhile, HHV8-positive solid lymphomas without lymphomatous effusions are considered extracavitary variants of PEL, which have been validated via gene expression profiling and proteomic analyses.⁵ In this context, we report herein another unique case of HHV8-negative and EBV-positive EBL, which developed from the bullous cavity of *Pneumocystis jirovecii* pneumonia (PJP) in a clinical background of HIV infection.

CASE REPORT

A 39-year-old man visited our hospital because of two enlarging dusky-colored patches on his chin and forehead, both of which appeared 1 month prior to his visit. Both skin lesions were diagnosed as Kaposi sarcoma, and the patient was diagnosed to be HIV positive. Two months later, he experienced sudden onset of chest pain and difficulty breathing. Laboratory tests showed high levels of white blood cells (10,600/ μ L) with 73.5% granulocytes and serum lactate dehydrogenase of 679 IU/L. The patient's CD4 T-cell count had decreased to 19 cells/ μ L. Hepatitis A, B, or C viruses were not detected. Computed tomographic scans of his chest revealed a 5.8-cm emphysematous bulla in the right middle lobe of his lung, while the left lobe showed diffuse ground glass opacities, suggestive of interstitial pneumonia (Fig. 1A). The patient underwent wedge resection of the lung, which grossly revealed a multilocular bullous cavity surrounded by whitish pneumonic consolidation (Fig. 1B). Microscopically, aggregates of atypical lymphoid cells were floating in the bullous cavity without forming solid masses. These cells showed medium to large pleomorphic nuclei with prominent nucleoli and basophilic cytoplasm, revealing plasmablastic features (Fig. 2). Th-

rough immunohistochemistry, tumor cells were found to exhibit a non-germinal center B-cell nature showing positivity for CD20, CD79a, and MUM1 but negativity for CD3, CD10, BCL6,

CD30, and CD138. The Ki-67 labeling index reached up to 80%–90%. Tumor cells were positive for EBV-encoded RNA *in situ* hybridization, EBV latent membrane protein-1 (LMP1),

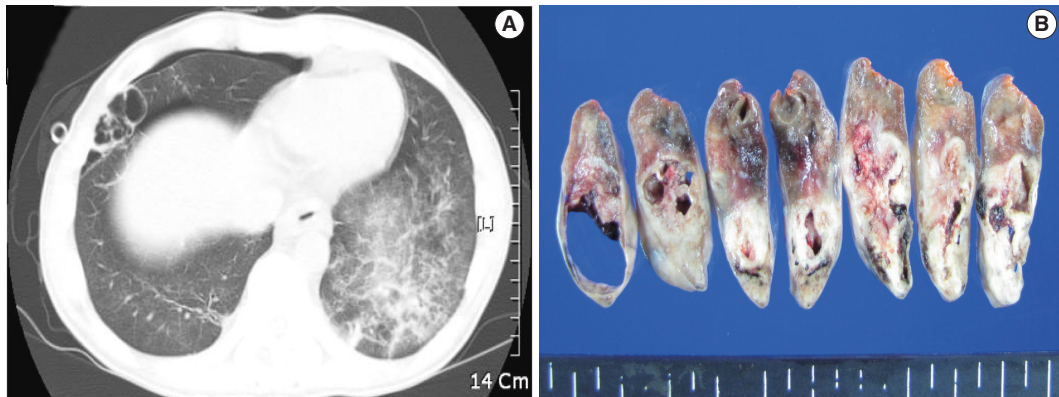


Fig. 1. A computed tomographic scan (A) and serial lung sections (B) displaying a 5.8-cm multilocular emphysematous bulla surrounded by pneumonic consolidation in the right middle lobe of the lung. The left lung shows diffuse ground glass opacities, which is consistent with interstitial pneumonia.

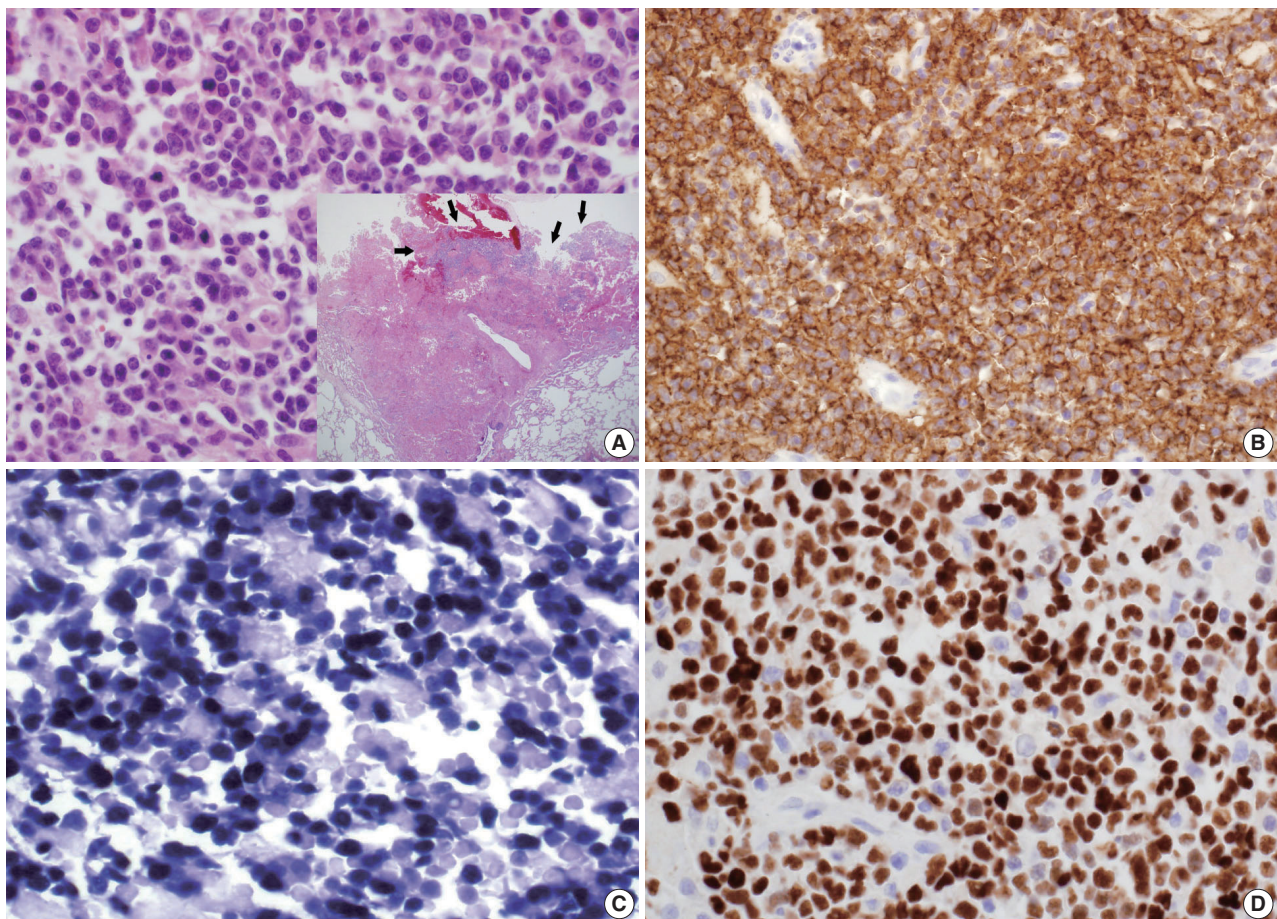


Fig. 2. Lymphoma cells have large eccentric pleomorphic nuclei and basophilic cytoplasm, showing plasmablastic features (A). Proliferating and necrotic tumor cells (arrows) are located in the bullous cavity, representing effusion-based nature (A inset). Tumor cells are positive for CD20 immunohistochemistry (IHC) (B), Epstein-Barr virus (EBV) *in situ* hybridization (C) and also EBV nuclear antigen-2 IHC (D).

Table 1. Main differential diagnoses of this case

	Present case	PEL	HHV8-negative EBL	DLBCL associated with chronic inflammation
Age at diagnosis	39 yr	Young or middle-aged	Old (median, 70 yr)	Old (median, 65–70 yr)
Underlying condition	<i>Pneumocystis jirovecii</i> pneumonia	ND	Fluid overload	Pyothorax or chronic pleuritis
Site of involvement	Pneumonic bullae	Body cavities	Body cavities	Body cavities
Immunophenotype	CD20(+), CD79a(+), MUM1(+), CD138(-), CD30(-)	CD20(-), CD79a(-), CD138(+), CD30(+/-)	CD20(+), CD79a(+), CD138(+/-), CD30(+/-)	CD20(+/-), CD79a(+/-), MUM1(+), CD138(+), CD30(+/-)
Viral infection	HIV(+), HHV8(-) EBV(+, latency III), HCV(-)	HIV(+), HHV8(+) EBV(+, latency II), HCV(-)	HIV(-), HHV8(-) EBV(-), HCV(+, 26.5%)	HIV(-), HHV8(-) EBV(+, latency III), HCV(-)
Prognosis	Unknown	Unfavorable (median survival, <6 mo)	Variable (median survival, 10 mo)	Unfavorable (5-yr survival, 20%–35%)

PEL, primary effusion lymphoma; HHV8, human herpesvirus 8; EBL, effusion-based lymphoma; DLBCL, diffuse large B-cell lymphoma; ND, not described; HIV, human immunodeficiency virus; EBV, Epstein-Barr virus; HCV, hepatitis C virus.

EBV nuclear antigen-2 (EBNA-2), but negative for HHV8. The background bullous cavity and adjacent alveolar cavities were filled with frothy exudates containing *Pneumocystis jirovecii* clearly visible after application of Gomori methenamine silver stain. Therefore, the patient was diagnosed with EBL, not PEL, arising in the PJP-associated cavitory lung lesion. He was treated with highly active antiretroviral therapy along with anti-microbes for 6 months, followed by chemotherapy.

DISCUSSION

This is a unique case of EBL occurring in the PJP-associated bullous cavity of the lung. The differential diagnosis of this case includes HHV8-negative EBL, PEL, and diffuse large B-cell lymphoma (DLBCL) associated with chronic inflammation (Table 1). While PEL is the only subtype of EBL listed in the 2008 WHO classification, HHV8-negative EBL has been steadily considered a separate entity, because the demographics, immunophenotype, and clinical outcome of HHV8-negative EBL are inconsistent with PEL.^{3,4} In contrast to this case, PEL is invariably positive for HHV8, and usually negative for pan-B-cell markers.¹ Compared to HHV8-negative EBL, this case did not show any clinical condition of fluid overload such as cirrhosis, protein-losing enteropathy, or cardiac disease. In addition, the tumor in this case developed in the setting of both HIV and EBV positivity, while negative for the hepatitis C virus, which is the reverse of HHV8-negative EBL. With regard to the tumor's origin, the present case is unique in that all previously reported cases of EBL involved pleural, peritoneal, or pericardial cavities, except for one, which was detected from scrotal effusion fluids.⁶ Although our case most closely resembles DLBCL associated with chronic inflammation, in that it is a lymphoid neoplasm often involving the body cavity and occurring in a condition of

chronic inflammation and EBV infection, DLBCL forms a detectable tumor mass and typically develops after a long-standing inflammation, usually over 10 years.⁷ It is unclear whether this particular tumor should be considered a previously undescribed subtype of DLBCL, or whether it corresponds with a rare variant of HHV8-negative EBL or DLBCL associated with chronic inflammation.

Interestingly, this tumor was accidentally discovered in the pneumothorax as a complication of PJP. The incidence of pneumothorax in HIV-positive patients is approximately 2%, but can reach up to 9% in those with PJP.^{8,9} It has been reported that chronic inflammation and localized immunosuppression may enhance the clonal evolution of EBV-infected lymphocytes.¹⁰ DLBCL cells in HIV-positive patients have been known to express the interleukin-6 (IL-6) receptor, which can respond to the IL-6 produced by adjacent non-neoplastic cells in a paracrine manner.¹¹ In addition, similar to DLBCL associated with chronic inflammation, the tumor cells in this case revealed EBV latency type III (LMP1-positive, EBNA-2-positive) infection, which represents the most complete form of latent gene expression.^{12,13} This finding is in contrast to PEL, in which the tumor cells are infected with the more restricted EBV latency type II (LMP1-positive, EBNA-2-negative) infection.¹⁴

In conclusion, the present case is a rare instance of HHV8-negative and EBV-positive EBL in an HIV-positive patient. This type of clinical presentation has never been described previously, and it should be kept in mind in order to diagnose occult lymphomas.

Conflicts of Interest

No potential conflict of interest relevant to this article was reported.

Acknowledgments

This work was supported by Basic Science Research Program through the National Research Foundation of Korea (NRF) funded by the Ministry of Science, ICT and Future Planning (grant number: 2013 R1A1A1058146).

REFERENCES

- Said J, Cesarman E. Primary effusion lymphoma. In: Swerdlow SH, Campo E, Harris NL, et al., eds. WHO classification of tumours of haematopoietic and lymphoid tissues. 4th ed. Lyon: IARC Press, 2008; 260-1.
- Raphael M, Said J, Borisch B, Cesarman E, Harris NL. Lymphomas associated with HIV infection. In: Swerdlow SH, Campo E, Harris NL, et al. eds. WHO classification of tumours of haematopoietic and lymphoid tissues. 4th ed. Lyon: IARC Press, 2008; 340-2.
- Alexanian S, Said J, Lones M, Pullarkat ST. KSHV/HHV8-negative effusion-based lymphoma, a distinct entity associated with fluid overload states. *Am J Surg Pathol* 2013; 37: 241-9.
- Wu W, Youm W, Rezk SA, Zhao X. Human herpesvirus 8-unrelated primary effusion lymphoma-like lymphoma: report of a rare case and review of 54 cases in the literature. *Am J Clin Pathol* 2013; 140: 258-73.
- Carbone A, Volpi CC, Caccia D, et al. Extracavitary KSHV-positive solid lymphoma: a large B-cell lymphoma within the spectrum of primary effusion lymphoma. *Am J Surg Pathol* 2013; 37: 1460-1.
- Nakamura Y, Tajima F, Omura H, Ishiga K, Kawatani T, Murawaki Y. Primary effusion lymphoma of the left scrotum. *Intern Med* 2003; 42: 351-3.
- Iuchi K, Aozasa K, Yamamoto S, et al. Non-Hodgkin's lymphoma of the pleural cavity developing from long-standing pyothorax: summary of clinical and pathological findings in thirty-seven cases. *Jpn J Clin Oncol* 1989; 19: 249-57.
- McClellan MD, Miller SB, Parsons PE, Cohn DL. Pneumothorax with *Pneumocystis carinii* pneumonia in AIDS: incidence and clinical characteristics. *Chest* 1991; 100: 1224-8.
- Sepkowitz KA, Telzak EE, Gold JW, et al. Pneumothorax in AIDS. *Ann Intern Med* 1991; 114: 455-9.
- Copie-Bergman C, Niedobitek G, Mangham DC, et al. Epstein-Barr virus in B-cell lymphomas associated with chronic suppurative inflammation. *J Pathol* 1997; 183: 287-92.
- Emilie D, Coumbaras J, Raphael M, et al. Interleukin-6 production in high-grade B lymphomas: correlation with the presence of malignant immunoblasts in acquired immunodeficiency syndrome and in human immunodeficiency virus-seronegative patients. *Blood* 1992; 80: 498-504.
- Cohen JL, Bollard CM, Khanna R, Pittaluga S. Current understanding of the role of Epstein-Barr virus in lymphomagenesis and therapeutic approaches to EBV-associated lymphomas. *Leuk Lymphoma* 2008; 49 Suppl 1: 27-34.
- Fukayama M, Ibuka T, Hayashi Y, Ooba T, Koike M, Mizutani S. Epstein-Barr virus in pyothorax-associated pleural lymphoma. *Am J Pathol* 1993; 143: 1044-9.
- Horenstein MG, Nador RG, Chadburn A, et al. Epstein-Barr virus latent gene expression in primary effusion lymphomas containing Kaposi's sarcoma-associated herpesvirus/human herpesvirus-8. *Blood* 1997; 90: 1186-91.

Oncocytic Renal Cell Carcinoma with Tubulopapillary Growth Having a Fat Component

Na Rae Kim · Hyun Yee Cho

Department of Pathology, Gachon University Gil Medical Center, Incheon, Korea

Received: April 24, 2015

Revised: June 3, 2015

Accepted: July 1, 2015

Corresponding Author

Hyun Yee Cho, MD

Department of Pathology, Gachon University Gil Medical Center, 21 Namdong-daero 774 beon-gil, Namdong-gu, Incheon 21565, Korea

Tel: +82-32-460-3865

Fax: +82-32-460-2394

E-mail: hicho@gilhospital.com

We report a rare case of oncocytic renal cell carcinoma (RCC) with tubulopapillary growth in the background of tuberculous end-stage kidney disease. Histology of the renal mass consisted of oncocytic cells forming solid, thin tubules and rare papillae. The tumor had abundant eosinophilic oncocytic cells containing occasional cytoplasmic Mallory body-like hyaline globules and a tiny focus of clear cells with intervening mature fat. Both the oncocytic cells and clear cells were immunoreactive for α -methylacyl-CoA racemase, vimentin, pancytokeratin, and CD10, and negative for transcription factor E3, CD15, human melanoma black 45, and c-kit. Mallory body-like hyaline globules were positive for CAM 5.2 and periodic acid-Schiff with or without diastase. Ultrastructurally, the tumor cells had abundant cytoplasmic mitochondria. The present case is a rare case of oncocytic RCC with tubulopapillary growth pattern. The case is unique in that the tumor was mixed with fat component, which is not common in RCC and thus can lead to misdiagnosis.

Key Words: Oxyphil cells; Carcinoma, renal cell; Adipocytes; Mycobacterium tuberculosis

Recent advances in cytogenetics have altered the traditional classification of renal cell carcinoma (RCC). According to the latest World Health Organization classification, renal cell tumors are classified based on their morphological, immunohistochemical, and genetic features.¹ The following subgroups can be used to classify these tumors: clear cell RCC (*VHL* and others on chromosome 3), papillary RCC (*MET*), chromophobe RCC (*TP53*), and collecting duct RCC.² Among them, papillary RCC can display extensive areas of solid and non-papillary architecture and extensive areas of oncocytic cytoplasm. As a rare morphological variant of papillary RCC, oncocytic RCC has been described as having papillotubular growth, as oncocytic papillary RCC with an inverted nuclear pattern, or as oncocytic papillary RCC with solid architecture.³⁻⁶ This new variant is composed of tumor cells with morphological, immunohistochemical, and ultrastructural characteristics of oncocytes, and frequently presents as high nuclear grade 3, type 2 papillary RCC with rare metastases, similar to type 1 papillary RCC. The present case of an oncocytic variant of RCC coexisted with renal tuberculosis.

Here, we report a rare case of oncocytic RCC with a tubulopapillary growth pattern and extracellular mature fat component in a tuberculous end-stage kidney and discuss its complex differential diagnosis.

CASE REPORT

A 52-year-old male had been treated for chronic renal failure and had been on continuous ambulatory peritoneal dialysis for 9 years. He visited our hospital due to a recent onset of vague left flank pain. Abdominopelvic computed tomography (CT) revealed a round mass in the lower pole of the left kidney and marked hydronephroureter with cortical thinning of bilateral kidneys (Fig. 1). Chest CT showed segmental consolidation with surrounding ground glass opacity in the right upper lobe, suggesting pulmonary tuberculosis. Bilateral nephrectomy was then performed.

Grossly, a well-circumscribed, round, solid mass measuring 2.5×2.0×1.5 cm was found at the lower pole of the left kidney. The cut surface of the mass was yellow-tan colored. Both kidneys showed severe hydronephrosis and pyelonephritic changes. The dilated pelvocalyces were covered with yellow-tan necrotic material. Microscopically, most of the mass was composed of solid and thin tubules of eosinophilic oncocytic cells mixed with mature fat (Fig. 2A, B). The polygonal-shaped tumor cells had abundant eosinophilic granular cytoplasm and round nuclei with prominent nucleoli (Fig. 2C). Elongated tubular architectures were predominant with occasional detachment from the lumens



Fig. 1. Coronal view of abdominopelvic computed tomography reveals severe hydronephrosis of bilateral kidneys. Note a round lesion in the left kidney (arrow).

(Fig. 2D). The tumor demonstrated only focal large papillary fronds that contained delicate fibrovascular cores (Fig. 2E, left) and aggregates of clear cells (Fig. 2E, right). Occasionally, the oncocytic cells had Mallory body–like eosinophilic cytoplasmic hyaline globules (Fig. 2E, left). Mitotic figures were counted up to 2 per 10 high power fields. The surrounding parenchyma showed a caseous necrotic cystic wall. Immunohistochemically, both the oncocytic and clear cells were diffusely strongly positive for vimentin (prediluted, V9, Dako, Glostrup, Denmark), pancytokeratin (prediluted, AE1/AE3, Dako), and α -methylacyl-CoA racemase (AMACR; 1:50, EPUM1, Novocastra, New Castle upon Tyne, UK). Some of the oncocytic cells were weakly positive for CD10 (1:100, 56C6, Dako). The tumor cells were negative for epithelial membrane antigen (prediluted, E29, Dako), cytokeratin 7 (CK7; 1:100, OV-TL, Dako), MOC31 (MOC31; 1:70, Novocastra), E-cadherin (1:50, 36B5, Dako), carcinoembryonic antigen (prediluted, Dako), progesterone receptor (1:50, PgR636, Dako), CD15 (1:50, C3D-1, Dako), human melanoma black 45 (HMB-45; prediluted, Dako), transcription factor E3 (1:50, MRQ-37, Cell Marque Corporation, Rocklin, CA, USA), and c-kit (1:30, T595, Novocastra). These cells were also

negative for Hale's colloidal iron and periodic acid–Schiff (PAS) staining. Mallory body–like eosinophilic hyaline globules were stained with PAS and diastase-resistant (Fig. 2F, right), and they were slightly positive for CAM 5.2 (prediluted, BD Bioscience, San Diego, CA, USA) and negative for α -fetoprotein (prediluted, Dako). The tumor was diagnosed as oncocytic papillary RCC of Fuhrman's nuclear grade 3. Surrounding parenchyma as well as renal pelvis and ureter showed chronic granulomatous inflammation with caseation necrosis. The oncocytic areas of the paraffin block were taken for ultrastructural examination. Electron microscopy revealed that the ovoid-shaped tumor cells had abundant cytoplasm and round nuclei with a euchromatic pattern. They had abundant mitochondria and some rough endoplasmic reticula (Fig. 3).

The mass was diagnosed as oncocytic RCC with a tubulopapillary growth pattern. During 9 years of postoperative follow up, the patient showed no recurrence or metastasis.

Institutional Review Board (IRB) of Gachon University Gil Medical Center (IRB No. GCIRB2015-192) approval was obtained for this case report.

DISCUSSION

Under light microscopy, the present renal tumor showed the characteristic pathologic findings of oncocytic tumor composed of mainly solid architecture with thin tubules, i.e., short papillae and intermixed fat. There are several oncocytic renal cell neoplasms with these histopathological features, which poses a diagnostic problem in differentiation between RCC with oncocytic features, oncocytoma-like epithelioid angiomyolipoma (AML), and renal oncocytoma.¹ Renal oncocytoma shows typical gross features of a solitary, well-circumscribed, slightly lobulated, solid appearance with a mahogany brown or dark red cut surface with a frequent central scar. Microscopically, the small, round, uniform tumor cells of oncocytoma have abundant, faintly eosinophilic granular cytoplasm, and the cells are arranged in nests and tubulocystic, solid, or trabecular patterns with a myxomatous or hyalinized stroma. Immunohistochemistry can be helpful for arriving at the correct diagnosis because the distinct immunopositivity for c-kit and the immunonegativity for CK7 and vimentin are characteristic of renal oncocytoma.¹ Clear cell RCC has diverse architecture of solid, alveolar, and acinar patterns, but prominent papillary architecture is not common. An extensive papillary architecture is one of the characteristic features of papillary RCC. A focal tubular growth pattern with small papillae may be also seen in papillary RCC, but extensive

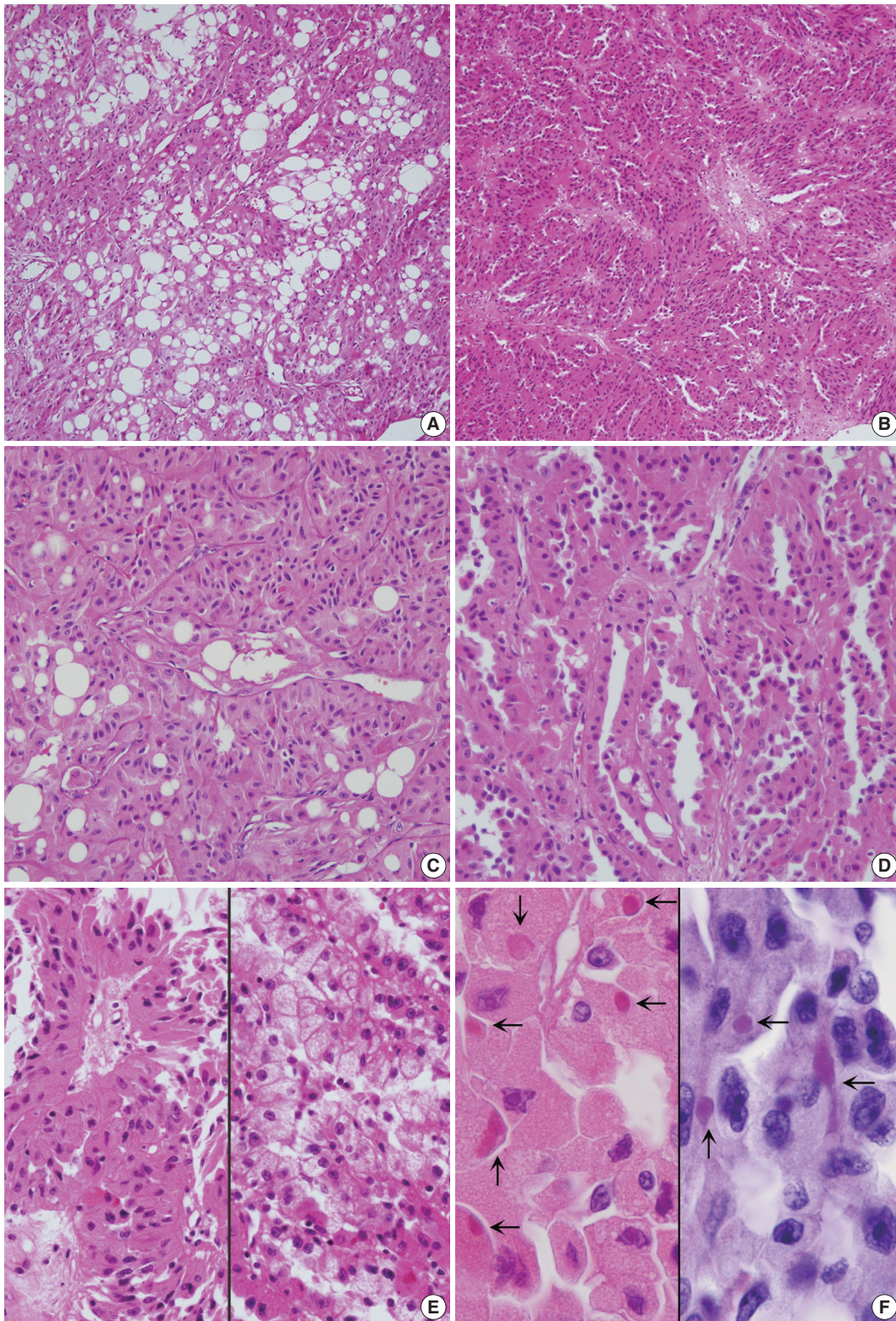


Fig. 2. (A) Tumor cells with abundant eosinophilic cytoplasm are arranged in solid papillae and tubules, intermingled with mature fat component. (B) The tumor is composed of a compact arrangement of small thin tubules. (C) At the solid area, lobules separated by thin capillaries consist of eosinophilic and granular tumor cells. Note fat vacuoles. (D) Eosinophilic tumor cells are lining the tubules with focal surface decapitation. (E) Oncocytic cells occasionally form papillary architecture (left). The tubules of clear tumor cells have the appearance of clear-type renal cell carcinoma (right). (F) The oncocytic cells have eosinophilic cytoplasmic globules (arrows, left) that are stained with periodic acid-Schiff (right).

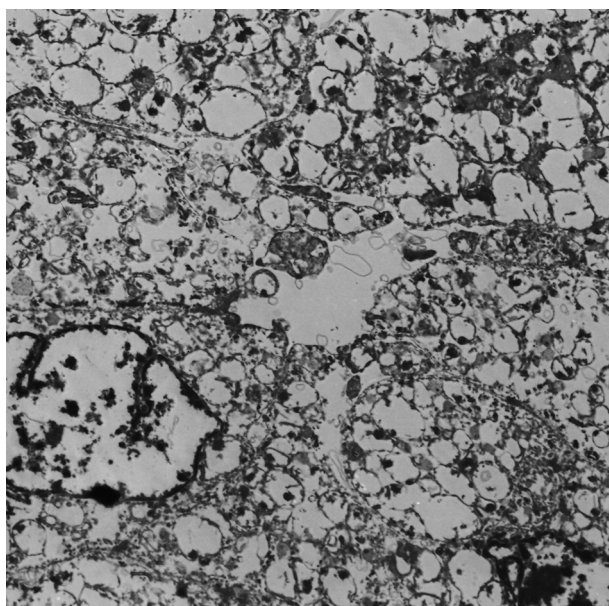


Fig. 3. Electron microscopy reveals oval-shaped tumor cells with abundant mitochondria and shelf-like cristae ($\times 3,000$).

tubular structures with intraluminal papillary projections have been rarely described.^{3,4} Recent studies reported that a variant of oncocytic RCC having papillotubular growth shows the histology of an extensive small tubular growth pattern, often with papillary fronds. Such tumors are mainly composed of oncocytic cells with eosinophilic granular cytoplasm and some scattered clear vacuolar cells.^{2,4} Either the oncocytic cells or the clear cells in those studies were positive for AMACR, CD10, CK7, epithelial membrane antigen, and vimentin, but they were negative for c-kit and E-cadherin. These histological and immunohistochemical findings are partly shared by those of the present case. Yet in the present case, the microscopic presence of mature fat among the monotonous polygonal cells with oncocytic cytoplasm suggested a possible diagnosis of oncocytoma-like epithelioid AML.⁷ Epithelioid AML was often misdiagnosed as granular, chromophobe, or high-grade unclassified RCC until it was included in the classification system of renal tumors. Intratumoral fat may be rarely found in RCC.⁸ Therefore, this uncommonly encountered histologic feature should be distinguished from perinephric and sinus fat invasion of RCC. Negative reaction for melanoma markers, such as HMB-45, Melan-A, microphthalmia transcription factor, and tyrosinase, and immunopositivity for such RCC markers as CD10 and epithelial membrane antigen, can exclude oncocytoma-like epithelioid AML.¹ The present immunohistochemical results matched those of the tumor cells of papillary RCC and partly matched those of the oncocytic cells of papillary RCC showing papillotubular growth, as re-

ported by Masuzawa *et al.*,³ whereas oncocytic cells are diffusely stained with AMACR and CK7.⁶ Recent molecular studies that have focused on oncocytic papillary RCC have revealed similar results to those of traditional papillary RCC showing frequent trisomies 7, 12, 16, 17, and 20.¹ Kunju *et al.*⁵ reported trisomy 7 and 17 and loss of the Y chromosome. Park *et al.*⁶ demonstrated that comparative genomic hybridization showed gains of 3p22 and 11q12-q13 in addition to chromosome 17 or loss of 4q. They also demonstrated a loss of chromosome 4 in one case of oncocytic papillary RCC. These molecular changes of oncocytic papillary RCC are similar to other types of papillary RCC. Immunopositivity for AMACR is similar to types 1 and 2 papillary RCC.

The Mallory body-like eosinophilic hyaline globules are not commonly encountered in RCC, but they were first reported by Datta in 1977.⁹ These structures are morphologically similar to those seen in alcoholic liver disease, which is composed of a parallel array or granular aggregates of intermediate filaments. These prekeratin-like structures show similar immunohistochemical and special staining results as the present case.

The present tumor arose in the background of tuberculous kidney. To date, less than 50 cases of RCC with renal tuberculosis have been reported.¹⁰ Establishing a causative relationship between the chronic inflammation of tuberculosis and RCC is rather complicated, especially since we know from previous literature that bacillus Calmette–Guérin interaction with the uroepithelium upregulates interleukins and various forms of interferon, which are currently the primary immunotherapies for RCC.

We emphasize a rare morphology of oncocytic RCC with tubulopapillary growth pattern containing a mature fat component. This combination of pathologic findings are rarely encountered and should be distinguished from other types of RCC as well as oncocytoma-like epithelioid AML.

Conflicts of Interest

No potential conflict of interest relevant to this article was reported.

REFERENCES

1. Eble JN, Sauter G, Epstein JI, Sesterhenn IA. World Health Organization classification of tumours: pathology and genetics of tumours of the urinary system and male genital organs. Lyon: IARC Press, 2004.
2. Shuch B, Amin A, Armstrong AJ, *et al.* Understanding pathologic variants of renal cell carcinoma: distilling therapeutic opportunities

- from biologic complexity. *Eur Urol* 2015; 67: 85-97.
3. Masuzawa N, Kishimoto M, Nishimura A, Shichiri Y, Yanagisawa A. Oncocytic renal cell carcinoma having papillotubular growth: rare morphological variant of papillary renal cell carcinoma. *Pathol Int* 2008; 58: 300-5.
 4. Mai KT, Kohler DM, Robertson SJ, Belanger EC, Marginean EC. Oncocytic papillary renal cell carcinoma with solid architecture: mimic of renal oncocytoma. *Pathol Int* 2008; 58: 164-8.
 5. Kunju LP, Wojno K, Wolf JS Jr, Cheng L, Shah RB. Papillary renal cell carcinoma with oncocytic cells and nonoverlapping low grade nuclei: expanding the morphologic spectrum with emphasis on clinicopathologic, immunohistochemical and molecular features. *Hum Pathol* 2008; 39: 96-101.
 6. Park BH, Ro JY, Park WS, *et al.* Oncocytic papillary renal cell carcinoma with inverted nuclear pattern: distinct subtype with an indolent clinical course. *Pathol Int* 2009; 59: 137-46.
 7. Sironi M, Spinelli M. Oncocytic angiomyolipoma of the kidney: a case report. *Int J Surg Pathol* 2003; 11: 229-34.
 8. Aron M, Aydin H, Sercia L, Magi-Galluzzi C, Zhou M. Renal cell carcinomas with intratumoral fat and concomitant angiomyolipoma: potential pitfalls in staging and diagnosis. *Am J Clin Pathol* 2010; 134: 807-12.
 9. Datta BN. Hyaline intracytoplasmic globules in renal carcinoma. *Arch Pathol Lab Med* 1977; 101: 391.
 10. Tickoo SK, dePeralta-Venturina MN, Harik LR, *et al.* Spectrum of epithelial neoplasms in end-stage renal disease: an experience from 66 tumor-bearing kidneys with emphasis on histologic patterns distinct from those in sporadic adult renal neoplasia. *Am J Surg Pathol* 2006; 30: 141-53.

Multifocal Polypoid Endometriosis Mimicking Malignancy in a Young Woman with a History of Hormonal Treatment

Ji-Young Kim · Tae-Jong Song¹ · Hye-Kyung Choi² · Jeong Yun Shim

Department of Pathology, CHA Gangnam Medical Center, CHA University School of Medicine, Seoul;

¹Department of Obstetrics and Gynecology, Kangbuk Samsung Medical Center, Sungkyunkwan University School of Medicine, Seoul;

²Department of Radiology, CHA Gangnam Medical Center, CHA University School of Medicine, Seoul, Korea

Polypoid endometriosis is a rare type of endometriosis that sometimes mimics the clinical presentation of malignancy. We report a case of a young woman with a history of hormone treatment who was suspected to have an ovarian malignancy with metastases.

CASE REPORT

A 30-year-old G0P0 woman with a history of left ovarian cystectomy due to endometriosis presented with a huge left adnexal mass detected on ultrasonography. After the previous cystectomy, she was administered a gonadotrophin releasing hormone (GnRH) agonist for four months and then a combined oral contraceptive (OC), Mercilon (Organon Ltd., Dublin, Ireland) (mixed ethinylestradiol and desogestrel), for about two years. Her menstrual cycle was regular, but she experienced severe dysmenorrhea. The patient's serum cancer antigen (CA) 125 level was increased (595.3 U/mL), while her CA 19-9 and carcinoembryonic antigen results were normal.

Ultrasonography showed an 11-cm-sized, mixed-echoic, semi-solid mass in the left adnexa. Abdominopelvic computed tomography revealed the mass to be solid with enhancement (Fig. 1A). Another mass was present in the left abdominal wall, extending to the peritoneum and the rectus abdominis muscle. A

small amount of ascites was observed in the perihepatic space (Fig. 1B).

A laparoscopic left salpingo-oophorectomy was performed to remove the 11-cm-sized tumor encasing and destroying the adnexal organs. Intraoperative frozen section examination indicated the lesion to be benign, most likely severe endometriosis. Other peritoneal foci were also resected.

Microscopically, the left adnexal mass was composed of endometrial-like tissue. Dilated endometrial-type glands were longitudinally arranged around grouped, thick-walled vessels, which were reminiscent of a typical endometrial polyp (Fig. 1C). Worrisome features, such as increased stromal cellularity or atypia, were not noted. The mitotic rate was less than 1 in 10 high-power fields (Fig. 1D). Immunohistochemically, both the epithelial and the stromal cells were positive for estrogen receptor and progesterone receptor. The stromal cells were also positive for CD10 (Fig. 1E, F). The absence of increased cellularity and/or stromal atypia easily excluded the possibility of adenocarcinoma. The endometrial-type stromal cells with CD10 positivity in our case were obviously different from the fibroblastic and CD34-positive stromal cells in adenofibroma.

The patient did not present residual disease at her follow-up six months after the operation.

DISCUSSION

Polypoid endometriosis is a rare type of endometriosis. In contrast to the usual cystic endometriosis, it is solid and frequently forms a nodular polypoid mass that can sometimes mimic malignancy at presentation.¹ Frequently involved sites are the vagi-

Corresponding Author

Jeong Yun Shim, MD, PhD

Department of Pathology, CHA Gangnam Medical Center, 566 Nonhyeon-ro, Gangnam-gu, Seoul 06135, Korea

Tel: +82-2-3468-2612, Fax: +82-2-3468-2619, E-mail: jyshim@cha.ac.kr

Received: March 19, 2015 Revised: April 30, 2015

Accepted: May 12, 2015

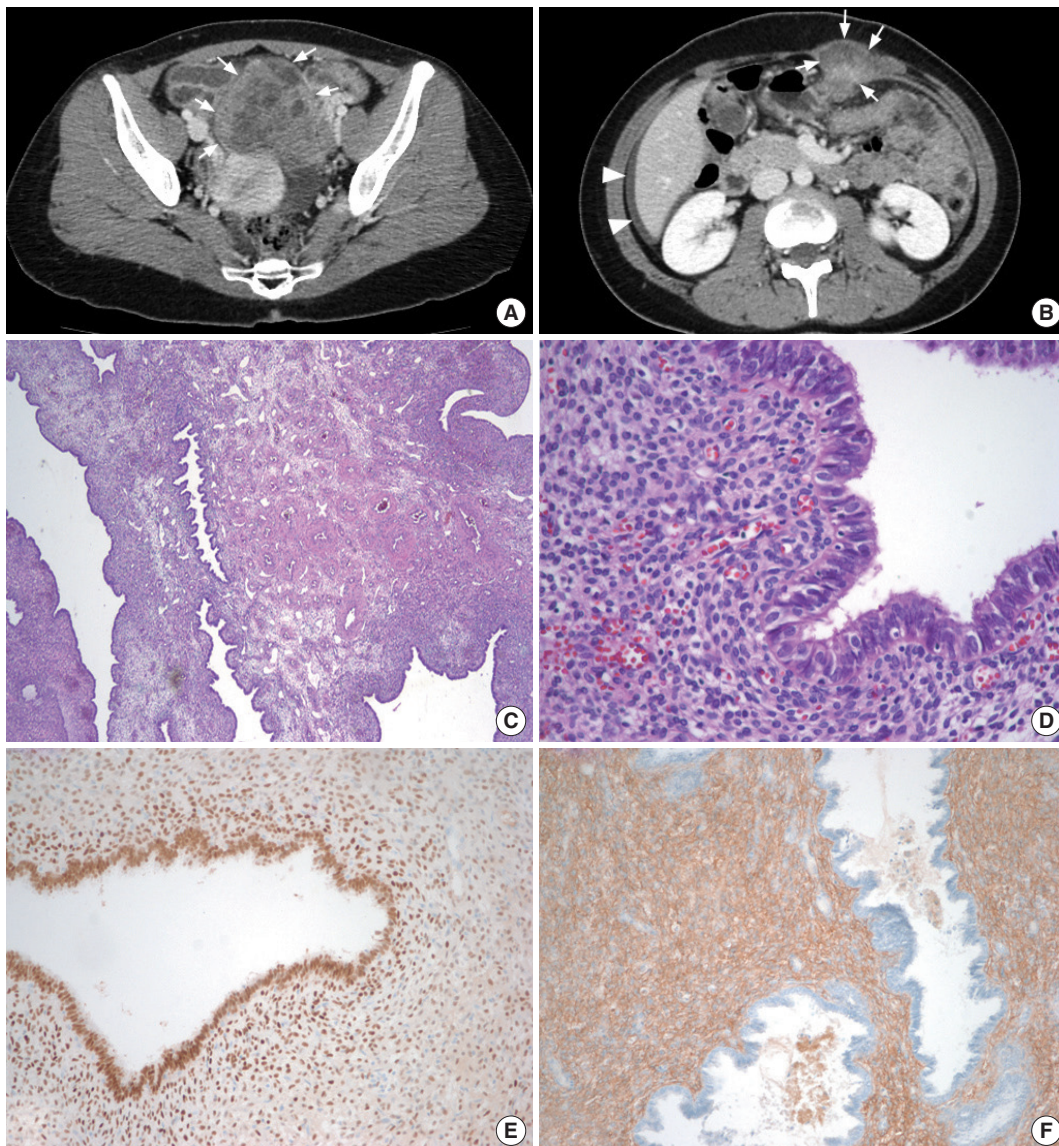


Fig. 1. (A) On axial computed tomography, a solid and cystic mass (arrows) with periuterine adhesions is visible in the left adnexa. (B) Another mass can be seen in the left upper abdominal wall (arrows) and extending to the rectus abdominis muscle. A small amount of ascites is present in the perihepatic area (arrowheads). (C) Microscopically, the mass is composed of endometrial-like tissue. Dilated endometrial-type glands are longitudinally arranged around grouped, thick-walled vessels with swollen and congested stroma, which is reminiscent of a typical endometrial polyp. (D) Some glandular epithelial cells demonstrate ciliated metaplasia. (E) On immunohistochemical staining, the glandular epithelial cells and some stromal cells are positive for estrogen receptor. (F) CD10 is positive only in stromal cells.

na, cervix, adnexa, and colorectum.²⁻⁴ It usually causes non-specific symptoms, such as dysmenorrhea, menorrhagia, or vaginal spotting.^{1,3,5}

The etiology of polypoid endometriosis is uncertain. Some reported cases have been associated with unopposed estrogen treatment, phytoestrogen, and tamoxifen, suggesting the role of estrogenic stimulation in the development of the disease.^{1,3-6} Withdrawal of a GnRH agonist was also reported to cause polypoid endometriosis as a rebound phenomenon.^{3,7} To our knowledge,

there is no previous report of polypoid endometriosis associated with OCs. In a collective review of 22 cases of polypoid endometriosis, Parker *et al.*¹ included four cases with mixed estrogen-progestin therapy. But it was in the form of hormone replacement therapy after menopause or oophorectomy rather than a contraceptive use. OCs, which are frequently used to prevent the recurrence of endometriosis after conservative surgery, have also been reported to increase the risk of endometriosis in certain conditions.⁸ In our patient, estrogen seems to have retained its

stimulatory effect despite being balanced with progesterone.

Polypoid endometriosis can sometimes mimic the clinical presentation of malignancy.¹ The presence of a large adnexal mass, multiple peritoneal and pelvic foci, ascites, and elevated CA 125 in our case gave the preoperative impression of a malignant ovarian tumor with peritoneal metastases. An elevated CA 125 level is one of the laboratory abnormalities associated with endometriosis and is also reported in some cases of polypoid endometriosis.^{4,9} It has been reported that ascites, though very rarely, can be associated with endometriosis, especially in the presence of severe disease.¹⁰ When it presents with ascites, particularly accompanied by multiple peritoneal lesions on radiology, adnexal polypoid endometriosis can be easily misinterpreted as ovarian malignancy with peritoneal metastases.

Our patient underwent laparoscopic surgery despite the preoperative suspicion of malignancy. Gynecological laparoscopy is increasingly performed, even in some early oncological conditions, because of its reduced invasiveness. In our case, an intraoperative frozen diagnosis of a benign mass prevented conversion of the procedure to a more extensive surgery with laparotomy. Despite the relatively typical microscopic findings, the confusing presentation of the mass, such as its large size, solid nodular nature, destruction of normal anatomical structures, multifocality, peritoneal involvement, ascites, and elevated CA 125, rendered doubt on the benign nature of the lesion. Pathologists' awareness of this rare form of endometriosis is vital in order to avoid unnecessary radical surgery. Yet again, a thorough microscopic examination with sufficient sampling is warranted in these patients in order to exclude complex hyperplasia or adenocarcinoma, which, although very rare, has arisen in polypoid endometriosis.¹ Polypoid endometriosis should also be included in the differential diagnosis of seemingly malignant adnexal tumors in a young woman, especially when associated with a history of hormone therapy, notably OCs, for endometriosis.

Conflicts of Interest

No potential conflict of interest relevant to this article was reported.

REFERENCES

1. Parker RL, Dadmanesh F, Young RH, Clement PB. Polypoid endometriosis: a clinicopathologic analysis of 24 cases and a review of the literature. *Am J Surg Pathol* 2004; 28: 285-97.
2. Jaiman S, Gundabattula SR, Pochiraju M, Sangireddy JR. Polypoid endometriosis of the cervix: a case report and review of the literature. *Arch Gynecol Obstet* 2014; 289: 915-20.
3. Othman NH, Othman MS, Ismail AN, Mohammad NZ, Ismail Z. Multiple polypoid endometriosis: a rare complication following withdrawal of gonadotrophin releasing hormone (GnRH) agonist for severe endometriosis: a case report. *Aust N Z J Obstet Gynaecol* 1996; 36: 216-8.
4. Kraft JK, Hughes T. Polypoid endometriosis and other benign gynaecological complications associated with tamoxifen therapy: a case to illustrate features on magnetic resonance imaging. *Clin Radiol* 2006; 61: 198-201.
5. Felix A, Nogales FF, Arias-Stella J. Polypoid endometriosis of the uterine cervix with Arias-Stella reaction in a patient taking phytoestrogens. *Int J Gynecol Pathol* 2010; 29: 185-8.
6. Chang CK, Chen P, Leu FJ, Lou SM. Florid polypoid endometriosis exacerbated by tamoxifen therapy in breast cancer. *Obstet Gynecol* 2003; 102(5 Pt 2): 1127-30.
7. Marugami N, Hirohashi S, Kitano S, et al. Polypoid endometriosis of the ureter mimicking fibroepithelial polyps. *Radiat Med* 2008; 26: 42-5.
8. Tu FF, Du H, Goldstein GP, Beaumont JL, Zhou Y, Brown WJ. The influence of prior oral contraceptive use on risk of endometriosis is conditional on parity. *Fertil Steril* 2014; 101: 1697-704.
9. Laird LA, Hoffman JS, Omrani A. Multifocal polypoid endometriosis presenting as huge pelvic masses causing deep vein thrombosis. *Arch Pathol Lab Med* 2004; 128: 561-4.
10. Gungor T, Kanat-Pektas M, Ozat M, Zayifoglu Karaca M. A systematic review: endometriosis presenting with ascites. *Arch Gynecol Obstet* 2011; 283: 513-8.

Gastric Langerhans Cell Histiocytosis: Case Report and Review of the Literature

So Jung Lee^{1,2} · Chung Su Hwang^{1,2} · Gi Young Huh^{1,2} · Chang Hun Lee^{1,2} · Do Youn Park^{1,2}

¹Department of Pathology, Pusan National University Hospital, Pusan National University School of Medicine, Busan;

²Biomedical Research Institute, Pusan National University Hospital, Busan, Korea

Langerhans cell histiocytosis (LCH) is a rare disease of unknown etiology and is characterized by a clonal proliferation of Langerhans cells.¹ The clinical presentation of LCH is variable, ranging from single organ to multisystem involvement; patients may experience benign to life-threatening outcomes.¹ Localization of LCH to the stomach is extremely rare and is most often found in pediatric patients with systemic disease.² Here we present a case of localized LCH to the stomach in a 64-year-old man who underwent a complete resection of the lesion by endoscopic submucosal dissection (ESD).

CASE REPORT

A 64-year-old man was referred to a gastroenterologist for further evaluation of an abnormality found during an upper gastrointestinal examination. This patient had nothing remarkable in his medical history except medical treatment for hyperthyroidism. Esophagogastroduodenoscopy revealed an elevated mucosal lesion approximately 1 cm in size in the gastric fundus (Fig. 1A). The surface of the lesion was smooth with focal erosion. Microscopic examination of the endoscopic biopsy specimen revealed increased eosinophilia, and a cluster of histiocytic cells infiltrated the lamina propria and were mixed with lymphocytes, neutrophils, and plasma cells (Fig. 1C). The histiocytic cells had elongated nuclei, intranuclear grooves, and irregular nuclear mem-

branes, as well as abundant fine granular eosinophilic to clear cytoplasm. Histiocytic cell clusters showed strong immunoreactivity to S100 and CD1a (Fig. 1D), while they were negative to cytokeratin AE1/AE3 and leukocyte common antigen. Through a combination of morphological and immunohistochemical analyses, a diagnosis of LCH was confirmed. A gastroenterologist performed ESD for complete removal of the lesion. The ESD specimen showed a very focal remnant LCH lesion that had been completely removed (Fig. 1B). Following complete resection of the gastric LCH lesion, a comprehensive evaluation was performed to determine the extent of the disease. No evidence of multisystem involvement was found. The patient's 6-month follow-up visit revealed no local or systemic recurrence, and the patient remained in good health.

DISCUSSION

LCH is a rare disease identified in both children and adults and is characterized by infiltration of histiocytic cells in various organs.³ The pathogenesis and etiology of LCH are not fully understood.¹ A recent hypothesis suggests that LCH cells are derived from bone marrow monocyte precursors that differentiate into antigen-presenting cells (i.e., Langerhans cells or dendritic cells) in the epidermis, respiratory tract, and lymph nodes. The presence of monoclonality itself has been used as evidence that this disease is a clonal neoplastic disorder. Despite the neoplastic nature of the condition, the clinical course of LCH is heterogeneous. Therefore, treatment of LCH depends on the extent and severity of the disease at the time of diagnosis, which includes the number of involved organs and the presence of normal organ function.¹

Corresponding Author

Do Youn Park, MD, PhD
Department of Pathology, Pusan National University Hospital, Pusan National University School of Medicine, 179 Gudeok-ro, Seo-gu, Busan 49241, Korea
Tel: +82-51-240-7422, Fax: +82-51-242-7422, E-mail: pdy220@pusan.ac.kr

Received: February 3, 2015 Revised: May 4, 2015

Accepted: May 19, 2015

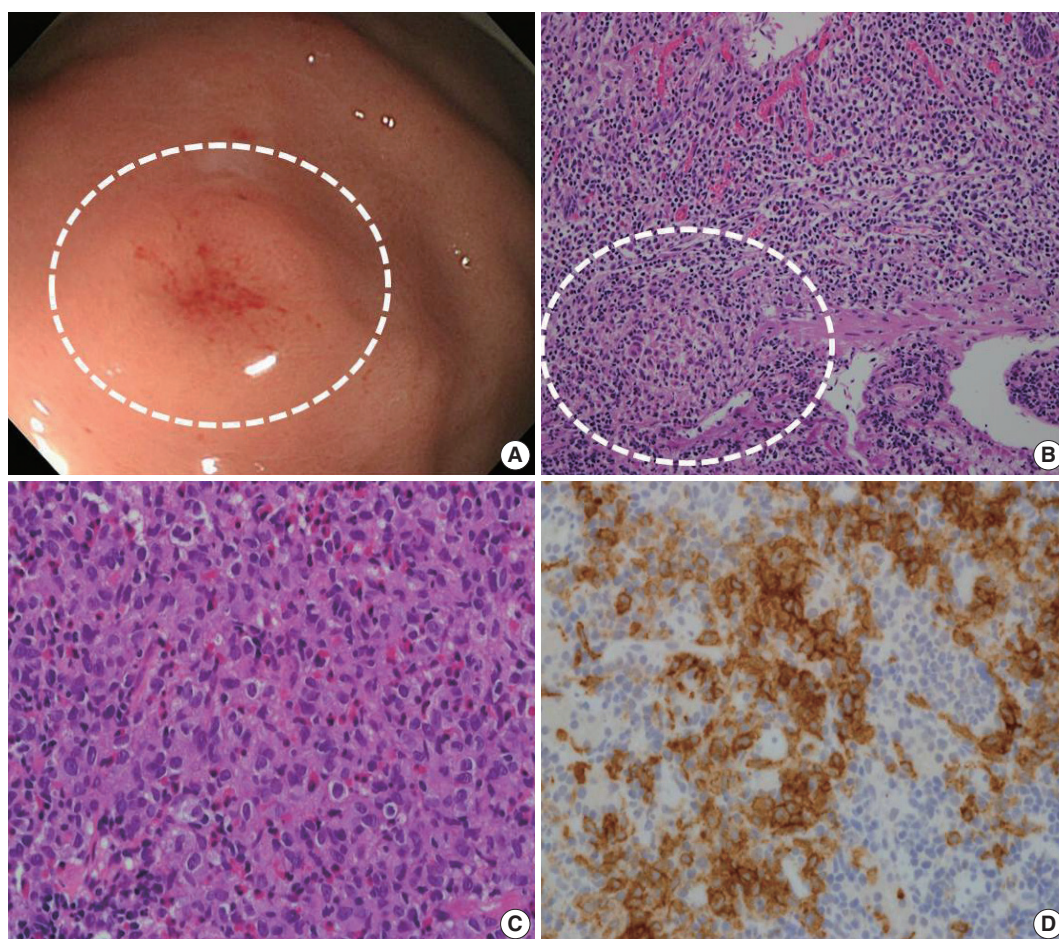


Fig. 1. Endoscopic and histologic finding of gastric Langerhans cell histiocytosis. (A) A mild elevated mucosal lesion (1 cm in size) with central erosion is observed upon gastroenteroscopy (circle). The lesion is located in the fundus of the stomach. (B) Microscopic analysis of the endoscopic submucosal dissection specimen. Focal histiocytic cell aggregates are present in the lamina propria and muscularis mucosa, with abundant eosinophils and other inflammatory cells. (C) Microscopic analysis of the endoscopic biopsy specimen reveals histiocytic cell aggregates in the lamina propria of the mucosa, with abundant eosinophil infiltration. Lymphocytes and plasma cells are also observed. The histiocytic cells show an irregular nuclear membrane and groove. These cells have abundant and granular eosinophilic to clear cytoplasm. (D) Immunohistochemistry for CD1a. The histiocytic cells show positive staining for CD1a.

Involvement of the gastrointestinal tract is very rare and has been associated with systemic involvement and poor prognosis.⁴ In pediatric patients, LCH in the gastrointestinal tract produces symptoms such as vomiting, loose stool, and abdominal pain and is related to a poor prognosis in the majority of neonatal cases; in these patients, skin lesions usually precede gastrointestinal LCH.^{4,5} In contrast to children, adult patients are asymptomatic and present with solitary polypoids or elevated lesions.⁴ Only six cases in adult of gastric LCH have been reported in the literature.^{4,6-10} In contrast to pediatric LCH, adult gastric LCH appears as a unifocal disease without recurrence or progression, in a similar manner to our case (Table 1). Like many other gastric LCH cases, an elevated mucosal lesion was noted in our patient by the gastroenterologist, whose initial impression was a sub-

mucosal tumor. Endoscopic findings of gastric LCH mucosa are sometimes confused with gastric tumors presenting as polypoids and ulcerative mucosa.^{2,4} Despite the absence of clinical features, gastric LCH shows the typical histological characteristics of LCH in other organs.^{3,4} Histologically, histiocytic cells resemble Langerhans cells of the epidermis. Langerhans cells form a sheet of islands with indistinct cell borders and abundant eosinophilic cytoplasm. Their nuclei are elongated and irregular, exhibiting vesicular chromatin with a nuclear groove and often presenting with a single prominent nucleoli.^{3,4} Langerhans cells are usually mixed with other inflammatory cells such as eosinophils, lymphocytes, plasma cells, and neutrophils. In the literature, predominant eosinophil infiltration has been reported in 50% of cases with gastric LCH.⁴ In a similar manner to a previous re-

Table 1. Comparison of reported cases and presented case

Case no.	Reference	Age (yr)/ Sex	Symptom	Endoscopic finding	Site	Multiplicity	Specimen	Multisystem ^a	Outcomes	Follow-up
1	Singhi and Montgomery ⁴	68/M	Dysphasia	Polyp	Antrum	Solitary	Biopsy	Absent	Remission	22 mo
2	Iwafuchi <i>et al.</i> ⁶	49/F	Asymptomatic	Sessile elevation	Throughout the stomach	Multiple	Biopsy	Absent	Remission	5.6 yr
3	Nihei <i>et al.</i> ⁷	47/F	R/O cancer	Flat	Body	Solitary	Resection	Absent	Remission	20 mo
4	Vazquez and Ayestaran ⁸	59/F	Epigastric pain	Ulcer	Lesser curvature	Solitary	Resection	N/A	N/A	N/A
5	Lee <i>et al.</i> ⁹	51/M	Asymptomatic	Elevated	Antrum	Solitary	Biopsy, ESD	Absent	Remission	12 mo
6	Wada <i>et al.</i> ¹⁰	53/F	Abdominal discomfort	Polypoid	Throughout the stomach	Multiple	Biopsy	Absent	Alive/skin lesion developed	2 yr
7	Present case	64/M	Asymptomatic	Elevated	Fundus	Solitary	Biopsy, ESD	Absent	Remission	6 mo

M, male; F, female; R/O, rule out; N/A, not applicable; ESD, endoscopic submucosal dissection.

^aMultisystem involvement at diagnosis.

port,⁴ our case showed aggregates of histiocytic cells with Langerhans cell nuclear features, which were mixed with inflammatory cells, mainly eosinophils. Immunohistochemical analysis is helpful to confirm the diagnosis, and Langerhans cells show diffuse immunoreactivity for S100 and CD1a.^{1,4} In such cases, we suggest that stomach LCH could appear as a submucosal tumor upon endoscopy. Pathologists should consider the possibility of LCH if microscopic observation of biopsy specimens reveals increased eosinophilia or histiocytic cells. In these cases, immunohistochemical staining for S100 and CD1a is needed.

Conflicts of Interest

No potential conflict of interest relevant to this article was reported.

Acknowledgments

This work was supported by the year 2014 clinical research grant from Pusan National University Hospital.

REFERENCES

1. Ablu O, Egeler RM, Weitzman S. Langerhans cell histiocytosis: current concepts and treatments. *Cancer Treat Rev* 2010; 36: 354-9.
2. Behdad A, Owens SR. Langerhans cell histiocytosis involving the gastrointestinal tract. *Arch Pathol Lab Med* 2014; 138: 1350-2.
3. Detlefsen S, Fagerberg CR, Ousager LB, *et al.* Histiocytic disorders of the gastrointestinal tract. *Hum Pathol* 2013; 44: 683-96.
4. Singhi AD, Montgomery EA. Gastrointestinal tract langerhans cell histiocytosis: a clinicopathologic study of 12 patients. *Am J Surg Pathol* 2011; 35: 305-10.
5. Vetter-Laracy S, Salinas JA, Martin-Santiago A, Guibelalde M, Balliu PR. Digestive tract symptoms in congenital langerhans cell histiocytosis: a fatal condition in an illness usually considered benign. *J Pediatr Hematol Oncol* 2014; 36: 426-9.
6. Iwafuchi M, Watanabe H, Shiratsuka M. Primary benign histiocytosis X of the stomach: a report of a case showing spontaneous remission after 5 1/2 years. *Am J Surg Pathol* 1990; 14: 489-96.
7. Nihei K, Terashima K, Aoyama K, Imai Y, Sato H. Benign histiocytosis X of stomach: previously undescribed lesion. *Acta Pathol Jpn* 1983; 33: 577-88.
8. Vazquez JJ, Ayestaran JR. Eosinophilic granuloma of the stomach similar to that of bone: light and electron microscopic study. *Virchows Arch A Pathol Anat Histol* 1975; 366: 107-11.
9. Lee CK, Lee SH, Cho HD. Localized Langerhans cell histiocytosis of the stomach treated by endoscopic submucosal dissection. *Endoscopy* 2011; 43 Suppl 2: E268-9.
10. Wada R, Yagihashi S, Konta R, Ueda T, Izumiyama T. Gastric polypoidosis caused by multifocal histiocytosis X. *Gut* 1992; 33: 994-6.